Conformal Field Theory and the Alpha Space Transform

DANIEL JOHN RUTTER

Conformal Field Theory and the Alpha Space Transform

& Counterterms in Truncated Theories

Daniel Rutter

A Thesis presented for the degree of
Doctor of Philosophy

Centre for Particle Theory
Department of Mathematical Sciences
Durham University
United Kingdom

May 2019

Conformal Field Theory and the Alpha Space Transform

& Counterterms in Truncated Theories

Daniel Rutter

Submitted for the degree of Doctor of Philosophy

May 2019

Abstract: This thesis can be split into two parts. In the first, we expound the alpha space formalism [1] and extend it beyond two dimensions. By performing a Sturm-Liouville analysis of the conformal quadratic Casimir differential equation, we define an invertible integral transform which maps functions on the Lorentzian square to alpha space. We explain how poles correspond to conformal blocks and provide numerous examples of interesting densities. After lifting the crossing equation to alpha space, we present a new representation of the accompanying kernel in terms of analytic Wilson functions. We also offer some comments on Regge physics and analyticity. In the second, we investigate the perturbative renormalisation of deformed conformal field theories from the Hamiltonian perspective. We discuss the relation with conformal perturbation theory, to which we provide an explicit match up to third order in the coupling, and show how second-order anomalous dimensions in the Wilson-Fisher fixed points are straightforwardly computed in the Hamiltonian framework. We then focus on the cut-off employed in the truncated conformal space approach of Yurov and Zamolodchikov [2]. We discuss the appearance of non-covariant and non-local counterterms to second order in the cut-off, explicitly in ϕ^4 theory, and find a smooth cut-off to tame subleading oscillations.

Declaration

The work in this thesis is based on research carried out in the Department of Mathematical Sciences at Durham University. No part of this thesis has been submitted elsewhere for any degree or qualification. A number of the results have been published during the course of my PhD [3].

Acknowledgements

Firstly, I would like to thank Amelia, who has made huge sacrifices for me throughout the course of my PhD. Her support and love have been unbounded and exceptional.

Secondly, I would like to thank my supervisor Balt van Rees, who is an extraordinarily talented physicist. He has consistently been patient, kind, humorous, inspiring, available and dedicated.

Finally, I would like to thank the Science and Technology Facilities Council and the Simons Collaboration on the Nonperturbative Bootstrap for their generous funding.

It's full of charts and facts and figures
and instructions for dancing.

— Stephin Merritt

Dedicated to

Amelia

and

our families

Contents

List of Figures

List of Tables

Chapter 0

Introduction

This thesis can be cleanly split into two parts. Making up the majority of the work, the first part consists of Chapters 2 and 3. Here, we extend the alpha space formalism of [1]. Chapter 4 makes up the second part, where we investigate cut-off dependent counterterms in the truncated conformal space approach of Yurov and Zamolodchikov [2].

The underlying link between these two projects is conformal field theory, a subject that is briefly reviewed in Chapter 1 and is a ubiquitous presence in modern physics. The important role played by conformal field theories has become increasingly apparent since the early pioneering work of Ferrera, Grillo, Gatto, Belavin, Parisi, Polyakov and Zamolodchikov [4, 5, 6, 7].

At critical points of phase transitions, quantum field theories typically enjoy an enlarged symmetry group as correlation lengths diverge. Supplementing this scale invariance, unitarity typically promotes the usual Lorentz group to the full conformal group [8].

Equivalently speaking, the space of quantum theories can be explored using the renormalisation group and, at fixed points of the flow, theories typically become conformal. This enhancement is discussed in Section 1.1. Due to the augmented symmetry group, these theories tend to be simpler and so they offer invaluable insight as important signposts in the space of all theories.

The bootstrap is a pivotal tool in the analysis of conformal field theories. It is a set of ideas which combines unitary, crossing symmetry and conformal invariance to constrain allowed theories. Introduced in the 1970s [5] and revived in 2008 [9], the bootstrap has provided an abundance of numerical and analytical insights; see for instance [10, 11, 12, 13].

Alpha space [1] is defined by performing a Sturm-Liouville analysis on the differential operator built from the quadratic Casimir of the conformal group. The output of this procedure is an invertible integral transform that allows us to naturally decompose a function into a linear combination of eigenfunctions. In the language of conformal field theory, these are the blocks which encode the contribution of an intermediate operator to a four-point correlation function.

In Chapter 2 we work in one and two dimensions, reviewing and then extending the results of [1]. That paper sought to initiate the study of the conformal bootstrap via an integral kernel by looking at the crossing equation in alpha space. Perhaps our most significant new contribution for $d = 1$ is Eq. (2.6.12), which gives the split kernel in terms of analytic Wilson functions.

In Chapter 3, we move beyond two dimensions and define alpha space more generally. In essence, poles in alpha space map to blocks in position space. Harmonic analyses of the conformal group are not new; see for instance [14, 15]. However, our approach is slightly different in that we do not start from the Euclidean inversion formula, which is essentially a statement about the orthogonality and completeness of conformal partial waves. Instead, we use the Sturm-Liouville approach to build a new orthogonal set of functions, defined in Eq. (3.1.7). In the future, it will be important to exactly understand how our integral transform differs from that of Caron-Huot [16] and this is something that we comment on in Section 3.1.2.

Finally, Chapter 4 is adapted from our paper [3] which deals with counterterms in truncated conformal field theories. One way to study renormalisation group flows is to start at a conformal fixed point and then perturb the system with some relevant operator. Under the assumption that the fixed point is solved (in the sense that we

fully understand the spectrum), the flow can be reproduced using the conformal data. In practice, we need to truncate the Hilbert space in order to put the computation on a computer. This cut-off is in general non-local and so the required counterterms are necessarily non-local too. However, we see in Section 4.2 that all hope is not lost and that the allowed guises of the counterterms are tractable. We illustrate our general results by considering ϕ^4 theory in Section 4.3.

Chapter 1

Conformal Field Theory

In this chapter, we present some well-established results in conformal field theory. The subject is vast and so we have cherry-picked calculations relevant to subsequent chapters without claiming to be encyclopaedic. There are a number of excellent review articles which go into much greater detail [17, 18].

Conformal field theories describe certain physical systems at critical points of phase transitions, where the correlation length becomes infinite. As such, there are no scales in a conformal field theory and there is no consistent interpretation in terms of particles.

Techniques for tackling conformal fixed points have typically involved Monte Carlo simulations, lattice calculations or epsilon expansions. Recently however, significant progress has been made using the bootstrap; a non-perturbative approach that looks to constrain the space of conformal field theories, usually through demanding consistency under crossing symmetry and unitarity.

Aside from phase transitions, conformal field theories are also widely studied because they make up half of the AdS/CFT correspondence. This is the statement that certain theories of quantum gravity in anti-de Sitter space are equivalent in some sense to conformal field theories with one fewer dimension. Early pioneering work includes [19, 20, 21] and a good review of gauge/gravity duality can be found at [22].

In Section 1.1, we discuss the interpretation of conformal field theories as fixed points along renormalisation group flows. We then go on to introduce the conformal algebra in Section 1.2. There we derive some constraints of conformal symmetry using the embedding space formalism, which thinks of Euclidean space as embedded in a higher-dimensional space where the conformal group acts as the linear Lorentz group. Following on from this, we investigate three- and four-point correlation functions in Section 1.3.

Crucially, the operator product expansion is convergent in conformal field theories and the significance of this fact is detailed in Section 1.4.

Within a conformal correlator, the contribution of an intermediate operator is encoded in a so-called conformal block. These are fixed by the symmetries and are studied in Section 1.5.

To conclude the chapter, we talk about crossing symmetry in Section 1.6. At the heart of this is the associativity of the operator product expansion, which places rigorous constraints on the spectra of conformal field theories.

1.1 Renormalisation Group

The physics governing a system is highly dependent on the pertinent energy scale. For example whilst the Navier-Stokes equation might accurately model the bulk dynamics of certain fluids, it is vastly different from the quantum equations of motion describing two of the constituent interacting molecules; both superficially and in terms of degrees of freedom.

A renormalisation group flow is the evolution of a quantum field theory from the ultraviolet to the infrared. As a group it is a misnomer because the flow from small scales to large ones is in general not invertible. The physical justification for this is that degrees of freedom are integrated away as we 'zoom out' from the ultraviolet.

The Wilsonian approach [23] to the renormalisation group heuristically starts with

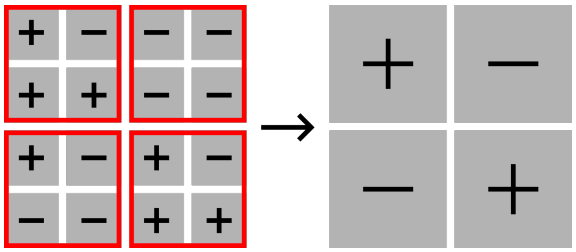

Figure 1.1: This figure represents a lattice of spins, modelling for example a ferromagnet. A discrete renormalisation group flow can be performed by grouping the spins into blocks. This is effectively zooming out from the ultraviolet regime. The effective Hamiltonian describing the interactions between lattices sites changes but the overall partition function remains the same. A scale invariant theory is found when the effective Hamiltonian is unchanged under a course of blocking.

a partition function

$$\begin{aligned} \mathcal{Z} &= \int \mathcal{D}\phi\, e^{-S[\phi]} \\ &= \int_{\text{low}} \mathcal{D}\phi\, e^{-S_{\text{eff}}[\phi]} \end{aligned} \tag{1.1.1}$$

where the path integral is in some manner split into high and low energy modes, with the effective action defined through the expression

$$e^{-S_{\text{eff}}[\phi]} \equiv \int_{\text{high}} \mathcal{D}\phi\, e^{-S[\phi]} \tag{1.1.2}$$

By altering the scale dividing high and low energy modes, the couplings evolve and the space of theories is explored. Fig. 1.1 shows a discrete lattice model equivalent, where spins are 'blocked' together. Each time this is done, the couplings in the effective action are altered despite the overall partition function remaining unchanged.

Along a renormalisation group flow, beta functions chronicle the development of the theory. These functions are derivatives of the couplings with respect to the renormalisation scale. Fixed points of the flow are defined by tuning the couplings to set the beta functions to zero. At these points, the theory is then by definition scale invariant. Under the assumption of unitarity, which demands that all physical

states have a non-negative norm, this enlarged symmetry group is typically enhanced further to include conformal transformations. These preserve angles in the sense that they only alter the metric by some local factor. The question of scale versus conformal symmetry is subtle and interesting but we do not consider theories that have the former without the latter in this work.

With this fixed point interpretation, conformal field theories can therefore be thought of as important signposts in the space of all quantum field theories. As they typically tend to be simpler, they are subsequently studied to learn about phenomena present in more general theories. The canonical sandbox is $\mathcal{N} = 4$ supersymmetric Yang-Mills theory as it shares some similarities with Quantum Chromodynamics and because it is dual to a string theory through the AdS/CFT correspondence [19].

Different ultraviolet theories may flow to the same infrared fixed point. This universality is typified by the Ising model, the critical exponents of which match a variety of experimentally observed phase transitions [8].

Formalising the notion that a quantum field theory has more degrees of freedom in the ultraviolet and that information is somehow lost as it flows to the infrared has been the topic of some notable work. One stand-out result is the c-theorem [24], which states that there exists a function that decreases monotonically along a two-dimensional renormalisation group flow and is equal to the central charge of the theory at the fixed points. Similar progress has been made in higher dimensions with the a- and F-theorems [25, 26, 27].

1.2 Conformal Algebra

At a reductive level, a conformal field theory is a quantum field theory that is invariant under the conformal group. This is the standard Poincaré group augmented by dilations and special conformal transformations, where the latter is an inversion-translation-inversion combination. Explicitly, the associated Lie algebra is $\mathfrak{so}(p{+}1, q{+}$

1) for a conformal field theory with metric signature (p, q) where $p + q = d$ is equal to the spacetime dimension. Concretely, d-dimensional Euclidean and Minkowskian conformal field theories have $\mathfrak{so}(d+1, 1)$ and $\mathfrak{so}(d, 2)$ respectively as their associated Lie algebras.

1.2.1 Embedding Space Formalism

We stated that the conformal algebra is $\mathfrak{so}(d + 1, 1)$ for a d-dimensional Euclidean conformal field theory. This is the familiar Lorentz algebra for $(d + 1, 1)$ spacetime, meaning that conformal transformations act linearly on $\mathbb{R}^{d+1,1}$ despite acting non-trivially on $\mathbb{R}^d$. Therefore, it is natural to embed the latter into the former and have some consistent prescription for projecting away two of the dimensions. This formalism was first introduced by Dirac in 1936 [28]. Usually, the recipe is to go to a specific section of the light-cone.

Putting this all together, a conformal spacetime transformation can be realised through the following algorithm.

1. Take a vector x in $\mathbb{R}^d$.

2. Lift this vector to the Euclidean sector of the light-cone to give $X = (1, x^2, x)$. In this basis, the inner product between the vectors $A = (A^+, A^-, a)$ and $B = (B^+, B^-, b)$ is $A.B \equiv a.b - (A^+B^- + A^-B^+)/2$. For vectors represented by lower-case letters, $a.b$ is the standard Euclidean inner product in $\mathbb{R}^d$.

3. Lorentz transform X and scale the resulting vector back to the Euclidean sector to give $Y = (1, y^2, y)$. Note that a Lorentz transformation will preserve the norm of the vector and so will not move it off of the light-cone.

4. Read off y from Y.

Throughout this work, a vector raised to some power is defined to be equal to the norm of that vector raised to that power.

Primary operators in a conformal field theory are those that transform homogeneously on the light-cone. As such, deriving their conformal kinematics becomes as straightforward as the Lorentzian counterpart. Other local operators are known as descendants and can be written as derivatives of primary operators.

Several of the quoted results in Section 1.3 can be neatly derived using this formalism. Below, we reproduce the simplest case but the embedding space logic is the same for higher-point correlators and is particularly powerful when dealing with spinning operators. In this work, we freely use the terms correlation function, correlator and n-point function interchangeably.

Consider $\langle\phi(X)\phi(Y)\rangle$, the correlation function of two identical scalar primary operators lifted up to $\mathbb{R}^{d+1,1}$. Homogeneity demands that

$$\phi(\lambda X) = \lambda^{-\Delta_\phi}\phi(X) \tag{1.2.1}$$

for some scale transformation parametrised by λ, where Δ_ϕ is known as the scaling dimension of ϕ. Therefore, the only consistent and Lorentz invariant object that can be written down is

$$\langle\phi(X)\phi(Y)\rangle = \frac{1}{(-2X.Y)^{\Delta_\phi}} \tag{1.2.2}$$

where we were free to scale the operators themselves to fix the overall factor. Terms like $X.X$ and $Y.Y$ are not present as they become zero on the light-cone. Note that if we had considered operators with different scaling dimensions then the two-point function would be necessarily zero to be consistent with homogeneity. Projecting down to $\mathbb{R}^d$, the inner product is

$$X.Y = x.y - \frac{x^2+y^2}{2} = -\frac{(x-y)^2}{2} \tag{1.2.3}$$

All in all, we have derived that the two-point function of identical scalar primaries in a conformal field theory is

$$\langle\phi(x)\phi(y)\rangle = \frac{1}{(x-y)^{2\Delta_\phi}} \tag{1.2.4}$$

That we have power-law rather than exponential fall-off is consistent with the fact that a conformal field theory describes the critical point of a phase transition, where the correlation length becomes infinite.

Similar logic can be applied to give other correlators involving potentially spinning operators. For example, the correlator between two identical spin-one primaries is

$$\langle j_\mu(x) j_\nu(y)\rangle = \left(\delta_{\mu,\nu} - \frac{2(x-y)_\mu (x-y)_\nu}{(x-y)^2}\right) \frac{1}{(x-y)^{2\Delta_j}} \tag{1.2.5}$$

where $\delta_{\mu,\nu}$ is the Kronecker delta symbol.

As clarification, the kinematics for operators with spin are additionally fixed using the transverse condition

$$X^M \langle \phi_M(X)...\rangle = 0 \tag{1.2.6}$$

and the operators themselves are projected to $\mathbb{R}^d$ using

$$\phi_\mu(x) = \phi_M(X) \frac{\partial X^M}{\partial x^\mu} \tag{1.2.7}$$

where μ and M are spacetime indices in $\mathbb{R}^d$ and $\mathbb{R}^{d+1,1}$ respectively.

1.2.2 A Comment on Virasoro Symmetry

In two dimensions, we acknowledge that local conformal transformations are captured by two copies of the infinite-dimensional Virasoro algebra. This leads to a significant simplification and has allowed for some great work to be done, notably the classification of the minimal models. For a comprehensive review, consult what is affectionately called the 'Yellow Pages' [29]. In this work, we do not offer any significant comments on theories with Virasoro symmetry but believe that their importance demanded at the very least a cursory comment.

1.3 Conformal Kinematics

In Section 1.2.1, we used the embedding space formalism to show that the correlation function between two identical scalar primary operators is equal to the distance between them raised to the inverse power of twice their scaling dimension, as given by Eq. (1.2.4). In this section, we discuss three- and four-point functions.

1.3.1 Three-Point Functions

For three scalar primaries, the embedding space formalism can analogously be used to show that conformal symmetry fixes the correlation function to be

$$\langle \phi_1 \phi_2 \phi_3 \rangle = \frac{\lambda_{123}}{x_{12}^{\Delta_1+\Delta_2-\Delta_3} x_{23}^{\Delta_2+\Delta_3-\Delta_1} x_{31}^{\Delta_3+\Delta_1-\Delta_2}} \tag{1.3.1}$$

where the operator ϕ_i has scaling dimension Δ_i and is located at position x_i. Also, we have introduced the shorthand expressions $\Delta_{ij} \equiv \Delta_i - \Delta_j$ and $x_{ij} \equiv x_i - x_j$.

We are not free to fix the coefficient λ_{123} as the operators have already been normalised to fix the two-point function to equal Eq. (1.2.4). λ_{123} is the operator product expansion coefficient introduced in Section 1.4, as we demonstrate for a particular case in Eq. (1.4.4).

1.3.2 Four-Point Functions

Things are slightly more complicated for the four-point correlation function. Conformal symmetry permits that one of the insertion points can be mapped to infinity. A second can then be shifted to zero and a third moved to the point $(1, 0, ..., 0)$ through a dilation and a rotation. This is ultimately why the two- and three-point functions are so simple. However, it does mean that the four-point correlator will only be fixed up to some function of the conformally invariant cross-ratios z and $\bar{z}$, which are related to the coordinates through the expressions

$$z\bar{z} = \frac{x_{12}^2 x_{34}^2}{x_{13}^2 x_{24}^2} \qquad (1-z)(1-\bar{z}) = \frac{x_{23}^2 x_{14}^2}{x_{13}^2 x_{24}^2} \tag{1.3.2}$$

The s-channel limit is defined by taking the first operator close to the second, or equivalently taking $z\bar{z}$ small. Comparably, the t-channel limit is defined by taking $(1-z)(1-\bar{z})$ small.

In a Lorentzian theory, z and $\bar{z}$ are independent real numbers and in a Euclidean theory z is a complex number with $\bar{z}$ as its conjugate (that is, $\bar{z} = z^*$).

Explicitly, the embedding space formalism can be used to show that conformal symmetry fixes the correlation function to the functional form

$$\langle \phi_1 \phi_2 \phi_3 \phi_4 \rangle = \frac{1}{x_{12}^{\Delta_1+\Delta_2} x_{34}^{\Delta_3+\Delta_4}} \left(\frac{x_{24}}{x_{14}}\right)^{\Delta_{12}} \left(\frac{x_{14}}{x_{13}}\right)^{\Delta_{34}} \mathcal{G}(z,\bar{z}) \tag{1.3.3}$$

where once again the operator ϕ_i has scaling dimension Δ_i and is located at position x_i.

1.4 Operator Product Expansion

In a quantum field theory, the product of two nearby operators within a correlation function can be approximated with a sum over operators. This is known as the operator product expansion (OPE).

With the addition of conformal symmetry, the OPE becomes a pivotal tool. Qualitatively, this is because scale invariance promotes the OPE to an exact, convergent statement. In essence, two operator insertions that can be separated by a hypersphere from any others define a state on the surface of that sphere. A local operator can then be defined by dilating the sphere to a point.

Foliating spacetime with hyperspheres such that the dilation operator evolves the theory like a Hamiltonian is the crux of radial quantisation. This leads to a state-operator correspondence in conformal field theories, whereby an operator insertion defines a unique state on any sphere that separates it from other operators and vice-versa.

Therefore, the product of two primary operators within a correlation function may

be written as

$$\mathcal{O}_i(x)\mathcal{O}_j(0) = \sum_k \lambda_{ijk} \mathrm{C}_{ijk}(x, \partial_y)\mathcal{O}_k(y)\big|_{y=0} \tag{1.4.1}$$

where we have here chosen to centre the sphere on the origin and have assumed that it only contains $\mathcal{O}_i$ and $\mathcal{O}_j$. Note that we have placed $\mathcal{O}_j$ and the sphere's centre at the origin only to make this expression cleaner; it was not required but no additional insight would have been gleaned from shifting things. In general, the operators have spin and we have suppressed any potential indices. The sum is over all primary operators in the theory and $\mathrm{C}_{ijk}(x, \partial_y)$ is a differential operator fixed by conformal invariance. Consequently, the contribution of a descendant (a derivative of a primary) is fixed by the contribution of the primary itself. In Eq. (1.4.4) we quote C_{ijk} for the simple scalar case with $\mathcal{O}_i = \mathcal{O}_j$.

The structure constants λ_{ijk} in the operator product expansion are known as OPE coefficients. These, along with the spectrum (the set of operator quantum numbers), define the theory and make up what is known as the conformal data.

Using the OPE to fuse two operators, an n-point correlator can be reduced to a sum over $(n-1)$-point correlators and so on and so forth. As an example, the three-point function $\langle\phi\phi\psi\rangle$ where ϕ and ψ are scalar primaries can be written in terms of two point functions like

$$\frac{\langle\phi(x)\phi(0)\psi(z)\rangle}{\lambda_{\phi\phi\psi}} = \mathrm{C}_{\phi\phi\psi}(x, \partial_y)\langle\psi(y)\psi(z)\rangle\big|_{y=0} = \mathrm{C}_{\phi\phi\psi}(x, \partial_y)\frac{1}{(y-z)^{2\Delta_\psi}}\bigg|_{y=0} \tag{1.4.2}$$

That this is the only term in the OPE contributing stems from the fact that two-point functions between non-identical scalars vanish.

However, we know from Eq. (1.3.1) that $\langle\phi\phi\psi\rangle$ is also equal to

$$\langle\phi(x)\phi(0)\psi(z)\rangle = \frac{\lambda_{\phi\phi\psi}}{x^{2\Delta_\phi-\Delta_\psi} z^{\Delta_\psi}(x-z)^{\Delta_\psi}} \tag{1.4.3}$$

and so, expanding both expressions in the limit that the two ϕ operators collide, we find

$$\mathrm{C}_{\phi\phi\psi}(x, \partial_y) = \frac{1}{x^{2\Delta_\phi-\Delta_\psi}}\left(1 + \frac{1}{2}x^\mu\frac{\partial}{\partial y^\mu} + \left(\frac{\Delta_\psi+2}{8(\Delta_\psi+1)}\right)x^\mu x^\nu\frac{\partial}{\partial y^\mu}\frac{\partial}{\partial y^\nu}\right.$$

$$-\left(\frac{\Delta_\psi}{16(\Delta_\psi-\frac{d}{2}+1)(\Delta_\psi+1)}\right)x^2\frac{\partial}{\partial y^\mu}\frac{\partial}{\partial y_\mu}+\ldots\Bigg) \tag{1.4.4}$$

where d is the spacetime dimension. Note that Δ_ϕ does not appear in $\mathrm{C}_{\phi\phi\psi}$. In general, C_{ijk} depends only on Δ_i and Δ_j through the combination $\Delta_i-\Delta_j$.

Convergent operator product expansions allow for the function $\mathcal{G}(z,\bar{z})$ in Eq. (1.3.3) to be decomposed into a sum over conformal blocks $G_{\alpha,\bar{\alpha}}(z,\bar{z})$, weighted by the theory-dependent OPE coefficients. Each block is fixed by conformal symmetry and encapsulates the contribution of an intermediate primary operator and its descendants. The nature of conformal blocks is discussed in more detail in Section 1.5.

The s-channel decomposition, where ϕ_1 fuses with ϕ_2 and ϕ_3 fuses with ϕ_4, is

$$\mathcal{G}(z,\bar{z})=\sum_{\mathcal{O}}\lambda_{12\mathcal{O}}\lambda_{34\mathcal{O}}\,G_{\alpha,\bar{\alpha}}(z,\bar{z}) \tag{1.4.5}$$

where the sum is over all of the primary operators in the theory and $\lambda_{12\mathcal{O}}$ is the coefficient of $\mathcal{O}$ in the $\phi_1\times\phi_2$ OPE. That is,

$$\phi_1(x)\phi_2(0)\supset\lambda_{12\mathcal{O}}\,x^{\Delta-\Delta_1-\Delta_2}\left(\frac{x^{\mu_1}\ldots x^{\mu_J}}{x^J}\right)\mathcal{O}_{\mu_1\ldots\mu_J}(0) \tag{1.4.6}$$

where we have made the possible spin indices explicit.

The intermediate operator $\mathcal{O}$ has dimension Δ and spin J, which are related to the variables that we have chosen to label the blocks with through the equalities

$$\Delta=\bar{\alpha}+\alpha+\frac{d}{2}\qquad J=\bar{\alpha}-\alpha+1-\frac{d}{2} \tag{1.4.7}$$

which invert to

$$\alpha=\frac{\Delta-J+1-d}{2}\qquad\bar{\alpha}=\frac{\Delta+J-1}{2} \tag{1.4.8}$$

These are the α and $\bar{\alpha}$ variables that play a leading role in the alpha space construction detailed in Chapters 2 and 3.

1.5 Conformal Blocks

In this section, we present some well-established results on conformal blocks; the functions encapsulating the contribution of an intermediate primary operator and all of its descendants to a four-point function.

Workable expressions for these blocks are required for many bootstrap calculations, both analytical and numerical. Impressive computations have been performed to find closed-form expressions in even dimensions and for spin-zero blocks, to derive recursion relations and to determine exact formulae on the diagonal where $z = \bar{z}$.

In this work, we only consider conformal blocks for external operators without spin. That is, we restrict ourselves to four-point functions of scalars. Recently, good progress has been made on spinning conformal blocks [30], which has allowed the bootstrap community to study more complicated configurations.

1.5.1 Casimir Equations

In Section 1.2, we gave the conformal algebra as $\mathfrak{so}(p+1, q+1)$ and so states in a theory lie in irreducible representations of this algebra. Furthermore, a differential operator can be built from the accompanying quadratic Casimir. Since a block encodes the contribution of an intermediate primary operator and its descendants, it ends up being an eigenfunction of the Casimir [31].

In one dimension, the quadratic Casimir equation is

$$D_z G_\alpha(z) = \left(\alpha^2 - \frac{1}{4}\right) G_\alpha(z) \tag{1.5.1}$$

with

$$D_z \equiv z^2(1-z)\frac{\partial^2}{\partial z^2} - (1 + \mathbf{a} + \mathbf{b})z^2\frac{\partial}{\partial z} - \mathbf{ab}z \tag{1.5.2}$$

$$\mathbf{a} \equiv -\frac{\Delta_{12}}{2} \qquad \mathbf{b} \equiv \frac{\Delta_{34}}{2} \tag{1.5.3}$$

Note that we only have one conformally invariant cross-ratio z in $d = 1$ and therefore the blocks only have an α label. The scaling dimension of the intermediate operator

is $\alpha + \frac{1}{2}$.

Eq. (1.5.1) is a hypergeometric differential equation and a solution is

$$G_\alpha(z) \equiv z^{\alpha+\frac{1}{2}}\, {}_2F_1\left(\frac{1}{2} + \mathbf{a} + \alpha, \frac{1}{2} + \mathbf{b} + \alpha; 2\alpha + 1; z\right) \tag{1.5.4}$$

Since the eigenvalue is invariant under $\alpha \to -\alpha$, $G_{-\alpha}(z)$ is also a solution. Around $z = 0$, Eq. (1.5.4) behaves like

$$G_\alpha(z) = z^{\alpha+\frac{1}{2}}(1 + O(z)) \tag{1.5.5}$$

and therefore, because we physically expect the contribution of a single operator of positive dimension to be non-singular in the s-channel limit (as dictated by the OPE), G_α is established as the true block as opposed to $G_{-\alpha}$. This hierarchy can be further justified mathematically by considering higher order Casimirs.

For spacetime dimension $d > 1$, the quadratic Casimir equation for the block $G_{\alpha,\bar{\alpha}}$ is

$$\mathcal{D}\, G_{\alpha,\bar{\alpha}} = \left(\bar{\alpha}^2 + \alpha^2 - \frac{d(d-2)+2}{4}\right) G_{\alpha,\bar{\alpha}} \tag{1.5.6}$$

with

$$\mathcal{D}(z,\bar{z}) \equiv D_z + D_{\bar{z}} + (d-2)\left(\frac{z\bar{z}}{z-\bar{z}}\right)\left((1-z)\frac{\partial}{\partial z} - (1-\bar{z})\frac{\partial}{\partial \bar{z}}\right) \tag{1.5.7}$$

which simplifies to $D_z + D_{\bar{z}}$ in two dimensions.

In addition, $G_{\alpha,\bar{\alpha}}$ satisfies a quartic Casimir eigen-equation given by

$$\begin{aligned}\left(\frac{z\bar{z}}{z-\bar{z}}\right)^{d-2}(D_z - D_{\bar{z}})\left(\frac{z\bar{z}}{z-\bar{z}}\right)^{2-d}(D_z - D_{\bar{z}})\, G_{\alpha,\bar{\alpha}}(z,\bar{z}) = \\ \left(\alpha^4 + \bar{\alpha}^4 - 2\left(\frac{d-2}{2}\right)^2(\alpha^2+\bar{\alpha}^2) - 2\alpha^2\bar{\alpha}^2 + \left(\frac{d-2}{2}\right)^4\right) G_{\alpha,\bar{\alpha}}(z,\bar{z})\end{aligned} \tag{1.5.8}$$

As all of these equations are invariant under $z \leftrightarrow \bar{z}$ (which is a consequence of the symmetric definitions in Eq. (1.3.2)), the blocks satisfy $G_{\alpha,\bar{\alpha}}(z,\bar{z}) = G_{\alpha,\bar{\alpha}}(\bar{z},z)$.

1.5.2 Normalisation Conventions

Analyses of Eqs. (1.5.6) and (1.5.8) show that the blocks can be written as a sum of so-called 'pure' functions like

$$G_{\alpha,\bar{\alpha}}(z,\bar{z}) = G^{\text{pure}}_{\alpha,\bar{\alpha}}(z,\bar{z}) + G^{\text{pure}}_{\bar{\alpha},\alpha}(z,\bar{z}) \tag{1.5.9}$$

Throughout this paper we have chosen to normalise the blocks so that

$$G^{\text{pure}}_{\alpha,\bar{\alpha}}(z,\bar{z}) \overset{z\to 0}{\longrightarrow} \gamma(\alpha-\bar{\alpha}) z^{\alpha+\frac{d-1}{2}} G_{\bar{\alpha}}(\bar{z}) \tag{1.5.10}$$

for finite $\bar{z}$ and the pure blocks are defined by these asymptotics. Fundamentally, the pure blocks are the independent solutions to the quadratic Casimir equation. There are eight due to the eigenvalue symmetries $\alpha \to -\alpha$, $\bar{\alpha} \to -\bar{\alpha}$ and $\alpha \leftrightarrow \bar{\alpha}$.

In Eq. (1.5.10), $G_{\bar{\alpha}}(\bar{z})$ is the one-dimensional block introduced in Eq. (1.5.4). The coefficient function is defined to be

$$\gamma(\alpha) \equiv \frac{\Gamma(d-1)\Gamma(-\alpha)}{2\Gamma(\frac{d}{2})\Gamma(\frac{d}{2}-1-\alpha)} \tag{1.5.11}$$

To assuage the fears of the reader, both $\gamma(\alpha-\bar{\alpha})$ and $\gamma(\bar{\alpha}-\alpha)$ are functions of spin (according to Eq. (1.4.8)) that are finite for physical values.

The normalisation chosen here means that a block is manifestly invariant under $\alpha \leftrightarrow \bar{\alpha}$. This is natural in the sense that the associated eigenvalues share this symmetry.

On the diagonal, it can be shown that a block behaves near the origin like

$$G_{\alpha,\bar{\alpha}}(z,z) \overset{z\to 0}{\longrightarrow} z^{\bar{\alpha}+\alpha+\frac{d}{2}} \tag{1.5.12}$$

and more generally

$$G_{\alpha,\bar{\alpha}}(z,\bar{z}) \overset{z,\bar{z}\to 0}{\longrightarrow} \tag{1.5.13}$$
$$(z\bar{z})^{\frac{d+2(\alpha+\bar{\alpha})}{4}} {}_2F_1\left(\frac{d}{2}-1+\alpha-\bar{\alpha}, \frac{d}{2}-1+\bar{\alpha}-\alpha, \frac{d-1}{2}, \frac{1-x}{2}\right)$$

where the limit is taken with $x \equiv \frac{z+\bar{z}}{2\sqrt{z\bar{z}}}$ fixed.

Recalling Eq. (1.4.8), the pure blocks behave like

$$\frac{G^{\text{pure}}_{\frac{\Delta-J+1-d}{2},\frac{\Delta+J-1}{2}}(z,\bar{z})}{\gamma\left(1-\frac{d}{2}-J\right)} = z^{\frac{\Delta-J}{2}}\bar{z}^{\frac{\Delta+J}{2}}(1+O(z/\bar{z},\bar{z})) \tag{1.5.14}$$

for $0 < z \ll \bar{z} \ll 1$, in terms of the dimension and spin of the intermediate operator.

Although Eqs. (1.5.6) and (1.5.8) are much more formidable than their one-dimensional counterparts, they are soluble in certain circumstances. For example, in even dimensions they can be solved in terms of $d = 1$ blocks. However, in odd dimensions the current state-of-the-art is to use recursion relations [32] for series expansions of $G_{\alpha,\bar{\alpha}}(z,\bar{z})$.

Two Dimensions

In two dimensions, the quadratic Casimir Eq. (1.5.6) reduces to $D_z + D_{\bar{z}}$ and so the block can immediately be written down as

$$G_{\alpha,\bar{\alpha}}(z,\bar{z}) \equiv \frac{G_\alpha(z)G_{\bar{\alpha}}(\bar{z}) + G_\alpha(\bar{z})G_{\bar{\alpha}}(z)}{2} \tag{1.5.15}$$

Four Dimensions

In four dimensions, Eqs. (1.5.6) and (1.5.8) can be solved to give the block as

$$G_{\alpha,\bar{\alpha}}(z,\bar{z}) \equiv \left(\frac{z\bar{z}}{\bar{z}-z}\right)\left(\frac{G_\alpha(z)G_{\bar{\alpha}}(\bar{z}) - G_\alpha(\bar{z})G_{\bar{\alpha}}(z)}{\bar{\alpha}-\alpha}\right) \tag{1.5.16}$$

Six Dimensions

In $d = 6$ (with $\mathbf{a}$ and $\mathbf{b}$ set equal to zero to ease notation), the block is

$$\begin{aligned} G_{\alpha,\bar{\alpha}}(z,\bar{z}) \equiv \Bigg(\Bigg(&-\frac{G_\alpha(z)}{\bar{\alpha}-\alpha}\left(\frac{z\bar{z}}{\bar{z}-z}\right)^3\left(\frac{6G_{\bar{\alpha}-1}(\bar{z})}{\bar{\alpha}-\alpha-1} + \frac{3(\bar{\alpha}+\alpha-1)(2\bar{\alpha}+1)^2 G_{\bar{\alpha}+1}(\bar{z})}{32\bar{\alpha}(\bar{\alpha}+1)((\bar{\alpha}+1)^2-\alpha^2)}\right) \\ &+ (z \leftrightarrow \bar{z})\Bigg) + (\alpha \leftrightarrow \bar{\alpha})\Bigg) \end{aligned} \tag{1.5.17}$$

Three Dimensions

Currently, a closed-form expression for the $d = 3$ block has only been derived on the diagonal ($z = \bar{z}$) [33]. It is equal to

$$G_{\alpha,\bar{\alpha}}(z,z) \equiv \tag{1.5.18}$$
$$\frac{z}{\sqrt{1-z}}\left(\frac{4z}{(1+\sqrt{1-z})^2}\right)^{\bar{\alpha}+\alpha+\frac{1}{2}} {}_4F_3\left(\begin{matrix}\alpha+\frac{1}{2},\bar{\alpha}+\frac{1}{2},\bar{\alpha}+\alpha+\frac{1}{2},\frac{1}{2}\\ \alpha+1,\bar{\alpha}+1,\bar{\alpha}+\alpha+1\end{matrix};\frac{z^2}{(1+\sqrt{1-z})^4}\right)$$

1.6 Crossing Symmetry

In Eq. (1.3.3), we gave the correlation function of four scalars. This expression is fixed by conformal symmetry up to a function $\mathcal{G}(z,\bar{z})$ of the conformal cross-ratios defined in Eq. (1.3.2).

The value of a correlator is independent of how the constituent operators are fused using their operator product expansions. If instead we had chosen to fuse in a 't-channel manner' (effectively swapping the operators $\phi_1 \leftrightarrow \phi_3$), we would have got a slightly different expression which must be non-trivially equal to the first.

All in all, this means that the function $\mathcal{G}$ can be related to its t-channel analogue $\mathcal{G}'$ via a simple crossing symmetry equation. Namely,

$$\mathcal{G}(z,\bar{z}) = \frac{(z\bar{z})^{\frac{\Delta_1+\Delta_2}{2}}}{((1-z)(1-\bar{z}))^{\frac{\Delta_3+\Delta_2}{2}}}\mathcal{G}'(1-z,1-\bar{z}) \tag{1.6.1}$$

where the prime on $\mathcal{G}'$ indicates that it naturally admits a t-channel decomposition. Specifically,

$$\mathcal{G}'(z,\bar{z}) = \sum_{\mathcal{O}} \lambda_{32\mathcal{O}}\lambda_{14\mathcal{O}}\, G'_{\alpha,\bar{\alpha}}(z,\bar{z}) \tag{1.6.2}$$

with $G'_{\alpha,\bar{\alpha}}$ being a t-channel block, equal to $G_{\alpha,\bar{\alpha}}$ up to the redefinitions

$$\mathbf{a} \to \mathbf{a}' \equiv \frac{\Delta_{23}}{2} \qquad \mathbf{b} \to \mathbf{b}' \equiv -\frac{\Delta_{41}}{2} \tag{1.6.3}$$

Eq. (1.6.1) therefore relates a sum over s-channel blocks to a sum over t-channel blocks. This non-trivial equivalence is represented schematically in Fig. 1.2.

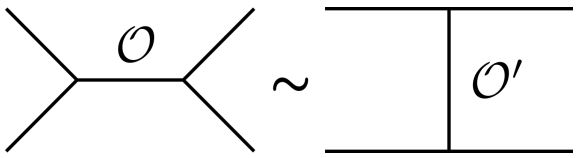

Figure 1.2: A common schematic for crossing symmetry, the left of the figure represents the sum over s-channel operators $\mathcal{O}$ following the fusion pattern $(\phi_1 \times \phi_2) \times (\phi_3 \times \phi_4)$. Likewise, the right of the figure represents the sum over t-channel operators $\mathcal{O}'$ following the fusion pattern $(\phi_4 \times \phi_1) \times (\phi_2 \times \phi_3)$. The bootstrap community uses this non-trivial equivalence to constrain the space of conformal field theories.

A lot of work has been done to constrain the space of conformal field theories by analysing crossing equations both numerically and analytically. Perhaps one of the most impressive results is a highly accurate determination of the 3d Ising spectrum [10].

Chapter 2

Alpha Space

In this chapter, we explain the philosophy behind alpha space before detailing the one-dimensional transform, which was first delineated in [1]. We then present several new results and applications of the formalism.

As discussed in Chapter 1, the correlation function of four primary scalar operators in a conformal field theory is

$$\langle \phi_1 \phi_2 \phi_3 \phi_4 \rangle = \frac{1}{x_{12}^{\Delta_1+\Delta_2} x_{34}^{\Delta_3+\Delta_4}} \left(\frac{x_{24}}{x_{14}}\right)^{\Delta_{12}} \left(\frac{x_{14}}{x_{13}}\right)^{\Delta_{34}} \mathcal{G}(z,\bar{z}) \tag{2.0.1}$$

where the operator ϕ_i has scaling dimension Δ_i and is located at position x_i. The cross-ratios are defined in Eq. (1.3.2) and, as before, $\Delta_{ij} \equiv \Delta_i - \Delta_j$ and $x_{ij} \equiv x_i - x_j$.

The function $\mathcal{G}(z,\bar{z})$ is known as the stripped correlator. It admits a decomposition into universal s-channel conformal blocks, weighted by theory-dependent operator product expansion (OPE) coefficients. That is,

$$\mathcal{G}(z,\bar{z}) = \sum_{\mathcal{O}} \lambda_{12\mathcal{O}} \lambda_{34\mathcal{O}} \, G_{\alpha,\bar{\alpha}}(z,\bar{z}) \tag{2.0.2}$$

Each block encodes the contribution of a primary operator $\mathcal{O}$ and its descendants. The scaling dimension and spin of $\mathcal{O}$ are related to α and $\bar{\alpha}$ through Eq. (1.4.8).

A natural question is then, what is the conformal block decomposition for a function $\mathcal{G}(z,\bar{z})$? This is what the alpha space approach sets out to answer. This is not new a

question; the harmonic analysis of the conformal group has been studied both in the 1970s [14] and more recently [15]. Furthermore, progress has been made both on a Lorentzian inversion formula and in Mellin space, with the latter seeming to offer a natural language for AdS/CFT correlators. We comment on these in Sections 3.1.2 and 3.6.

All of this detail is really necessary because the blocks themselves to do not form a complete orthogonal basis. Therefore, we cannot integrate a block against $\mathcal{G}(z,\bar{z})$ to 'pick out' its contribution.

The alpha space approach differs slightly from previous attempts as it looks to apply Sturm-Liouville theory directly to the quadratic Casimir differential operator in Eq. (1.5.7). This delivers an orthogonal basis of eigenfunctions and an invertible integral transform.

Illustratively, the alpha space algorithm is as follows. Start with a function $f(z,\bar{z})$ (it need not be a stripped correlator in general). Then, use the alpha space integral transform $f(z,\bar{z}) \mapsto \hat{f}(\alpha,\bar{\alpha})$ to get the density. Next, read off the conformal data from $\hat{f}(\alpha,\bar{\alpha})$. The pole locations end up giving the dimensions and spins of the intermediate operators and the residues give the weightings (OPE coefficients).

Another motivation for working in alpha space is that it allows for Eq. (1.6.1) to be written as an integral equation. The consequences of crossing symmetry can then be investigated by studying the analytic properties of the kernel. This is done in Section 2.6.1.

In this work, we focus on the Lorentzian square $z,\bar{z} \in (0,1)$. This is done so that the Casimir operator is elliptic and so that both the s- and t-channel decompositions converge.

After introducing the $d = 1$ case in Section 2.1, we explain how large imaginary α corresponds to the $z \to 1$ limit in Section 2.2 before discussing how Casimir singular and regular terms have different alpha space signatures in Section 2.3.

Since polylogarithms are simply expressed in alpha space, we make a comment in Section 2.4 on Witten diagram calculations, where such functions are abundant.

We then move on to $d = 2$ alpha space in Section 2.5. This turns out to be no more difficult than the $d = 1$ case because of the simplicity of the quadratic Casimir differential equation.

To conclude the chapter, we return to the crossing equation in Section 2.6. There we introduce an integral equivalent of the crossing equation in Eq. (1.6.1), delve into the analytic properties of the kernel and compute anomalous dimensions.

In Sections 2.1, 2.5 and 2.6, we allow for non-equal external scalars. For the rest of the chapter, we implicitly work with $\mathbf{a} = \mathbf{b} = 0$ and take the external operators to have scaling dimension Δ_ϕ.

2.1 Alpha Space in One Dimension

In this section, we present the Sturm-Liouville analysis of the $d = 1$ quadratic Casimir. This is a more tractable problem than the higher dimensional case because there is only one cross-ratio and the differential equation can be easily put into standard Sturm-Liouville form.

The integral transform itself is fleshed out in Section 2.1.2, some simple examples are given in Section 2.1.3 and the interesting case of logarithms is discussed in Section 2.1.4.

Working with $d = 1$ theories may seem restrictive but they in fact display much of the salient features of higher dimensions. For example, they appear naturally as line defects and in the light-cone limit of $d > 1$ theories [34, 35].

2.1.1 Sturm-Liouville

A second-order ordinary differential operator which is linear and Hermitian on some interval is known as a Sturm-Liouville operator. The associated eigen-equation,

along with a set of boundary conditions to guarantee a Hermitian inner product, is called a Sturm-Liouville equation. Hypergeometric, Bessel, Legendre and simple harmonic equations are common examples.

All of these properties ensure that the eigenvalues are real and the eigenfunctions can form an orthogonal basis on the interval. An integral transform can then naturally be defined by using the orthogonality of the eigenbasis.

2.1.2 Defining the Transform

In one dimension, there is only a single cross-ratio and the blocks are given by Eq. (1.5.4). They satisfy Eq. (1.5.1) and so a general eigenfunction of the quadratic Casimir operator D_z can be written as a linear combination of $G_\alpha(z)$ and $G_{-\alpha}(z)$.

The Sturm-Liouville analysis of D_z on $z \in (0,1)$ begins by defining an appropriate measure μ and a bracket for which the operator is self-adjoint. This is done by first defining the bracket

$$\langle f, g\rangle \equiv \int_0^1 dz\, \mu(z) f^*(z) g(z) \tag{2.1.1}$$

for two functions f, g taking $(0,1) \to \mathbb{C}$ and then by requiring that

$$\int_0^1 dz\, \mu(z)\Big(f^*(z) D_z g(z) - g(z) D_z f^*(z)\Big) \tag{2.1.2}$$

is zero up to boundary terms. This fixes the measure to be

$$\mu(z) \equiv \frac{(1-z)^{\mathbf{a}+\mathbf{b}}}{z^2} \tag{2.1.3}$$

so that Eq. (2.1.2) becomes

$$\int_0^1 dz \frac{d}{dz}\left((1-z)^{1+\mathbf{a}+\mathbf{b}}\left(f^*(z)\frac{dg(z)}{dz} - g(z)\frac{df^*(z)}{dz}\right)\right) \tag{2.1.4}$$

which is a boundary term.

The measure in Eq. (2.1.3) tells us that if a function f has power-law behaviour around $z = 0$, a necessary condition for $\langle f, f\rangle$ to be finite is that the exponent must be greater than $\frac{1}{2}$. Unfortunately, this means that a stripped correlator containing

an identity operator contribution will always have a divergent norm with respect to the bracket. This is because the leading term will be

$$\mathcal{G}(z) \xrightarrow{z\to 0} 1 \qquad \text{if there is an intermediate identity operator.} \tag{2.1.5}$$

Here we have assumed that each of the other intermediate operators has a positive scaling dimension, as is the case in a unitary theory. However, we show in Section 2.1.3 that such problems can be rigorously circumnavigated through contour deformations.

The blocks themselves are divergent at $z = 1$. That a single block has power-law behaviour as $z \to 0$ but is logarithmically (for $\mathbf{a} = \mathbf{b} = 0$) divergent in the limit $z \to 1$ is physically linked to the fact that a t-channel operator can only be reproduced by an infinite sum of s-channel operators. By way of illustration, the block behaves asymptotically like

$$G_\alpha(z)|_{\mathbf{a}=\mathbf{b}=0} \xrightarrow{z\to 1} -\frac{\Gamma(1+2\alpha)}{\Gamma^2(\frac{1}{2}+\alpha)}\log(1-z) \tag{2.1.6}$$

The next step in the Sturm-Liouville procedure is to find the linear combinations of G_α and $G_{-\alpha}$ that are orthogonal with respect to the bracket. Defining $Q(\alpha)$ as

$$Q(\alpha) \equiv \frac{2\Gamma(-2\alpha)\Gamma(1+\mathbf{a}+\mathbf{b})}{\Gamma(\frac{1}{2}+\mathbf{a}-\alpha)\Gamma(\frac{1}{2}+\mathbf{b}-\alpha)} \tag{2.1.7}$$

we have that

$$\begin{aligned}\Psi_\alpha(z) &\equiv \frac{1}{2}\Big(Q(\alpha)G_\alpha(z) + Q(-\alpha)G_{-\alpha}(z)\Big) \\ &= z^{-\mathbf{a}}\,{}_2F_1\left(\frac{1}{2}+\mathbf{a}+\alpha, \frac{1}{2}+\mathbf{a}-\alpha; 1+\mathbf{a}+\mathbf{b}; -\frac{1-z}{z}\right)\end{aligned} \tag{2.1.8}$$

is finite in the $z \to 1$ limit. In fact, we have normalised the function to $\Psi_\alpha(1) = 1$. The second line of Eq. (2.1.8) is derived by combining the two terms in the first line using a hypergeometric identity. Interestingly, $\Psi_\alpha(z)$ is not the standard conformal partial wave that appears in the Euclidean inversion formula [14].

Often in this work, we employ a Mellin-Barnes integral representation for the function

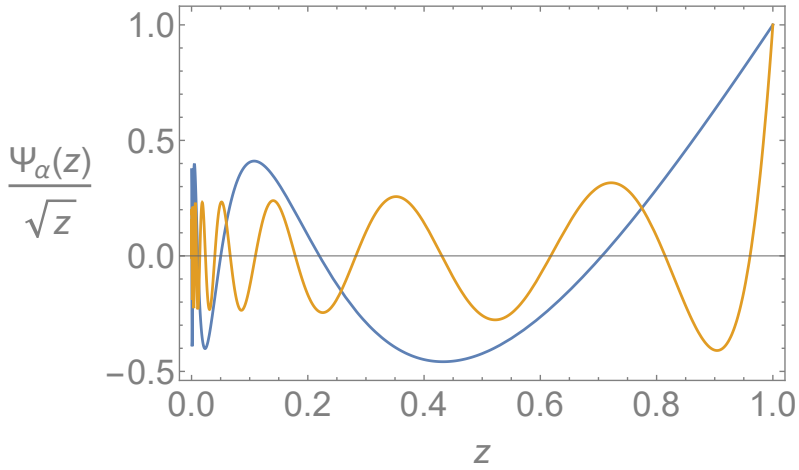

Figure 2.1: $\Psi_\alpha(z)/\sqrt{z}$ is plotted against z for imaginary $\alpha = 2i$ (blue) and $\alpha = 6i$ (orange) with $\mathbf{a} = \mathbf{b} = 0$. Note that both functions equal 1 at $z = 1$ despite being sums of two divergent blocks. Inspiration for this plot came from an almost identical figure in [1].

$\Psi_\alpha(z)$. After defining $\Gamma(x \pm y) \equiv \Gamma(x+y)\Gamma(x-y)$, the two most common are

$$\begin{aligned}\Psi_\alpha(z) &= \frac{z^{-\mathbf{a}}\,\Gamma(1+\mathbf{a}+\mathbf{b})}{\Gamma(\frac{1}{2}+\mathbf{a}\pm\alpha)}\int [ds]\,\frac{\Gamma(-s)\Gamma(\frac{1}{2}+\mathbf{a}+s\pm\alpha)}{\Gamma(1+\mathbf{a}+\mathbf{b}+s)}\left(\frac{1-z}{z}\right)^s \\ &= \frac{z^{-\mathbf{a}}\,\Gamma(1+\mathbf{a}+\mathbf{b})}{\Gamma(\frac{1}{2}+\mathbf{a}\pm\alpha)\Gamma(\frac{1}{2}+\mathbf{b}\pm\alpha)}\int [ds]\,\Gamma(-s)\Gamma(\mathbf{b}-\mathbf{a}-s)\Gamma\Big(\frac{1}{2}+\mathbf{a}+s\pm\alpha\Big)\Big(\frac{1}{z}\Big)^s\end{aligned} \tag{2.1.9}$$

where we have introduced the shorthand expression

$$\int [d\beta] \equiv \int_{-i\infty}^{i\infty} \frac{d\beta}{2\pi i} \tag{2.1.10}$$

for which the integration contour is deformed off of the imaginary axis to separate left- and right-running, semi-infinite sequences of poles, if necessary.

Up to some simple redefinitions, $\Psi_\alpha(z)$ is the main ingredient in the Jacobi transform [36] which maps between Jacobi and Wilson polynomials. Consequently, $\Psi_\alpha(z)$ with $\alpha \in i\mathbb{R}$ forms an orthogonal basis. Explicitly, this statement means that for some function $\hat{f}$ defined along the imaginary axis, it is true that

$$\int [d\beta]\,\langle \Psi_\alpha, \Psi_\beta\rangle \hat{f}(\beta) = \frac{Q(\alpha)Q(-\alpha)}{2}\left(\frac{\hat{f}(\alpha)+\hat{f}(-\alpha)}{2}\right) \tag{2.1.11}$$

which essentially means that $\langle \Psi_\alpha, \Psi_\beta\rangle$ acts like a delta function along the imaginary α-axis.

Duly, one-dimensional alpha space can be defined through the transform

$$\boxed{\hat{f}(\alpha) = \int_0^1 dz\, \mu(z)\Psi_\alpha(z) f(z)} \tag{2.1.12}$$

and an alpha space density can be taken back to position space using the inverse transform

$$\boxed{f(z) = \int [d\alpha]\, \frac{2\Psi_\alpha(z)\hat{f}(\alpha)}{Q(\alpha)Q(-\alpha)}} \tag{2.1.13}$$

Formally, this is a map between the Hilbert spaces

$$L^2\Big((0,1), \mu(z)dz\Big) \to L^2\Big((-i\infty, i\infty), \frac{d\alpha}{i\pi\, Q(\alpha)Q(-\alpha)}\Big) \tag{2.1.14}$$

and the associated Parseval's formula is $\langle f, g\rangle = \left[\hat{f}, \hat{g}\right]$ where

$$\left[\hat{f}, \hat{g}\right] \equiv \int [d\alpha]\, \frac{2\hat{f}^*(\alpha)\hat{g}(\alpha)}{Q(\alpha)Q(-\alpha)} \tag{2.1.15}$$

Fig. 2.1 plots $\Psi_\alpha(z)/\sqrt{z}$ for two different imaginary α values. In hindsight, it is natural for the inverse alpha space transform to be defined along the imaginary axis. For real alpha, the power-law behaviour of $\Psi_\alpha(z)$ near the origin has exponent $\frac{1}{2} - |\alpha|$ and so it is not formally normalisable. Conversely, the oscillatory behaviour for imaginary α gives us some faith in Eq. (2.1.11).

2.1.3 Some Examples

Here we present the alpha space densities for some simple functions. This is done to seed some intuition for the following sections.

Densities are straightforwardly related to conformal block decompositions. The symmetry $\alpha \leftrightarrow -\alpha$ allows for $\Psi_\alpha(z)$ in Eq. (2.1.13) to be replaced with $Q(\alpha)G_\alpha(z)$ to give the split inverse transform

$$f(z) = \int [d\alpha]\, \frac{2G_\alpha(z)\hat{f}(\alpha)}{Q(-\alpha)} \tag{2.1.16}$$

Under the assumption that $\hat{f}(\alpha)$ decays sufficiently fast at infinity, the contour can then be closed in the right half-plane. If $\hat{f}(\alpha)$ is a meromorphic function then closing

the contour picks up poles to give a sum over conformal blocks. The semi-infinite series of poles from the $1/Q(-\alpha)$ factor is left-running and so the contour only picks up poles from $\hat{f}(\alpha)$.

Blocks

As the first example, consider a (symmetrised) pole in alpha space, located at $\alpha = \pm\beta$ with residue $-Q(-\beta)/2$. This maps to $G_\beta(z)$ because the split inverse transform is

$$-\int [d\alpha]\, \frac{Q(-\beta)G_\alpha(z)}{Q(-\alpha)} \left(\frac{1}{\alpha-\beta} - \frac{1}{\alpha+\beta}\right) \tag{2.1.17}$$

and the contour can be closed to the right to give a single block. That is,

$$G_\beta(z) \mapsto -\frac{Q(-\beta)}{2} \left(\frac{1}{\alpha-\beta} - \frac{1}{\alpha+\beta}\right) \tag{2.1.18}$$

where we have used the notation $f(z) \mapsto \hat{f}(\alpha)$ for a map from position to alpha space.

All-in-all, simple poles in $d = 1$ alpha space are conformal blocks in position space, and the residues are simply related to the OPE coefficients.

$$\begin{aligned} \text{A pole at } \beta &\implies \Delta = \beta + \frac{1}{2} \\ \text{Residue equal to } R &\implies \lambda_{12\mathcal{O}}\lambda_{34\mathcal{O}} = -\frac{2R}{Q(-\beta)} \end{aligned}$$

In deriving Eq. (2.1.18), we have assumed that $\beta > 0$ so that closing the contour picks up the pole at $\alpha = \beta$ but not the one at $\alpha = -\beta$. However, the range of scaling dimensions $0 < \Delta < \frac{1}{2}$ corresponds to $-\frac{1}{2} < \beta < 0$. Therefore to encode an operator in this range, the contour must be deformed to an 's-bend' to separate the two poles correctly. This is illustrated in Fig. 2.2.

It is this deformation prescription that solves the normalisation problem raised in Section 2.1.2. There we saw that $\langle f, f\rangle$ diverges if $f(z)$ behaves like z^p near $z = 0$ as p is dialled below $\frac{1}{2}$. Now we understand this as two poles crossing the imaginary axis in alpha space and the remedy is to deform the inverting contour off of the

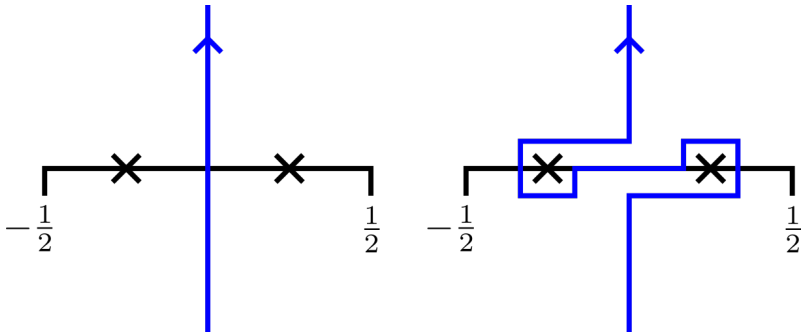

Figure 2.2: This figures illustrates the importance of the contour prescription for the inverse alpha space transform. Each plot shows the contour for an inverse alpha space transform of the form Eq. (2.1.13) and the crosses represent simple poles. The density is assumed to be the same for both plots but the left integral produces an operator with scaling dimension $\frac{1}{2} < \Delta < 1$ whereas $0 < \Delta < \frac{1}{2}$ on the right. The take-home lesson is that we need both the density *and* the contour to go back to position space.

imaginary axis to separate the 'right-hand' pole on the left of the axis from the 'left-hand' one on the right.

There are two limit cases that deserve a mention. We present these for $\mathbf{a} = \mathbf{b} = 0$ but the generalisation is straightforward. Firstly, $1/Q(-\alpha)$ itself has a pole at $\alpha = -\frac{1}{2}$ and so a density only needs to be finite at this point for an identity contribution, with the 's-bend' contour prescription now going around $\alpha = \pm\frac{1}{2}$. Secondly, $1/Q(-\alpha)$ has a zero at $\alpha = 0$ and so a density requires a double pole here for an operator of dimension $\frac{1}{2}$, with the contour deformed slightly to the left of the origin.

Powers

Simple powers are mapped to gamma functions in alpha space. This is shown by using the first Mellin-Barnes representation in Eq. (2.1.9) to get

$$\int_0^1 dz\, \mu(z) z^p \Psi_\alpha(z) = \frac{\Gamma(1+\mathbf{a}+\mathbf{b})}{\Gamma(p+\mathbf{b})\Gamma(\frac{1}{2}+\mathbf{a}\pm\alpha)} \int [ds]\, \Gamma(-s)\Gamma(p-1-\mathbf{a}-s)\Gamma\Big(\frac{1}{2}+\mathbf{a}+s\pm\alpha\Big) \tag{2.1.19}$$

where we have integrated away z. This integral can be computed by using Barnes' first lemma, which is

$$\int [ds]\,\Gamma(a+s)\Gamma(b+s)\Gamma(c-s)\Gamma(d-s) = \frac{\Gamma(a+c)\Gamma(a+d)\Gamma(b+c)\Gamma(b+d)}{\Gamma(a+b+c+d)} \quad (2.1.20)$$

The resultant map from position to alpha space is

$$z^p \mapsto \frac{\Gamma(1+\mathbf{a}+\mathbf{b})\Gamma(p-\frac{1}{2}\pm\alpha)}{\Gamma(p+\mathbf{a})\Gamma(p+\mathbf{b})} \quad (2.1.21)$$

which basically says that z^p is a sum over blocks with integer-spaced scaling dimensions, starting at p. The OPE coefficients can be read off from Eq. (2.1.21) using Eq. (2.1.18) and the fact that the residues of the gamma function are

$$\mathrm{Res}\,(\Gamma(\alpha))|_{\alpha=-n} = \frac{(-1)^n}{n!} \quad (2.1.22)$$

for any natural number $n \in \mathbb{N} \equiv \mathbb{Z}^{\geq 0}$.

A similar calculation yields the result

$$\left(\frac{z}{1-z}\right)^p \mapsto \frac{\Gamma(1-p)\Gamma(p-\frac{1}{2}\pm\alpha)}{\Gamma(p)\Gamma(\frac{1}{2}\pm\alpha)} \qquad (\mathbf{a}=\mathbf{b}=0) \quad (2.1.23)$$

which we use in Sections 2.2 and 2.3.

Jacobi and Wilson Polynomials

More generally, the $d=1$ alpha space transform maps Jacobi to Wilson polynomials according to

$$z^p P_n^{(x,\,\mathbf{a}+\mathbf{b})}(1-2z) \mapsto \quad (2.1.24)$$
$$\frac{\Gamma(1+\mathbf{a}+\mathbf{b})\Gamma(p-\frac{1}{2}\pm\alpha)}{n!\,\Gamma(p+\mathbf{a}+n)\Gamma(p+\mathbf{b}+n)}\mathfrak{p}_n\Big(\alpha; p-\frac{1}{2}, \frac{3}{2}-p+x, \frac{1}{2}+\mathbf{a}, \frac{1}{2}+\mathbf{b}\Big)$$

The Jacobi polynomial is

$$P_n^{(x,y)}(z) \equiv \frac{(1+x)_n}{n!}\,{}_2F_1\left(-n, 1+x+y+n; 1+x; \frac{1-z}{2}\right) \quad (2.1.25)$$

and the Wilson polynomial is

$$\mathfrak{p}_n(\alpha; a, b, c, d) \equiv \tag{2.1.26}$$
$$(a+b)_n(a+c)_n(a+d)_n\, {}_4F_3\left(\begin{matrix}-n, a+\alpha, a-\alpha, n+a+b+c+d-1 \\ a+b, a+c, a+d\end{matrix}; 1\right)$$

where we have introduced the Pochhammer symbol,

$$(x)_n \equiv \frac{\Gamma(x+n)}{\Gamma(x)} \tag{2.1.27}$$

The simple z^p map in Eq. (2.1.21) can then be recovered by setting $n = 0$.

Eq. (2.1.24) is slightly more general then the analogous result of [1] in that it includes the free parameter x.

The Wilson polynomial and the more general Wilson function play a pivotal role in the split kernel introduced in Section 2.6.1.

2.1.4 Logarithms

Since simple poles in alpha space map to conformal blocks, it is sensible to also appraise higher-order poles. These singularities roughly correspond to derivatives of blocks. As an example, consider the integral

$$-\frac{Q(-\beta)}{2}\int [d\alpha]\,\frac{2\Psi_\alpha(z)}{Q(\alpha)Q(-\alpha)}\left(\frac{1}{(\alpha-\beta)^2}+\frac{1}{(\alpha+\beta)^2}\right) \tag{2.1.28}$$

Once again, the symmetry of the integrand allows for the substitution $\Psi_\alpha(z) \to Q(\alpha)G_\alpha(z)$. After this split, the contour can be closed to the right to pick up the double pole and give

$$Q(-\beta)\frac{\partial}{\partial\beta}\left(\frac{G_\beta(z)}{Q(-\beta)}\right) = \frac{\partial G_\beta(z)}{\partial\beta} + \tilde{\psi}(\beta)G_\beta(z) \tag{2.1.29}$$

where the function $\tilde{\psi}(\beta)$ is defined to be

$$\tilde{\psi}(\beta) \equiv -\frac{d\log Q(-\beta)}{d\beta} = \psi\left(\frac{1}{2}+\beta+\mathbf{a}\right)+\psi\left(\frac{1}{2}+\beta+\mathbf{b}\right)-2\psi(2\beta) \tag{2.1.30}$$

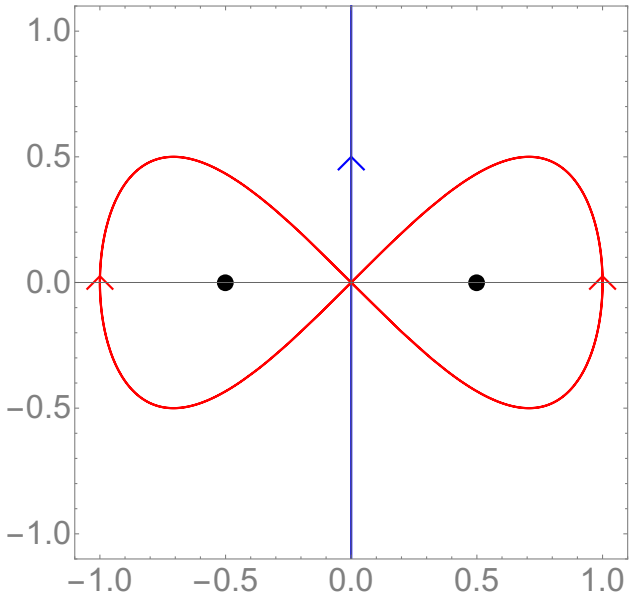

Figure 2.3: Plotted are the contours for the integral Eq. (2.1.33). The blue contour gives $\log(1-z)$ whereas the figure-of-eight red one gives $2(1-\log(z))$. The double poles at $\alpha = \pm 1/2$ are marked by black dots.

and $\psi(\beta)$ is the digamma function

$$\psi(\beta) \equiv \frac{d \log \Gamma(\beta)}{d\beta} \tag{2.1.31}$$

Putting this all together, the first derivative of a block maps to alpha space like

$$\frac{\partial G_\beta(z)}{\partial \beta} \mapsto -\frac{Q(-\beta)}{2(\alpha-\beta)}\left(\frac{1}{\alpha-\beta} - \tilde{\psi}(\beta)\right) + (\alpha \to -\alpha) \tag{2.1.32}$$

Such block derivatives produce $\log(z)$ terms and so the alpha space density for the logarithm deserves some attention. With $\mathbf{a} = 0$ and $\mathbf{b} = 0$, consider the integral

$$\int \frac{d\alpha}{2\pi i} \frac{2\Psi_\alpha(z)}{Q(\alpha)Q(-\alpha)(\alpha-\frac{1}{2})(\alpha+\frac{1}{2})} \tag{2.1.33}$$

over the two contours plotted in Fig. 2.3. The blue contour is the standard alpha space one. Therefore, Ψ_α can be replaced by $Q(\alpha)G_\alpha$ under the integral and the contour closed in the right half plane to give the single block

$$-\frac{2G_{\frac{1}{2}}(z)}{Q(-\frac{1}{2})} = -G_{\frac{1}{2}}(z) = \log(1-z) \tag{2.1.34}$$

However, two double poles are enclosed by the red contour because of the Q factors and so the integral is

$$-4\lim_{\alpha\to-1/2}\frac{\partial}{\partial\alpha}\left(\frac{\Psi_\alpha(z)(\alpha+\frac{1}{2})}{Q(\alpha)Q(-\alpha)(\alpha-\frac{1}{2})}\right)=2(1-\log(z)) \tag{2.1.35}$$

We note that in terms of the derivative of a block, the logarithm is

$$\log z=\left.\frac{\partial G_\alpha(z)}{\partial\alpha}\right|_{\alpha=-1/2} \tag{2.1.36}$$

The red contour may appear to be peculiar, but it arises naturally via the following argument.

The derivative of z^p with respect to p is $z^p\log(z)$ and so a regularised alpha space density for the logarithm can be defined through

$$z^p\log(z)\mapsto\frac{\partial}{\partial p}\left(\frac{\Gamma(p-\frac{1}{2}\pm\alpha)}{\Gamma^2(p)}\right) \tag{2.1.37}$$

where we have used the density for z^p in Eq. (2.1.21). We can get higher powers of the logarithm by taking further p derivatives. The standard alpha space contour for this density is pinched at $\alpha=\pm\frac{1}{2}$ as $p\to0$ and so it makes sense to pull the contour through $\alpha=\pm(\frac{1}{2}-p)$ with p small, picking up the residues at these points and leaving an integral along the imaginary axis. The contribution of this integral vanishes as $p\to0$ because the integrand vanishes, and so it can be dropped. The contribution of the residues as $p\to0$ amounts to

$$\left.\frac{\partial\Psi_\alpha(z)}{\partial\alpha}\right|_{\alpha=-1/2}=\log(z) \tag{2.1.38}$$

and we see that everything is consistent. The two small contours around $\alpha=\pm(\frac{1}{2}-p)$ giving rise to these residues can be joined up nicely to give a figure-of-eight path analogous to the red contour in Fig. 2.3.

Similar alpha space densities can be defined by substituting Eq. (2.1.21) into various Taylor series expansions. Two interesting examples are

$$\log(z)\log(1-z)\mapsto\frac{1}{(\frac{1}{2}+\alpha)(\frac{1}{2}-\alpha)}\left(2\,\Gamma\Big(\frac{1}{2}\pm\alpha\Big)-\frac{1}{(\frac{1}{2}+\alpha)(\frac{1}{2}-\alpha)}\right) \tag{2.1.39}$$

and the polylogarithm

$$\mathrm{Li}_s(z) \mapsto \sum_{p=1}^{\infty} \frac{\Gamma(p - \frac{1}{2} \pm \alpha)}{p^s \Gamma^2(p)} = \Gamma\left(\frac{1}{2} \pm \alpha\right) {}_{s+1}F_s \left(\begin{matrix} \frac{1}{2} + \alpha, \frac{1}{2} - \alpha, 1, ..., 1 \\ 2, ..., 2 \end{matrix} ; 1 \right) \tag{2.1.40}$$

for $s \in \mathbb{Z}^{\geq 1}$.

Now that we understand the logarithm, we can also think about constant alpha space densities. In Fourier space, the inverse transform of a constant gives a delta function and we expect something similar to happen in alpha space. In fact, since

$$\log(1 - z) \mapsto \frac{1}{\alpha^2 - \frac{1}{4}} \tag{2.1.41}$$

we can use Parseval's formula from Eq. (2.1.15) to say that

$$\begin{aligned} \langle D_z \log(1 - z), f(z) \rangle &= \int_0^1 \frac{dz}{z^2} f(z) D_z \log(1 - z) \\ &= \int [d\alpha] \, \frac{2\hat{f}(\alpha)}{Q(\alpha)Q(-\alpha)} \left(\frac{\alpha^2 - \frac{1}{4}}{\alpha^2 - \frac{1}{4}} \right) \\ &= \int [d\alpha] \, \frac{2\Psi_\alpha(1)\hat{f}(\alpha)}{Q(\alpha)Q(-\alpha)} \\ &= f(1) \end{aligned} \tag{2.1.42}$$

where we have used the fact that

$$D_z f(z) \mapsto \left(\alpha^2 - \frac{1}{4}\right) \hat{f}(\alpha) \tag{2.1.43}$$

which follows from Eq. (2.1.13) along with the observation that $\Psi_\alpha(z)$ is an eigenfunction of D_z. Therefore, an alpha space density of 1 corresponds to the position space function $D_z \log(1 - z)$, which is equivalent to $\delta(1 - z)$ in the context of the integral above.

2.2 Large Alpha Limit

Analogously to how large momenta probe short distances through the Fourier transform, the large imaginary α limit in alpha space corresponds to taking the cross-ratio

z close to 1. This can be seen by applying the quadratic Casimir n times to an inverse alpha space integral. Since Ψ_α is an eigenfunction, we get

$$D_z^n f(z) = \int [d\alpha] \frac{2\hat{f}(\alpha)}{Q(\alpha)Q(-\alpha)} \left(\alpha^2 - \frac{1}{4}\right)^n \Psi_\alpha(z) \tag{2.2.1}$$

Now because $\Psi_\alpha(1) = 1$, if $f(1)$ is well-defined but $D_z f(z)|_{z=1}$ is not then

$$\int [d\alpha] \frac{2\hat{f}(\alpha)}{Q(\alpha)Q(-\alpha)} \qquad \text{converges but} \tag{2.2.2}$$

$$\int [d\alpha] \frac{2\hat{f}(\alpha)}{Q(\alpha)Q(-\alpha)} \left(\alpha^2 - \frac{1}{4}\right) \qquad \text{does not converge.} \tag{2.2.3}$$

All we have done is modify the integrand by a polynomial factor and so we conclude that the large imaginary α behaviour of $\hat{f}(\alpha)$ reflects the $z \to 1$ limit of $f(z)$.

As an explicit example, consider the function

$$f(z) = 4\arccos(\sqrt{z}) - 2\pi = 4\sqrt{1-z} - 2\pi + O((1-z)^{3/2}) \tag{2.2.4}$$

After applying the Casimir, this function becomes

$$D_z f(z) = \sqrt{\frac{z}{1-z}} \tag{2.2.5}$$

Crucially, $D_z f(z)$ is undefined at $z = 1$ in this instance. From Eqs. (2.1.23) and (2.2.1), the corresponding alpha space densities are

$$\sqrt{\frac{z}{1-z}} \mapsto \pi\, Q(\alpha)Q(-\alpha) = \frac{1}{\sqrt{-\alpha^2}} + ... \tag{2.2.6}$$

$$4\arccos(\sqrt{z}) - 2\pi \mapsto \pi\, Q(\alpha)Q(-\alpha) \left(\frac{1}{\alpha^2 - \frac{1}{4}}\right) = \frac{1}{\alpha^2\sqrt{-\alpha^2}} + ...$$

where the ellipses here represent subordinate terms in the large imaginary α limit. Indeed, the inverse alpha space integral clearly converges for the $f(z)$ density but not for the $D_z f(z)$ density, mirroring the worsening $z \to 1$ behaviour.

More generally, if a function behaves like

$$f(z) = (1-z)^{-p}(1 + O(1-z)) \tag{2.2.7}$$

then

$$\hat{f}(\alpha) = (-\alpha^2)^{p-1}\frac{\Gamma(1-p)}{\Gamma(p)}(1+O(\alpha^{-2})) \tag{2.2.8}$$

as can be seen from the large α limit of Eq. (2.1.23).

To conclude this section, if $D_z^n f(z)|_{z=1}$ remains well-defined for arbitrarily large n then Eq. (2.2.1) tells us that $\hat{f}(\alpha)$ must fall off faster than any power for large imaginary α. This is exemplified by the density for z^p in Eq. (2.1.21), which falls off exponentially like

$$z^p \mapsto \frac{\Gamma(p-\frac{1}{2}\pm\alpha)}{\Gamma^2(p)} = \frac{2\pi e^{-\pi\sqrt{-\alpha^2}}(-\alpha^2)^{p-1}}{\Gamma^2(p)}(1+O(\alpha^{-2})) \tag{2.2.9}$$

2.3 Casimir Regular Terms

A Casimir singular term is defined as a function that becomes arbitrarily divergent in the $z \to 1$ limit after repeated applications of the Casimir D_z. Terms that do not suffer this fate are known as Casimir regular. By way of example, $\sqrt{\frac{1-z}{z}}$ and $\frac{z}{1-z}$ are Casimir singular whereas $z^p, G_\alpha(z), \frac{1-z}{z}$ and $(1-z)^2\log(1-z)$ are all regular.

In alpha space language, if a density behaves asymptotically like

$$\hat{f}(\alpha) = (-\alpha^2)^p(1+O(\alpha^{-2})) \quad p \notin \mathbb{Z} \tag{2.3.1}$$

then the corresponding function $f(z)$ is Casimir singular.

This distinction is useful because the addition of any regular term will not alter the asymptotic Casimir singular part of the density, which itself can be unambiguously related to the associated asymptotic $z \to 1$ behaviour through equations such as Eq. (2.2.8).

As an example of a density corresponding to a Casimir regular function, we note that

$$1+\left(\frac{1-z}{z}\right)\log(1-z) \mapsto \frac{1}{2}\left(\frac{1}{(\alpha-\frac{3}{2})(\alpha+\frac{3}{2})} - \frac{1}{(\alpha+\frac{1}{2})(\alpha-\frac{1}{2})}\right) = \alpha^{-4}+O(\alpha^{-6}) \tag{2.3.2}$$

It is worth bearing in mind that not all Casimir singular functions behave like Eq. (2.3.1) in alpha space. Take for example $z/(1-z)$. Expanding Eq. (2.1.23) around $p = 1$ and dropping the divergent term gives us the density

$$\frac{z}{1-z} \mapsto -\left(H_{-\frac{1}{2}+\alpha} + H_{-\frac{1}{2}-\alpha}\right) \tag{2.3.3}$$

where H_n is the n^{th} Harmonic number.

Asymptotically away from the real axis, this density behaves like

$$-\left(H_{-\frac{1}{2}+\alpha} + H_{-\frac{1}{2}-\alpha}\right) = -2\left(\gamma_E + \log(\sqrt{-\alpha^2})\right) + O(\alpha^{-2}) \tag{2.3.4}$$

where γ_E is the Euler–Mascheroni constant. This logarithmic behaviour does not fit into the pattern of Eq. (2.3.1) but it still cannot be reproduced by Casimir regular terms.

Why we were allowed to simply drop the divergent term to find this density is not immediately obvious and so it needs to be retrospectively justified. This can be done by numerically checking that the integral

$$-\int [d\alpha] \left(\frac{2\Psi_\alpha(z)}{Q(\alpha)Q(-\alpha)}\right) \frac{H_{-\frac{1}{2}+\alpha} + H_{-\frac{1}{2}-\alpha}}{(\alpha^2 - \frac{1}{4})^2} \tag{2.3.5}$$

is equal to

$$\begin{aligned} &3\left(\mathrm{Li}_3(z) + \mathrm{Li}_3(1-z)\right) - 2\left(\log(z)\mathrm{Li}_2(z) + \log(1-z)\mathrm{Li}_2(1-z)\right) \\ &-\frac{1}{2}\log(z)\log(1-z)\left(\log(z) + \log(1-z)\right) - 3\zeta(3) \end{aligned} \tag{2.3.6}$$

which reduces to $z/(1-z)$ after two applications of D_z. In this expression, we have introduced the Riemann zeta function $\zeta(s) \equiv \sum_{n=1}^{\infty} n^{-s}$. Another justification is that the divergent term is a constant in alpha space, and so it simply maps to a delta function in position space.

The author of [37] procured a formula relating a Casimir singular term to a sum over conformal blocks, up to a sum over regular terms. In the remainder of this section, we re-derive their expression using the alpha space formalism.

A sum over derivatives of some function f can be represented like

$$\sum_{k=0}^{\infty} \frac{df(k)}{dk} = -\int \frac{ds}{2\pi i} \left(\frac{\pi}{\sin(\pi s)}\right)^2 f(-s) \tag{2.3.7}$$

for a suitable contour. As such, the sum

$$\left(\frac{1-z}{z}\right)^p + \frac{\Gamma(\beta-\frac{1}{2}-p)}{\Gamma^2(-p)\Gamma(\beta+\frac{1}{2}+p)} \sum_{k=0}^{\infty} \frac{\partial}{\partial k} \left(\frac{\Gamma(\beta+\frac{1}{2}+k)}{(k!)^2(k-p)\Gamma(\beta-\frac{1}{2}-k)} \left(\frac{1-z}{z}\right)^k\right) \tag{2.3.8}$$

which is a Casimir singular term plus an infinite sum over regular terms, is equal to

$$\left(\frac{1-z}{z}\right)^p + \frac{\Gamma(\beta-\frac{1}{2}-p)}{\Gamma^2(-p)\Gamma(\beta+\frac{1}{2}+p)} \int \frac{ds}{2\pi i} \frac{\Gamma^2(s)\Gamma(\beta+\frac{1}{2}-s)}{(s+p)\Gamma(\beta-\frac{1}{2}+s)} \left(\frac{1-z}{z}\right)^{-s} \tag{2.3.9}$$

where the contour encircles the (double) poles at $s = -\mathbb{N}$ in a counter-clockwise manner.

Pulling this contour up to lie along the imaginary axis picks up the pole at $s = -p$, which contributes

$$-\left(\frac{1-z}{z}\right)^p \tag{2.3.10}$$

to cancel against the $\left(\frac{1-z}{z}\right)^p$ term already present.

The remaining integral can then be taken to alpha space by transforming the z-dependent factor under the integral according to

$$\left(\frac{1-z}{z}\right)^{-s} \mapsto \frac{\Gamma(1-s)\Gamma(s-\frac{1}{2}\pm\alpha)}{\Gamma(s)\Gamma(\frac{1}{2}\pm\alpha)} \tag{2.3.11}$$

to give

$$\frac{\Gamma(\beta-\frac{1}{2}-p)}{\Gamma^2(-p)\Gamma(\beta+\frac{1}{2}+p)\Gamma(\frac{1}{2}\pm\alpha)} \int [ds] \frac{\Gamma(s)\Gamma(1-s)\Gamma(\beta+\frac{1}{2}-s)\Gamma(s-\frac{1}{2}\pm\alpha)}{(s+p)\Gamma(\beta-\frac{1}{2}+s)} \tag{2.3.12}$$

This integral produces poles in the α plane because the s contour separating left- and right-running semi-infinite sequences of poles is pinched whenever $\alpha = \pm(\beta+\mathbb{N})$. As usual, these poles encode a block decomposition. The residues at the pinch-points prove that Eq. (2.3.8) is equal to

$$\frac{1}{\Gamma^2(-p)} \sum_{n=0}^{\infty} \frac{\Gamma^2(\beta+\frac{1}{2}+n)\Gamma(\beta-\frac{1}{2}-p+n)}{\Gamma(2(\beta+n))\Gamma(\beta+\frac{3}{2}+p+n)} G_{\beta+n}(z) \tag{2.3.13}$$

which reduces to the block decomposition of $\left(\frac{1-z}{z}\right)^p$ when β is tuned to $-p-\frac{1}{2}$.

The significance of this equality is that the residue of the pole at $\alpha = \beta + n$ in alpha space is

$$-\left(\frac{Q(-\beta-n)}{2}\right)\frac{\Gamma^2(\beta+\frac{1}{2}+n)\Gamma(\beta-\frac{1}{2}-p+n)}{\Gamma^2(-p)\Gamma(2(\beta+n))\Gamma(\beta+\frac{3}{2}+p+n)} \tag{2.3.14}$$

which is asymptotically equal to

$$-\frac{n^{-2(1+p)}}{\Gamma^2(-p)}\left(1+O\left(\frac{1}{n}\right)\right) \tag{2.3.15}$$

That is, the leading asymptotic behaviour is independent of β and is exactly equal to the leading large n asymptotic behaviour of

$$-\frac{\Gamma(-2p-1+n)}{n!\,\Gamma^2(-p)} \tag{2.3.16}$$

which is the residue of the alpha space density for $\left(\frac{1-z}{z}\right)^p$ at $\alpha = -p-\frac{1}{2}+n$. In conclusion, the addition of the Casimir regular terms has shifted the locations of the blocks and their OPE coefficients without changing the leading asymptotics. A more complete discussion can be found in [37].

2.4 Witten Diagrams

We have shown that functions such as logarithms and polylogarithms can be taken to $d = 1$ alpha space in a fairly straight forward manner. Therefore it is our hope that the alpha space formalism can one day say something about Witten diagram calculations, where these functions are abundant. While this may seem optimistic, some confidence can be drawn from the progress made in Mellin space [38, 39, 40].

As a first baby-step, consider the tree-level Witten diagram in AdS_2 for four identical external scalars of scaling dimension 1. The stripped correlator is then

$$2z^2\left(\frac{\log(1-z)}{z}+\frac{\log(z)}{1-z}\right) \tag{2.4.1}$$

The Mellin-Barnes representations in Eq. (2.1.9) can be used to show that the

relevant alpha space density is

$$2z^2\left(\frac{\log(1-z)}{z}+\frac{\log(z)}{1-z}\right)\mapsto -4\,\frac{\partial^2}{\partial\alpha^2}\left(\log\Gamma\Big(\frac{3}{4}\pm\frac{\alpha}{2}\Big)\right) \tag{2.4.2}$$

This goes like $2/\alpha^2$ for large α, which is consistent with the fact that the function is Casimir regular.

The density in Eq. (2.4.2) has double poles at $\alpha=\pm(\frac{3}{2}+2n)$ for $n\in\mathbb{N}$, meaning that the decomposition is made up of both blocks and their derivatives for operators of dimension $2(1+n)$. Reading off the residues, we have

$$\begin{aligned}2z^2\left(\frac{\log(1-z)}{z}+\frac{\log(z)}{1-z}\right)&=8\sum_{n=0}^{\infty}\frac{\partial}{\partial\beta}\left(\frac{G_\beta(z)}{Q(-\beta)}\right)\Big|_{\beta=\frac{3}{2}+2n}\\&=8\sum_{n=0}^{\infty}\frac{1}{Q(-\beta)}\left(\tilde{\psi}(\beta)G_\beta(z)+\frac{\partial G_\beta(z)}{\partial\beta}\right)\Big|_{\beta=\frac{3}{2}+2n}\end{aligned} \tag{2.4.3}$$

where $\tilde{\psi}(\beta)$ was defined in Eq. (2.1.30). The anomalous dimensions and tree-level corrections to the OPE constants can then be directly read off.

A similar function appearing in a discussion of $d=4$ supergravity [41] is

$$\frac{z}{1-z}-\frac{2z^2}{(1-z)^2}-\frac{2z^3\log(z)}{(1-z)^3}=-\frac{1}{2}D_z(D_z-2)\frac{z\log(z)}{1-z} \tag{2.4.4}$$

Using the fact that applying the quadratic Casimir to a function only changes the alpha space density by a polynomial factor and that

$$\frac{z\log(z)}{1-z}\mapsto-\Gamma^2\Big(\frac{1}{2}\pm\alpha\Big) \tag{2.4.5}$$

we immediately arrive at the result

$$\frac{z}{1-z}-\frac{2z^2}{(1-z)^2}-\frac{2z^3\log(z)}{(1-z)^3}\mapsto\frac{1}{2}\left(\alpha^2-\frac{1}{4}\right)\left(\alpha^2-\frac{9}{4}\right)\Gamma^2\Big(\frac{1}{2}\pm\alpha\Big) \tag{2.4.6}$$

whence the OPE data can be easily extracted in the usual manner. This function is Casimir regular, which is consistent with the exponential suppression of the density at large imaginary α.

It is not much more of a leap to consider comparable functions composed of even

higher derivatives of blocks. By way of example, we found that

$$\frac{z(12\mathrm{Li}_3(z) - 6\log(z)\mathrm{Li}_2(z) - \log^3(z) - 3\pi^3\log(z) - 12\zeta(3))}{6(1-z)} \mapsto \Gamma^4\left(\frac{1}{2} \pm \alpha\right) \quad (2.4.7)$$

That such a complicated position space function can be packaged up nicely makes us sanguine about the prospect of investigating objects like the D-functions in alpha space.

2.5 Two Dimensions

The Sturm-Liouville analysis in two dimensions is no more difficult than the $d = 1$ case because the quadratic Casimir equation of Eq. (1.5.6) factorises nicely, reducing to

$$(D_z + D_{\bar{z}})G_{\alpha,\bar{\alpha}}(z,\bar{z}) = \left(\alpha^2 + \bar{\alpha}^2 - \frac{1}{2}\right) G_{\alpha,\bar{\alpha}}(z,\bar{z}) \quad (2.5.1)$$

which is effectively like the sum of two $d = 1$ equations. The block in two dimensions is defined in Eq. (1.5.15). This factorisation means that we do not need a new bracket or a new measure and we can use many of the earlier results. This all being so, alpha space for $d = 2$ can immediately be defined through the integral transform

$$\hat{f}(\alpha,\bar{\alpha}) = \int_0^1 dz \int_0^1 d\bar{z}\, \mu(z)\mu(\bar{z}) \left(\frac{\Psi_\alpha(z)\Psi_{\bar{\alpha}}(\bar{z}) + \Psi_\alpha(\bar{z})\Psi_{\bar{\alpha}}(z)}{2}\right) f(z,\bar{z}) \quad (2.5.2)$$

and the inverse transform

$$f(z,\bar{z}) = \int [d\alpha] \int [d\bar{\alpha}]\, \frac{4\,\hat{f}(\alpha,\bar{\alpha})}{Q(\alpha)Q(\bar{\alpha})Q(-\alpha)Q(-\bar{\alpha})} \left(\frac{\Psi_\alpha(z)\Psi_{\bar{\alpha}}(\bar{z}) + \Psi_\alpha(\bar{z})\Psi_{\bar{\alpha}}(z)}{2}\right) \quad (2.5.3)$$

From this, is it clear that we can only accommodate for functions satisfying $f(z,\bar{z}) = f(\bar{z},z)$. Assuming this symmetry, the two equivalent terms can be combined, meaning that the transform simplifies to

$$\hat{f}(\alpha,\bar{\alpha}) = \int_0^1 dz \int_0^1 d\bar{z}\, \mu(z)\mu(\bar{z})\Psi_\alpha(z)\Psi_{\bar{\alpha}}(\bar{z}) f(z,\bar{z}) \quad (2.5.4)$$

and the inverse transform to

$$f(z,\bar{z}) = \int [d\alpha] \int [d\bar{\alpha}] \, \frac{4\,\hat{f}(\alpha,\bar{\alpha})\Psi_{\alpha}(z)\Psi_{\bar{\alpha}}(\bar{z})}{Q(\alpha)Q(\bar{\alpha})Q(-\alpha)Q(-\bar{\alpha})} \tag{2.5.5}$$

Scaling dimension and spin are related to α and $\bar{\alpha}$ through Eq. (1.4.8) with $d = 2$. Explicitly, this means that

$$\alpha = \frac{\Delta - J - 1}{2} \qquad \bar{\alpha} = \frac{\Delta + J - 1}{2} \tag{2.5.6}$$

or equivalently

$$\Delta = \bar{\alpha} + \alpha + 1 \qquad J = \bar{\alpha} - \alpha \tag{2.5.7}$$

Generalising Eq. (2.1.18) using Eq. (2.5.3), a block once again maps to a symmetrised pole according to

$$G_{\beta,\bar{\beta}}(z,\bar{z}) \mapsto \left(\frac{Q(-\beta)Q(-\bar{\beta})}{8(\alpha-\beta)(\bar{\alpha}-\bar{\beta})} + \text{`seven images'} \right) \tag{2.5.8}$$

and we recall that $G_{\beta,\bar{\beta}}(z,\bar{z})$ is a two-dimensional conformal block for an operator of dimension $\bar{\beta} + \beta + 1$ and spin $\bar{\beta} - \beta$. The seven images are found from the three $\mathbb{Z}_2$ symmetries of the Casimir eigenvalues, which are

$$\alpha \to -\alpha, \quad \bar{\alpha} \to -\bar{\alpha}, \quad \alpha \leftrightarrow \bar{\alpha} \tag{2.5.9}$$

2.5.1 Ising Model in Two Dimensions

As a simple check of the two-dimensional alpha space formalism, consider the four-point function $\langle \sigma\epsilon\sigma\epsilon \rangle$ of the Ising model. $\Delta_\sigma = \frac{1}{8}$ and $\Delta_\epsilon = 1$ and so $\mathbf{a} = \frac{7}{16}$ and $\mathbf{b} = -\frac{7}{16}$. The stripped correlator is

$$\mathcal{G}_{\sigma\epsilon\sigma\epsilon}(z,\bar{z}) = g(z)g(\bar{z}) \tag{2.5.10}$$

with

$$g(z) = \frac{z^{1/16}(1-2z)}{2\sqrt{1-z}} \tag{2.5.11}$$

Expanding around $z = 0$, $g(z)$ is

$$g(z) = -\frac{z^{1/16}}{4\sqrt{\pi}} \sum_{n=0}^{\infty} \frac{(1+2n)\Gamma(n-\frac{1}{2})}{n!} z^n \tag{2.5.12}$$

Using Eq. (2.1.21), $g(z)$ can be converted to alpha space by replacing each power of z to give

$$\begin{aligned} \hat{g}(\alpha) =& -\frac{1}{4\sqrt{\pi}} \sum_{n=0}^{\infty} \frac{(1+2n)\Gamma(n-\frac{1}{2})}{n!} \frac{\Gamma(n-\frac{7}{16} \pm \alpha)}{\Gamma(n+\frac{1}{2})\Gamma(n-\frac{3}{8})} \\ =& \frac{\Gamma(-\frac{7}{16} \pm \alpha)}{96\sqrt{\pi}\Gamma(-\frac{3}{8})} \left(48\, {}_3F_2\left(-\frac{1}{2}, -\frac{7}{16} - \alpha, -\frac{7}{16} + \alpha; -\frac{3}{8}, \frac{1}{2}; 1\right) + \right. \\ & \left. (49 - 256\alpha^2)\, {}_3F_2\left(\frac{1}{2}, \frac{9}{16} - \alpha, \frac{9}{16} + \alpha; \frac{5}{8}, \frac{3}{2}; 1\right)\right) \end{aligned} \tag{2.5.13}$$

This has poles at $\alpha = \pm(\mathbb{N} - \frac{7}{16})$ and so, according to Eq. (2.1.18), the conformal block decomposition of $g(z)$ is then

$$g(z) = \sum_{n=0}^{\infty} \chi_n G_{n-\frac{7}{16}}(z) \tag{2.5.14}$$

where

$$\begin{aligned} \chi_n \equiv& \frac{(-1)^n 2^{\frac{7}{4}-2n}\Gamma(n+\frac{1}{2})\Gamma(2n-\frac{7}{4})}{3n!\Gamma(-\frac{3}{8})\Gamma(2n-\frac{7}{8})} \left(3\, {}_3F_2\left(-\frac{1}{2}, n-\frac{7}{8}, -n; -\frac{3}{8}, \frac{1}{2}; 1\right) - \right. \\ & \left. 2n(8n-7)\, {}_3F_2\left(\frac{1}{2}, n+\frac{1}{8}, -n+1; \frac{5}{8}, \frac{3}{2}; 1\right)\right) \end{aligned} \tag{2.5.15}$$

Therefore, the conformal block decomposition of $\mathcal{G}_{\sigma\epsilon\sigma\epsilon}$ consists of operators $\sigma_{m,n}$ with dimensions $\Delta_{\sigma_{m,n}} \equiv \frac{1}{8} + m + n$, spins $J_{\sigma_{m,n}} \equiv m - n$ and squared OPE coefficients given by

$$\lambda^2_{\sigma\epsilon\sigma_{m,n}} \equiv \left(\frac{2}{1+\delta_{m,n}}\right) \chi_m \chi_n \tag{2.5.16}$$

The Kronecker delta is necessary to ensure that we do not double count the spin-0 operators. All together, the stripped correlator decomposes into

$$\mathcal{G}_{\sigma\epsilon\sigma\epsilon}(z, \bar{z}) = \sum_{\substack{m,n=0 \\ m \geq n}}^{\infty} \lambda^2_{\sigma\epsilon\sigma_{m,n}} G_{n-\frac{7}{16}, m-\frac{7}{16}}(z, \bar{z}) \tag{2.5.17}$$

The sum is limited to $m \geq n$ to avoid double counting and to ensure that the decomposition only contains operators with positive scaling dimensions.

2.6 Split Kernel and Crossing Symmetry

Beside from decomposing functions into conformal blocks, one of the initial goals of the alpha space construction was to further understand the consequences of crossing symmetry.

The crossing symmetry equation in Eq. (1.6.1) equates a stripped correlator in the s-channel to one in the t-channel, up to some kinematical pre-factor. The bootstrap community have done some impressive work to numerically constrain conformal field theories using this equation. Furthermore, analytic insight can be gained from studying the crossing equation in various limits. As an example, the light-cone limit can be used to show that every conformal field theory contains families of operators within which dimensions asymptote to the generalised free field values at large spin [12, 42]. It is also known that the anomalous dimensions of these operators are determined by the minimal twist sector of the theory, where twist is defined as the difference between dimension and spin. We recover this result for $d = 2$ in Section 2.6.2.

To clarify terminology, if we consider the four-point function $\langle\phi\phi\phi\phi\rangle$ then the tower of operators whose dimensions approach the generalised free field values $2\Delta_\phi + J + 2n$ make up the n^{th} double-twist family in this work. Asymptotically, the operators can be schematically thought of as $\phi\partial^J\Box^n\phi$.

2.6.1 Split Kernel

In two dimensions, the alpha space transform in Eq. (2.5.2) can be applied to the crossing equation of Eq. (1.6.1) to give

$$\hat{\mathcal{G}}(\alpha,\bar{\alpha}) = \int_0^1 dz \int_0^1 d\bar{z}\, \mu(z)\mu(\bar{z})\Psi_\alpha(z)\Psi_{\bar{\alpha}}(\bar{z})\frac{(z\bar{z})^{\frac{\Delta_1+\Delta_2}{2}}\mathcal{G}'(1-z,1-\bar{z})}{((1-z)(1-\bar{z}))^{\frac{\Delta_3+\Delta_2}{2}}} \qquad (2.6.1)$$

where we have used the fact that $\mathcal{G}'(z,\bar{z}) = \mathcal{G}'(\bar{z},z)$ to combine the two equivalent terms. The t-channel stripped correlator can be written like

$$\mathcal{G}'(1-z,1-\bar{z}) = \int [d\alpha] \int [d\bar{\alpha}] \, \frac{4\,\hat{\mathcal{G}}'(\alpha,\bar{\alpha})\Psi'_{\alpha}(1-z)\Psi'_{\bar{\alpha}}(1-\bar{z})}{Q'(\alpha)Q'(\bar{\alpha})Q'(-\alpha)Q'(-\bar{\alpha})} \tag{2.6.2}$$

where $Q'(\alpha)$ and $\Psi'_{\alpha}(z)$ are equal to $Q(\alpha)$ and $\Psi_{\alpha}(z)$ respectively, up to the redefinitions in Eq. (1.6.3).

Putting these two expressions together, we arrive at

$$\hat{\mathcal{G}}(\alpha,\bar{\alpha}) = \int [d\beta] \int \left[d\bar{\beta}\right] K(\alpha;\beta|\Delta_i) K(\bar{\alpha};\bar{\beta}|\Delta_i) \hat{\mathcal{G}}'(\beta,\bar{\beta}) \tag{2.6.3}$$

where Δ_i is shorthand for the set of external scaling dimensions and the crossing kernel is defined as

$$K(\alpha;\beta|\Delta_i) \equiv \frac{2}{Q'(\beta)Q'(-\beta)} \int_0^1 dz\, \mu(z) \frac{z^{\frac{\Delta_1+\Delta_2}{2}}}{(1-z)^{\frac{\Delta_3+\Delta_2}{2}}} \Psi_{\alpha}(z)\Psi'_{\beta}(1-z) \tag{2.6.4}$$

However, the crossing equation integrand is even in β and $\bar{\beta}$. Therefore, an equally valid integral equation can be build by splitting $\Psi'_{\beta}(1-z)$ in the definition of the kernel to give

$$\boxed{\hat{\mathcal{G}}(\alpha,\bar{\alpha}) = \int [d\beta] \int \left[d\bar{\beta}\right] K_{\text{split}}(\alpha;\beta|\Delta_i) K_{\text{split}}(\bar{\alpha};\bar{\beta}|\Delta_i) \hat{\mathcal{G}}'(\beta,\bar{\beta})} \tag{2.6.5}$$

where the split kernel is defined as

$$\boxed{K_{\text{split}}(\alpha;\beta|\Delta_i) \equiv \frac{2}{Q'(-\beta)} \int_0^1 dz\, \mu(z) \frac{z^{\frac{\Delta_1+\Delta_2}{2}}}{(1-z)^{\frac{\Delta_3+\Delta_2}{2}}} \Psi_{\alpha}(z) G'_{\beta}(1-z)} \tag{2.6.6}$$

and $G'_{\alpha}(z)$ equals $G_{\alpha}(z)$ up to the redefinitions in Eq. (1.6.3).

The instantaneous advantage of expressing crossing symmetry as an integral equation is that some physical consequences can be probed by investigating the analytic structure of the kernel itself. The first step in doing this is to write the crossing kernel in a more lucid form. It turns out that the split kernel can be written in terms of analytic Wilson functions. All of the divergent structure then comes from the multiplying gamma functions.

Here, we present our derivation of the split kernel in terms of Wilson functions for equal external scalars to make the argument more cogent. Then we quote our general result in Eq. (2.6.25).

Taking the external scalars to be identical and of dimension Δ_ϕ, Eq. (2.6.6) simplifies to

$$K_{\text{split}}(\alpha;\beta|\Delta_\phi) = \frac{2}{Q(-\beta)}\int_0^1 \frac{dz}{z^2}\left(\frac{z}{1-z}\right)^{\Delta_\phi}\Psi_\alpha(z)G_\beta(1-z) \tag{2.6.7}$$

Now we replace $\Psi_\alpha(z)$ and $G_\beta(1-z)$ in this integral with the Mellin-Barnes representations

$$\Psi_\alpha(z) = \frac{1}{\Gamma(\frac{1}{2}\pm\alpha)}\int [ds]\,\frac{\Gamma(-s)\Gamma(\frac{1}{2}+s\pm\alpha)}{\Gamma(1+s)}\left(\frac{1-z}{z}\right)^s \tag{2.6.8}$$

and

$$G_\beta(1-z) = (1-z)^{\frac{1}{2}+\beta}\frac{\Gamma(1+2\beta)}{\Gamma^2(\frac{1}{2}+\beta)}\int [dt]\,\Gamma^2(-t)\Gamma^2\Big(\frac{1}{2}+\beta+t\Big)\,z^t \tag{2.6.9}$$

The cross-ratio z can then be integrated out to give a double contour integral. The resultant t-dependent part can be solved using Barnes' first lemma in Eq. (2.1.20) to contribute

$$\int [dt]\,\Gamma^2(-t)\,\Gamma\Big(\frac{1}{2}+\beta+t\Big)\,\Gamma(\Delta_\phi-1-s+t) = \frac{\Gamma(\frac{1}{2}+\beta)\Gamma^2(\Delta_\phi-1-s)}{\Gamma(\Delta_\phi-\frac{1}{2}+\beta-s)} \tag{2.6.10}$$

Putting this all together, we are left with the single contour integral

$$K_{\text{split}}(\alpha;\beta|\Delta_\phi) = \tag{2.6.11}$$
$$\frac{2\beta}{\Gamma(\frac{1}{2}\pm\alpha)}\int [ds]\,\frac{\Gamma(-s)\Gamma^2(\Delta_\phi-1-s)\Gamma(\frac{1}{2}+s\pm\alpha)\Gamma(\frac{3}{2}-\Delta_\phi+s+\beta)}{\Gamma(1+s)\Gamma(\Delta_\phi-\frac{1}{2}+\beta-s)}$$

The pole structure of Eq. (2.6.11) in the α- and β-planes can be determined by looking at the where the s contour gets pinched. Doing this, we find that there are single poles at $\beta = -\frac{1}{2}-\mathbb{N}$ and $\beta = \Delta_\phi - \frac{3}{2}-\mathbb{N}$. There are also double poles at the generalised free field values $\alpha = \pm(\Delta_\phi - \frac{1}{2}+\mathbb{N})$.

The advantage of using the split rather than the full kernel is now apparent. The split kernel does not have any sequences of poles running to the right in the β-plane. Therefore, it is conceivable that the contours in Eq. (2.6.5) can be closed to the right

to only pick up poles in $\hat{\mathcal{G}}'(\beta,\bar{\beta})$. Then, an s-channel density can be thought of as a sum over t-channel residues weighted by split kernels and vice-versa. It also means that we can consider the contribution to one channel of a single operator in the crossed channel. In particular, the fact that there are double poles in the split kernel establishes the well known result that a t-channel operator cannot be reproduced by a finite sum of s-channel operators. This is simply because a double pole cannot be written as a finite sum of single poles.

The authors of [1] took the contour integral in Eq. (2.6.11) and closed it to the left to give a sum over three ${}_4F_3$ functions. Unfortunately, each of these hypergeometrics is non-analytic in α and β. Furthermore, these terms introduce additional singularities that cancel amongst one another. Therefore, it is difficult to study the analytic structure of the split kernel with this representation. However, we found that a series of hypergeometric identities can be employed to massage the sum into

$$\begin{aligned} K_{\text{split}}(\alpha;\beta|\Delta_\phi) = &2\beta\Gamma(\Delta_\phi)\Gamma(1-\Delta_\phi)\Gamma\Big(\Delta_\phi-\frac{1}{2}\pm\alpha\Big)\Gamma\Big(\frac{1}{2}\pm\beta\Big) \\ &\left(\frac{\Gamma(\Delta_\phi-\frac{1}{2}\pm\alpha)W_\alpha(\beta;\frac{1}{2},\frac{1}{2},\Delta_\phi-\frac{1}{2},\Delta_\phi-\frac{1}{2})}{\Gamma(\frac{1}{2}\pm\alpha)}-\right. \\ &\left.\frac{\Gamma(\frac{3}{2}-\Delta_\phi+\beta)W_\alpha(\beta;\frac{1}{2},\frac{1}{2},\Delta_\phi-\frac{1}{2},\frac{3}{2}-\Delta_\phi)}{\Gamma(\Delta_\phi-\frac{1}{2}+\beta)}\right) \end{aligned} \tag{2.6.12}$$

where

$$W_\alpha(\beta;a,b,c,d) \equiv \frac{\Gamma(d-a)\,{}_4F_3\left(\begin{matrix}\tilde{a}-\alpha,\tilde{a}+\alpha,a-\beta,a+\beta\\ a+b,a+c,a-d+1\end{matrix};1\right)}{\Gamma(a+b)\Gamma(a+c)\Gamma(\tilde{d}\pm\alpha)\Gamma(d\pm\beta)}+(a\leftrightarrow d) \tag{2.6.13}$$

is called the Wilson function [43]. It is symmetric in its final four arguments and the dual variables are

$$\begin{pmatrix}\tilde{a}\\ \tilde{b}\\ \tilde{c}\\ \tilde{d}\end{pmatrix} \equiv \frac{a+b+c+d}{2}-\begin{pmatrix}d\\ c\\ b\\ a\end{pmatrix} \tag{2.6.14}$$

such that

$$W_\alpha(\beta;a,b,c,d) = W_\beta(\alpha;\tilde{a},\tilde{b},\tilde{c},\tilde{d}) \tag{2.6.15}$$

Another useful representation in terms of a single well-poised ${}_7F_6$ hypergeometric function is

$$W_\alpha(\beta;a,b,c,d) = \tag{2.6.16}$$
$$\frac{\Gamma(2a+\tilde{d}-\alpha)\,{}_7F_6\left(\begin{matrix}\tilde{a}-\alpha,\tilde{b}-\alpha,\tilde{c}-\alpha,2a+\tilde{d}-1-\alpha,\frac{2a+\tilde{d}+1-\alpha}{2},a-\beta,a+\beta\\ a+b,a+c,a+d,\frac{2a+\tilde{d}-1-\alpha}{2},\frac{a+b+c+d}{2}-\alpha-\beta,\frac{a+b+c+d}{2}-\alpha+\beta\end{matrix};1\right)}{\Gamma(a+b)\Gamma(a+c)\Gamma(a+d)\Gamma(\tilde{d}+\alpha)\Gamma(\frac{a+b+c+d}{2}-\alpha\pm\beta)}$$

The Wilson function reduces to the polynomial introduced in Eq. (2.1.26) through the equality

$$W_{\tilde{a}+n}(\beta;a,b,c,d) = \frac{(-1)^n\mathfrak{p}_n(\beta;a,b,c,1-d)}{\Gamma(a+b+n)\Gamma(a+c+n)\Gamma(b+c+n)\Gamma(d\pm\beta)} \tag{2.6.17}$$

when $n\in\mathbb{N}$.

The main argument in favour of the representation in Eq. (2.6.12) is that the Wilson function $W_\alpha(\beta;a,b,c,d)$ is analytic in both α and β. Therefore, all of the singularities come from the gamma functions. The only blemish is that there naively seems to be simple poles in Eq. (2.6.12) for $\beta=\frac{1}{2}+\mathbb{N}$ from the overall $\Gamma(\frac{1}{2}-\beta)$ factor. However, it can be shown that the associated residues vanish.

The asymptotic properties of the Wilson function are well understood and so it is not difficult to establish the large α and β behaviours of the split kernel. For large non-real α, $K_{\text{split}}(\alpha;\beta|\Delta_\phi)$ goes like

$$K_{\text{split}}(\alpha;\beta|\Delta_\phi) = \frac{2\Gamma(\frac{3}{2}-\Delta_\phi+\beta)}{Q(-\beta)\Gamma(\Delta_\phi-\frac{1}{2}-\beta)}(-\alpha^2)^{\Delta_\phi-\frac{3}{2}-\beta}(1+O(\alpha^{-2})) \tag{2.6.18}$$

Eq. (2.6.7) tells us that the split kernel is ultimately the alpha space transform of a single t-channel block, up to an overall factor. That is,

$$\frac{2}{Q(-\beta)}\left(\frac{z}{1-z}\right)^{\Delta_\phi}G_\beta(1-z)\mapsto K_{\text{split}}(\alpha;\beta|\Delta_\phi) \tag{2.6.19}$$

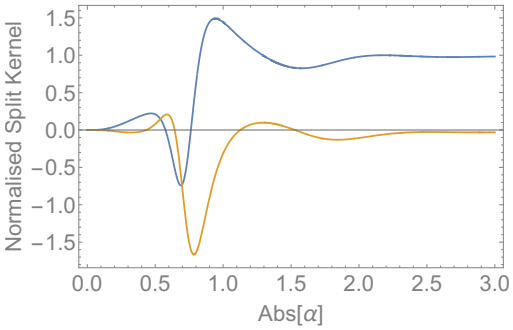

(a) $\beta = \frac{1}{3}$, $\Delta_\phi = \frac{1+i}{5}$, $\arg(\alpha) = \frac{\pi}{6}$

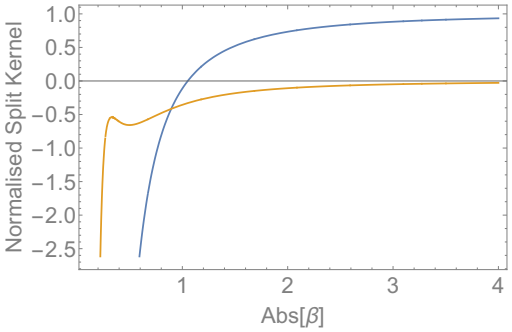

(b) $\alpha = \frac{8}{7} - i$, $\Delta_\phi = \frac{1-4i}{3}$, $\mathrm{Arg}(\beta) = \frac{\pi}{4}$

Figure 2.4: Fig. 2.4a plots $K_{\text{split}}(\alpha;\beta|\Delta_\phi)$ normalised by the leading term in Eq. (2.6.18) against the absolute value of α. Likewise, the split kernel in Fig. 2.4b is plotted against $\mathrm{Abs}(\beta)$ and is normalised by Eq. (2.6.21). The real part (blue) asymptotes to 1 whereas the imaginary part (orange) falls to zero. Peculiar values for the parameters have been picked to demonstrate that the asymptotic formulae hold for $\mathrm{Arg}(\alpha) \neq 0, \pi$ and $\mathrm{Arg}(\beta) \neq \pi$ respectively.

In addition, in the limit $z \to 1$ this function is

$$\left(\frac{z}{1-z}\right)^{\Delta_\phi} G_\beta(1-z) = (1-z)^{\frac{1}{2}+\beta-\Delta_\phi}(1+O(1-z)) \tag{2.6.20}$$

and so, the asymptotic behaviour at large α in Eq. (2.6.18) is in exact agreement with what was expected from Eq. (2.2.8).

Similarly, the split kernel in the large non-negative β limit is

$$\begin{aligned} K_{\text{split}}(\alpha;\beta|\Delta_\phi) = Q(-\alpha)\,\Gamma^2\left(\Delta_\phi - \frac{1}{2} - \alpha\right)\beta^{2(1+\alpha-\Delta_\phi)}(1+O(\beta^{-2})) \\ + (\alpha \to -\alpha) \end{aligned} \tag{2.6.21}$$

where either term can dominate. Fig. 2.4 plots the split kernel normalised by the large α and β expressions.

Using Eq. (2.6.21), we can investigate how asymptotic t-channel discontinuities map into the s-channel. An alpha space density can be taken from the s-channel to the t-channel by integrating against the split kernel. By default, the contour lies along the imaginary axis. If it is deformed to embrace the positive real axis, this integral

schematically becomes

$$\int^{\infty} d\beta\, K_{\text{split}}(\alpha;\beta|\Delta)\,\text{disc}_{\beta}(f(\beta)) \tag{2.6.22}$$

where

$$\text{disc}_{\alpha}(f(\alpha)) \equiv \lim_{\epsilon\to 0}\left(\frac{f(\alpha+i\epsilon)-f(\alpha-i\epsilon)}{2\pi i}\right) \tag{2.6.23}$$

is effectively a sum over delta functions. For example, $\text{disc}_{\alpha}(\alpha^{-1}) = -\delta(\alpha)$.

The question now is, how does the discontinuity need to asymptotically behave in order to develop the opposite channel in a certain way?

From Eq. (2.6.21), it seems to be the case that if along the real, positive β axis

$$\text{disc}_{\beta}(f(\beta)) = \beta^{-2x}(1+O(\beta^{-2})) \tag{2.6.24}$$

then in the s-channel, poles are produced at $\alpha = \pm(x+\Delta_{\phi}-\frac{3}{2})$. The subleading asymptotics will produce additional poles further away from the origin, the first correction being at $\alpha = \pm(x+1+\Delta_{\phi}-\frac{3}{2})$. Importantly, this means that subordinate contributions to the double-twist operators are seemingly captured by Casimir regular terms (i.e. with $x = 1,2,3,...$). In Section 2.6.2 and Appendix A, we talk about asymptotic discontinuities more rigorously using a Tauberian theorem.

To conclude this section, we found that the split kernel in Eq. (2.6.6) can be written as

$$\begin{aligned} K_{\text{split}}(\alpha;\beta|\Delta_i) = {} & \frac{2\beta\Gamma(1+\mathbf{a}+\mathbf{b})\Gamma(\Delta_1)\Gamma(1-\Delta_1)\Gamma(\frac{\Delta_3+\Delta_4-1}{2}\pm\alpha)\Gamma(\frac{1}{2}\pm(\mathbf{a}'+\beta))}{\Gamma(1+\mathbf{a}'+\mathbf{b}')\Gamma(\frac{1}{2}-\mathbf{b}'+\beta)\Gamma(\frac{1}{2}+\mathbf{a}\pm\alpha)\Gamma(\frac{1}{2}\pm(\frac{\Delta_1+\Delta_4}{2}+\beta))} \\ & \left[\Gamma\Big(\frac{1}{2}+\mathbf{b}'+\beta\Big)\Gamma\Big(\frac{\Delta_1+\Delta_2-1}{2}\pm\alpha\Big)\Gamma\left(\frac{1}{2}\pm\left(\frac{\Delta_1+\Delta_4}{2}+\beta\right)\right)W\right. \\ & \left.+\,\Gamma\Big(\frac{1}{2}-\mathbf{b}'+\beta\Big)\Gamma\Big(\frac{1}{2}+\mathbf{a}\pm\alpha\Big)\Gamma\left(\frac{3-\Delta_1-\Delta_4}{2}\pm\beta\right)W\right] \end{aligned} \tag{2.6.25}$$

for non-zero $\mathbf{a}$ and $\mathbf{b}$, where the first W is

$$W_{\beta}\left(\alpha\,;\frac{1}{2}-\mathbf{a},\frac{1}{2}+\mathbf{b},\frac{\Delta_1+\Delta_2-1}{2},\frac{\Delta_3+\Delta_4-1}{2}\right) \tag{2.6.26}$$

and the second is

$$W_\beta\left(\alpha\,;\frac{1}{2}+\mathbf{a},\frac{1}{2}+\mathbf{b},\frac{3-\Delta_1-\Delta_2}{2},\frac{\Delta_3+\Delta_4-1}{2}\right) \tag{2.6.27}$$

This result is also new and enjoys the same advantages as Eq. (2.6.12).

2.6.2 Anomalous Dimensions

Using the pole map in Eq. (2.5.8) and the crossing equation in Eq. (2.6.5), a single t-channel block in $d=2$ alpha space is

$$\int[d\sigma]\int[d\bar{\sigma}]\,K_{\text{split}}(\alpha;\sigma|\Delta_i)K_{\text{split}}(\bar{\alpha};\bar{\sigma}|\Delta_i)\left(\frac{Q'(-\beta)Q'(-\bar{\beta})}{8(\sigma-\beta)(\bar{\sigma}-\bar{\beta})}+\text{`seven images'}\right) \tag{2.6.28}$$

This double integral is solved by closing both the σ and $\bar{\sigma}$ contours to the right to pick up the poles at β and $\bar{\beta}$, to become

$$\frac{Q'(-\beta)Q'(-\bar{\beta})}{8}\Big(K_{\text{split}}(\alpha;\beta|\Delta_i)K_{\text{split}}(\bar{\alpha};\bar{\beta}|\Delta_i)+(\alpha\leftrightarrow\bar{\alpha})\Big) \tag{2.6.29}$$

As a quick sanity check, setting $\beta=\bar{\beta}=-\frac{1}{2}$ should reproduce the identity contribution when $\mathbf{a}=\mathbf{b}=0$. Specialising to equal external scalars for the remainder of this section, we found that

$$\begin{aligned}\lim_{\beta\to-\frac{1}{2}}&\left(\frac{Q^2(-\beta)K_{\text{split}}(\alpha;\beta|\Delta_\phi)K_{\text{split}}(\bar{\alpha};\beta|\Delta_\phi)}{4}\right)\\&=\frac{\Gamma^2(1-\Delta_\phi)\Gamma(\Delta_\phi-\frac{1}{2}\pm\alpha)\Gamma(\Delta_\phi-\frac{1}{2}\pm\bar{\alpha})}{\Gamma^2(\Delta_\phi)\Gamma(\frac{1}{2}\pm\alpha)\Gamma(\frac{1}{2}\pm\bar{\alpha})}\end{aligned} \tag{2.6.30}$$

Using Eq. (2.1.23), this is the $d=2$ alpha space density for the function

$$\left(\frac{z\bar{z}}{(1-z)(1-\bar{z})}\right)^{\Delta_\phi}\mapsto\frac{\Gamma^2(1-\Delta_\phi)\Gamma(\Delta_\phi-\frac{1}{2}\pm\alpha)\Gamma(\Delta_\phi-\frac{1}{2}\pm\bar{\alpha})}{\Gamma^2(\Delta_\phi)\Gamma(\frac{1}{2}\pm\alpha)\Gamma(\frac{1}{2}\pm\bar{\alpha})} \tag{2.6.31}$$

which is the identity operator in the t-channel according to crossing symmetry through Eq. (1.6.1). The constituent operators in the block decomposition of this function are generalised free fields at the double-twist values.

For future reference, we take the residue of Eq. (2.6.30) at $\alpha=\Delta_\phi-\frac{1}{2}+n$ for $n\in\mathbb{N}$

and expand in large imaginary $\bar{\alpha}$ to give

$$\begin{aligned}\text{Res}\left(\frac{\Gamma^2(1-\Delta_\phi)\Gamma(\Delta_\phi-\frac{1}{2}\pm\alpha)\Gamma(\Delta_\phi-\frac{1}{2}\pm\bar{\alpha})}{\Gamma^2(\Delta_\phi)\Gamma(\frac{1}{2}\pm\alpha)\Gamma(\frac{1}{2}\pm\bar{\alpha})}\right)\Big|_{\alpha=\Delta_\phi-\frac{1}{2}+n} \\ = -\frac{\Gamma(1-\Delta_\phi)\Gamma(2\Delta_\phi-1+n)}{n!\,\Gamma^3(\Delta_\phi)}(-\bar{\alpha}^2)^{\Delta_\phi-1}\Big(1+O(\bar{\alpha}^{-2})\Big)\end{aligned} \tag{2.6.32}$$

It is worth taking a moment to think about this expression more carefully. We have expanded in large (imaginary) $\bar{\alpha}$, which corresponds to taking $\bar{z}$ close to 1. Likewise, we are looking at an α pole, which arises from the z behaviour near the origin. Therefore, this is tantamount to taking the light-cone limit. Equivalently, Eq. (2.6.32) is the leading term (i.e. from the t-channel identity) in the light-cone bootstrap [44, 13].

After changing variables from $\bar{\alpha}$ to J, Eq. (2.6.32) matches the asymptotic $d = 2$ OPE coefficient found using the light-cone bootstrap [45]. In comparing our results to the literature, it is important to understand how to go from large imaginary J to real spins. This is detailed below in Eq. (2.6.35) and in Appendix A. Furthermore, we have to pencil in a factor of 2 because the spin can only take on even values when the external scalars are equal. We also have to dress the answer with a factor of $4/Q(-\bar{\alpha})Q(-(\Delta_\phi-\frac{1}{2}+n))$ as usual to go from residue to OPE coefficient.

A complete density is made up of a weighted sum over contributions like Eq. (2.6.29). That is,

$$\hat{\mathcal{G}}(\alpha,\bar{\alpha}) = \sum_{\beta,\bar{\beta}}\lambda_{\beta,\bar{\beta}}\frac{Q(-\beta)Q(-\bar{\beta})}{8}\Big(K_{\text{split}}(\alpha;\beta|\Delta_\phi)K_{\text{split}}(\bar{\alpha};\bar{\beta}|\Delta_\phi)+(\alpha\leftrightarrow\bar{\alpha})\Big) \tag{2.6.33}$$

where $\lambda_{\beta,\bar{\beta}}$ is the t-channel OPE coefficient for the fusion $\phi\times\phi\to\mathcal{O}_{\beta,\bar{\beta}}$. Eq. (2.6.33) is subtle and we must exercise prudence. Firstly, there must be a infinite number of terms because a split kernel has double-poles at the double-twist locations whereas the full density does not. Secondly, the sum is asymptotic and will not converge when there is an identity operator present. This is because $K_{\text{split}}(\alpha;\beta|\Delta_\phi)$ goes like $\beta^{2(1-\Delta_\phi\pm\alpha)}$ according to Eq. (2.6.21) and the discontinuity of the density goes like $\beta^{2(\Delta_\phi-1)}$ to reproduce the correct $z\to 1$ behaviour (i.e. $p=\Delta_\phi$ in Eq. (2.2.8), for

the identity). The total summand then has terms that go like β^{α} and $\beta^{-\alpha}$, making the sum divergent. When there is not an identity operator in the spectrum the sum may converge for some range of α and $\bar{\alpha}$, as we demonstrate in Section 2.6.3.

In order to loosely gain some control over the sum, we expand in large and imaginary $\bar{\alpha}$. This is done because the split kernel behaves as in Eq. (2.6.18) and so if there is a twist gap above the (t-channel) identity then the we can focus on the terms in the sum with lowest β. Eq. (2.6.33) then becomes

$$\hat{\mathcal{G}}(\alpha,\bar{\alpha}) = \sum_{\beta,\bar{\beta}} \frac{\lambda_{\beta,\bar{\beta}}\, Q(-\bar{\beta})\Gamma(\frac{3}{2}-\Delta_\phi+\beta)K_{\text{split}}(\alpha;\bar{\beta}|\Delta_\phi)}{4\Gamma(\Delta_\phi-\frac{1}{2}-\beta)}(-\bar{\alpha}^2)^{\Delta_\phi-\frac{3}{2}-\beta}\Big(1+O(\bar{\alpha}^{-2})\Big) \tag{2.6.34}$$

where we have dropped the $K_{\text{split}}(\alpha;\beta|\Delta_\phi)$ term because $\bar{\beta} > \beta$. An exception to this rule is a scalar in $d = 2$ for which $\beta = \bar{\beta}$. In this case, we must pencil in a factor of 2.

In Eq. (2.6.34) we are expanding in large imaginary $\bar{\alpha}$ but we ideally want to be working in the large *real* $\bar{\alpha}$ limit to be confident of the twist suppression. Going from asymptotic imaginary values to the large positive limit boils down to the replacement[1]

$$(-\bar{\alpha}^2)^p \implies -\frac{\bar{\alpha}^{2p}}{\Gamma(p)\Gamma(1-p)} \tag{2.6.35}$$

This is of course not exactly true because the density has poles along the real axis. In fact, it is only true in an aggregate sense for the discontinuity and this is justified more properly in Appendix A using a Tauberian theorem. A rough vindication follows from thinking about the complex function $(-\bar{\alpha}^2)^p$ itself. Splitting this using the identity

$$(-\bar{\alpha}^2)^p = \frac{(-\bar{\alpha})^{2p}+\bar{\alpha}^{2p}}{2\cos(\pi p)} \tag{2.6.36}$$

we see that it is made up of two functions; one with a right-running cut and one with a left-running cut. Therefore across the positive real axis, the discontinuity as

[1] With this replacement, the expression picks up a factor of $\sin(\pi p)$. Perhaps this is somehow linked to Caron-Huot's double discontinuity [16], which gives a factor of $\sin^2(\pi p)$ to a term like $(1-z)^p$.

defined in Eq. (2.6.23) is

$$\text{disc}_{\bar{\alpha}}(-\bar{\alpha}^2)^p = \frac{\text{disc}_{\bar{\alpha}}(-\bar{\alpha})^{2p}}{2\cos(\pi p)} = -\frac{\bar{\alpha}^{2p}}{\Gamma(p)\Gamma(1-p)} \tag{2.6.37}$$

All in all, Eq. (2.6.34) becomes

$$\text{disc}_{\bar{\alpha}}\Big(\hat{\mathcal{G}}(\alpha,\bar{\alpha})\Big) = \sum_{\beta,\bar{\beta}} \frac{\lambda_{\beta,\bar{\beta}}\, Q(-\bar{\beta}) K_{\text{split}}(\alpha;\bar{\beta}|\Delta_\phi)}{4\Gamma^2(\Delta_\phi - \frac{1}{2} - \beta)} \bar{\alpha}^{2\Delta_\phi - 3 - 2\beta}\Big(1 + O(\bar{\alpha}^{-2})\Big) \tag{2.6.38}$$

and $1/\bar{\alpha}$ is now the small and real parameter that we can expand in. As we mentioned before, the operators with lowest twist (i.e. smallest β) will dominate and we can focus on these terms in the sum.

It is clear from Eq. (2.6.12) that the split kernel has double poles at the generalised free field values $\alpha = \pm(\Delta_\phi - \frac{1}{2} + \mathbb{N})$ in general. The split kernel is the s-channel alpha space incarnation of a t-channel block and we have seen that adding an identity operator to one channel establishes a double-twist sector in the other. Additional operators then correct this contribution in some sense. Here, we formalise this argument and recover an important result in Eq. (2.6.46).

The coefficient of the double pole in $K_{\text{split}}(\alpha;\beta|\Delta_\phi)$ at $\alpha = \Delta_\phi - \frac{1}{2} + n$ with $n \in \mathbb{N}$ can be written as a Wilson polynomial using Eq. (2.6.17). We found that it is $\mathfrak{q}_n(\beta,\Delta_\phi)$ where

$$\mathfrak{q}_n(\beta,\Delta) \equiv \frac{2\beta\,\Gamma(2\Delta-1+n)}{(n!)^2\Gamma^2(\Delta+n)} \mathfrak{p}_n\Big(\beta;\frac{1}{2},\frac{1}{2},\Delta-\frac{1}{2},\Delta-\frac{1}{2}\Big) \tag{2.6.39}$$

Likewise, the residue is $\mathfrak{h}_n(\beta,\Delta_\phi)$ where

$$\begin{aligned}\mathfrak{h}_n(\beta,\Delta) \equiv{}& \mathfrak{q}_n(\beta,\Delta)\Big(\pi\tan(\pi\beta) + 2H_{2(\Delta-1)+n} - 2H_n\Big) \\ &+ (-1)^n \frac{2\beta\,\Gamma(\frac{1}{2}\pm\beta)\Gamma^2(2\Delta-1+n)}{(n!)^2} \frac{\partial}{\partial\alpha} W_\alpha\Big(\beta;\frac{1}{2},\frac{1}{2},\Delta-\frac{1}{2},\Delta-\frac{1}{2}\Big)\Big|_{\alpha=\Delta-\frac{1}{2}+n}\end{aligned} \tag{2.6.40}$$

Putting this all together, we can take the identity from Eq. (2.6.32) along with a single operator of small twist in Eq. (2.6.38), expand around $\alpha = \Delta_\phi - \frac{1}{2} + n$ and

divide by $\bar{\alpha}^{2(\Delta_\phi-1)}$ to give

$$\frac{a_{\mathbf{1}}}{\alpha-(\Delta-\frac{1}{2}+n)}+\frac{1}{\bar{\alpha}^{2\beta+1}}\left(\frac{a^{(2)}_{\beta,\bar{\beta}}}{(\alpha-(\Delta-\frac{1}{2}+n))^2}+\frac{a^{(1)}_{\beta,\bar{\beta}}}{\alpha-(\Delta-\frac{1}{2}+n)}\right)+\dots \quad (2.6.41)$$

where

$$\begin{aligned} a_{\mathbf{1}} &\equiv -\frac{\Gamma(2\Delta_\phi-1+n)}{n!\,\Gamma^4(\Delta_\phi)} \\ a^{(2)}_{\beta,\bar{\beta}} &\equiv \frac{\lambda_{\beta,\bar{\beta}}\,Q(-\bar{\beta})\text{Ч}_n(\bar{\beta})}{4\Gamma^2(\Delta_\phi-\frac{1}{2}-\beta)} \\ a^{(1)}_{\beta,\bar{\beta}} &\equiv \frac{\lambda_{\beta,\bar{\beta}}\,Q(-\bar{\beta})\text{Ћ}_n(\bar{\beta})}{4\Gamma^2(\Delta_\phi-\frac{1}{2}-\beta)} \end{aligned} \quad (2.6.42)$$

The final expression should of course have simple rather than double poles, and so terms should exponentiate to something like

$$\text{disc}_{\bar{\alpha}}\big(\hat{\mathcal{G}}(\alpha,\bar{\alpha})\big)\sim\frac{R_n(\bar{\alpha})}{\alpha-(\Delta_\phi-\frac{1}{2}+n+\frac{1}{2}\Gamma_n(\bar{\alpha}))} \quad (2.6.43)$$

close to the pole. Expanding in large $\bar{\alpha}$ and comparing to Eq. (2.6.41), we interpret the residue and the anomalous dimension as

$$R_n(\bar{\alpha})=\bar{\alpha}^{2(\Delta_\phi-1)}\left(a_{\mathbf{1}}+\frac{a^{(1)}_{\beta,\bar{\beta}}}{\bar{\alpha}^{2\beta+1}}+\dots\right) \quad (2.6.44)$$

$$\Gamma_n(\bar{\alpha})=\frac{2a^{(2)}_{\beta,\bar{\beta}}}{a_{\mathbf{1}}\bar{\alpha}^{2\beta+1}}+\dots \quad (2.6.45)$$

That is, the first contribution to the anomalous dimension is

$$\frac{2a^{(2)}_{\beta,\bar{\beta}}}{a_{\mathbf{1}}\bar{\alpha}^{2\beta+1}}=-\frac{\lambda_{\beta,\bar{\beta}}}{\bar{\alpha}^{2\beta+1}}\left(\frac{Q(-\bar{\beta})\Gamma^4(\Delta_\phi)}{2\Gamma^2(\Delta_\phi-\beta-\frac{1}{2})}\right)\left(\frac{n!\,\text{Ч}_n(\bar{\beta},\Delta_\phi)}{\Gamma(2\Delta_\phi-1+n)}\right) \quad (2.6.46)$$

to leading order in large positive $\bar{\alpha}$. As a recap, Eq. (2.6.46) is the leading anomalous contribution to the scaling dimension of $\phi\partial^{m-n}\Box^n\phi$ due to an operator in the t-channel of dimension $\bar{\beta}+\beta+1$ and spin $\bar{\beta}-\beta$ in the large $\bar{\alpha}=m-n$ limit with n finite. Eq. (2.6.46) matches the literature [12] for $n=0$ and it is clear that there is a suppression in (s-channel) spin to the power of (t-channel) twist. Note that we are of course restricting ourselves to $d=2$ theories *without* Virasoro symmetry, so that we can assume a twist gap above the identity.

The subleading terms in Eq. (2.6.44) come from t-channel operators with higher twist but also from subordinate terms in the expansion of the split kernel. For the latter case, the expansion is in integer powers of $1/\bar{\alpha}^2$ with respect to the leading split kernel term, as we saw in Eq. (2.6.18).

The expansion of the split kernel in integer powers of $\bar{\alpha}^{-2}$ corresponds to the 'reciprocity principle' for the double-twist operators that was highlighted in [42]. To see this, we again have to realise that $\mathrm{disc}_{\bar{\alpha}}\Big(\hat{\mathcal{G}}(\alpha,\bar{\alpha})\Big)$ is really a sum of delta functions and that we can undo the averaging in the above formulae by realising that a pole at a given α can only give rise to poles in $\bar{\alpha}$ at the values $\bar{\alpha} = J + \alpha$ with J an (in our case) even integer. The poles in α are at $\Delta_\phi - \frac{1}{2} + n + \frac{1}{2}\Gamma_n(\bar{\alpha})$, which implies that we can substitute $\bar{\alpha}$ for J through

$$\bar{\alpha} = \Delta_\phi - \frac{1}{2} + n + \frac{1}{2}\Gamma_n(\bar{\alpha}) + J \tag{2.6.47}$$

The expansion in even powers of $\bar{\alpha}$ then becomes an expansion in even powers of the square of the right-hand side. For $n = 0$ this is (up to a constant shift) precisely the two-dimensional version of the 'Casimir' defined in [42], whereas the case $n > 0$ was not discussed in that work.

To finish this section, we make a quick comment on the exponentiation of poles. A single split kernel only has double poles but we need to have arbitrarily high-order ones to compare to an expansion of Eq. (2.6.43). This equation gives the requisite poles upon expansion for small $\Gamma_n(\bar{\alpha})$, allowing us to determine the anomalous dimensions as written in Eq. (2.6.46). However if Eq. (2.6.43) is correct then the higher-order terms in the small $\Gamma_n(\bar{\alpha})$ expansion require higher-order poles in α. More precisely, one would expect terms in the discontinuity like

$$\frac{\bar{\alpha}^{2\Delta_\phi - 3 - 2\beta k}}{(\alpha - (\Delta_\phi - \frac{1}{2} + n))^m} \qquad \text{for } k, m \in \mathbb{N} \text{ and } m \leq k + 1 \tag{2.6.48}$$

near the double-twist α-values. A single t-channel block only gives double poles, so this exponentiation of the anomalous dimension is not automatic. What would the t-channel density have to look like to reproduce these singularities?

First of all, the power of $\bar{\alpha}$ in the above expansion indicates that such operators come from t-channel operators with twists that equal $2k\beta + 1$. In other words, the exponentiation of the s-channel anomalous dimensions due to a single t-channel operator $\mathcal{O}_t$ of twist $2\beta + 1$ requires the existence of further t-channel operators with twist $2k\beta + 1$ (the multi-twist versions of the original t-channel operator). A single such multi-twist t-channel operator will not produce the higher-order pole in $\bar{\alpha}$ that the above expression requires, and therefore we actually need an infinite family of such multi-twist t-channel operators. If we think of $\mathcal{O}_t$ as 'single-particle exchange', then a k-particle exchange diagram is necessary to reproduce the $(k+1)$-th order pole in the above expression. Notice furthermore that this k-particle exchange must somehow conspire to give the corresponding higher-order pole for all n.

Whilst we do not fully understand exactly how all of the poles will exponentiate, the take home lesson is that towers of operators are seemingly more natural than isolated poles. This is something that we return to in Section 3.5, where we discuss Regge trajectories.

2.6.3 Crossing Symmetric Example

Here we investigate a density with $\mathbf{a} = \mathbf{b} = 0$ that can be written as a convergent sum over split kernels in some region of the $\alpha, \bar{\alpha}$ plane. The example we have chosen does not have an identity operator in its spectrum because this would shrink away the region of convergence, as discussed in Section 2.6.2.

The function

$$\left(\frac{z\bar{z}}{(1-z)(1-\bar{z})}\right)^{\Delta_\phi/2} \tag{2.6.49}$$

is crossing symmetric, according to Eq. (1.6.1). Therefore, we expect from Eq. (2.1.23) that

$$\frac{\Gamma(\frac{1}{2} \pm \alpha)}{\Gamma(\frac{\Delta_\phi - 1}{2} \pm \alpha)} \int [d\beta]\, K_{\text{split}}(\alpha; \beta | \Delta_\phi) \left(\frac{\Gamma(\frac{\Delta_\phi - 1}{2} \pm \beta)}{\Gamma(\frac{1}{2} \pm \beta)}\right) = 1 \tag{2.6.50}$$

Assuming that the contour can be closed to the right, the left-hand side of Eq. (2.6.50)

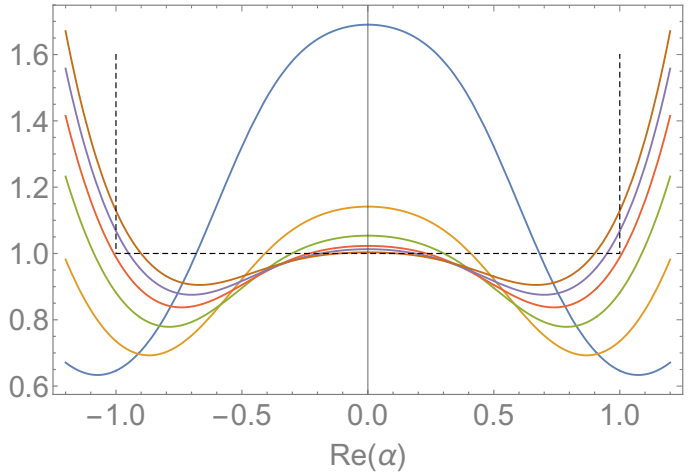

Figure 2.5: The absolute value of the truncated sum in Eq. (2.6.51) is plotted against the real part of α for n_{max} between 0 (blue) and 5 (brown) with $\Delta_\phi = 3$ and $\text{Im}(\alpha) = \frac{1}{2}$. The sum appears to be converging to the dotted black line as n_{max} increases, in agreement with Eq. (2.6.52).

is

$$\frac{\Gamma(\frac{1}{2} \pm \alpha)}{\Gamma(\frac{\Delta_\phi - 1}{2} \pm \alpha)} \sum_{n=0}^{\infty} K_{\text{split}} \left(\alpha \,;\, \frac{\Delta_\phi - 1}{2} + n \,\middle|\, \Delta_\phi \right) \frac{\Gamma(\Delta_\phi - 1 + n)}{n!\,\Gamma(\frac{\Delta_\phi}{2})\Gamma(1 - \frac{\Delta_\phi}{2})} \tag{2.6.51}$$

and so Eq. (2.6.50) can by tested by plugging in values of α, truncating the sum and checking convergence with increasing n_{max}.

Physically, this truncation corresponds to only crossing the $n_{\text{max}} + 1$ t-channel primaries of lowest weight. When it comes to reproducing the correct poles, this approach will never work because a finite sum of split kernels only has double-twist singularities. Note that this is effectively a one-dimensional problem because of the factorisation of the density, and so spin does not play a role.

Using the large β asymptotics of Eq. (2.6.21), the sum will in fact converge whenever

$$2\,|\text{Re}(\alpha)| < \text{Re}(\Delta_\phi) - 1 \tag{2.6.52}$$

and this convergence is tested numerically in Fig. 2.5.

More generally, if the lowest operator contributing to the crossing-symmetric function in Eq. (2.6.50) had been of weight p (rather than simply $\Delta_\phi/2$), then the residue series would have asymptotically gone like $\beta^{2(\Delta_\phi - p - 1)}$ and the region of convergence

would have been

$$2\,|\mathrm{Re}(\alpha)| < 2\mathrm{Re}(p) - 1 \tag{2.6.53}$$

Notice that this means that summing over split kernels will not converge anywhere in the α-plane if there is an identity operator present, as was discussed in Section 2.6.2.

2.6.4 Doubly-Split Kernel

In Eq. (2.6.5), we wrote an s-channel alpha space density as an integral against the product of a t-channel density and the split kernel of Eq. (2.6.6). We then argued that closing the contours to the right gives a sum over split kernels which is formally asymptotic. One way to bypass the issue of non-convergence is to instead consider the doubly-split kernel, built from breaking up Ψ_α. That is,

$$\begin{aligned}\hat{\mathcal{G}}(\alpha,\bar{\alpha}) = \Bigg(\Bigg(\int [d\beta]\int \left[d\bar{\beta}\right] K_{\text{dsplit}}(\alpha;\beta|\Delta_i)K_{\text{dsplit}}(\bar{\alpha};\bar{\beta}|\Delta_i)\hat{\mathcal{G}}'(\beta,\bar{\beta}) \\ + (\alpha\to-\alpha)\Bigg) + (\alpha\leftrightarrow\bar{\alpha})\Bigg)\end{aligned} \tag{2.6.54}$$

where the doubly-split kernel is defined as

$$K_{\text{dsplit}}(\alpha;\beta|\Delta_i) \equiv \frac{Q(\alpha)}{Q'(-\beta)}\int_0^1 dz\,\mu(z)\frac{z^{\frac{\Delta_1+\Delta_2}{2}}}{(1-z)^{\frac{\Delta_3+\Delta_2}{2}}}G_\alpha(z)G'_\beta(1-z) \tag{2.6.55}$$

From the large β asymptotics in Eq. (2.6.21), we see that a sum over doubly-split kernels might converge in one half-plane. The images then need to be added by hand via some analytic continuation. We can see this explicitly by returning to the example of Section 2.6.3. Indeed, we have numerically checked that

$$\begin{aligned}\frac{\Gamma(\frac{1}{2}\pm\alpha)}{\Gamma(\frac{\Delta_\phi-1}{2}\pm\alpha)}\sum_{n=0}^{\infty}K_{\text{dsplit}}\left(\alpha\,;\,\frac{\Delta_\phi-1}{2}+n\,\middle|\,\Delta_\phi\right)\frac{\Gamma(\Delta_\phi-1+n)}{n!\,\Gamma(\frac{\Delta_\phi}{2})\Gamma(1-\frac{\Delta_\phi}{2})} \\ = \frac{1}{2}\left(1-\frac{\tan(\pi\alpha)}{\tan(\pi\Delta_\phi/2)}\right)\end{aligned} \tag{2.6.56}$$

when the real part of α is sufficiently large. Notice that we were fortunate to find the true analytic continuation in this case (we gracelessly broke apart the full density with an educated guess); it is generally not possible to add the images by hand.

Chapter 3

Beyond Two Dimensions

In this chapter, we look to extend the alpha space formalism beyond two dimensions. Once again, the philosophy is to apply a Sturm-Liouville analysis to the quadratic Casimir differential operator in Eq. (1.5.7), which we reproduce here for convenience:

$$\mathcal{D}(z,\bar{z}) \equiv D_z + D_{\bar{z}} + (d-2)\left(\frac{z\bar{z}}{z-\bar{z}}\right)\left((1-z)\frac{\partial}{\partial z} - (1-\bar{z})\frac{\partial}{\partial \bar{z}}\right)$$

$$D_z \equiv z^2(1-z)\frac{\partial^2}{\partial z^2} - (1+\mathbf{a}+\mathbf{b})z^2\frac{\partial}{\partial z} - \mathbf{ab}z$$

Life was made easier for $d = 2$ because $\mathcal{D}(z,\bar{z})$ reduced to $D_z + D_{\bar{z}}$, the sum of two $d = 1$ Casimirs. However, we are not afforded this luxury beyond two dimensions where the differential operator does not factorise as neatly.

In one dimension, the process was fairly algorithmic. Firstly, an inner product was built for which the Casimir is a self-adjoint operator. Secondly, a linear combination of eigenfunctions was found such that the singularities at $z = 1$ cancel to leave us with something finite. This defined $\Psi_\alpha(z)$, which is detailed in Eq. (2.1.8). Since $\langle \Psi_\alpha, \Psi_\beta \rangle$ acts like a delta function along the imaginary axis according to Eq. (2.1.11), an invertible transform could be written down in Eq. (2.1.12). Mathematically speaking, this turned out to be equal to the Jacobi transform up to some substitutions.

The hope is that a similar procedure works in higher dimensions. The asymptotic form of the conformal blocks is known for when z or $\bar{z}$ approaches 1 and so in principle

we can build a combination of eigenfunctions without logarithmic divergences. This defines $\Psi_{\alpha,\bar{\alpha}}(z,\bar{z})$, which can be used as the kernel in an integral transform. Whether or not this is a well-defined and invertible transform will be a matter of debate since the process is somewhat precipitous with two variables to consider. In this work, we offer some corroborating evidence in favour of our transform and we also recognise its limitations. Perhaps most convincingly, the transform seems to reproduce the correct block decompositions, so it is probably a good transform for CFT correlators at least.

After discussing the general transform in Section 3.1 we present the alpha space density for generalised free fields in Section 3.2. Following this, we substantiate the alpha space formalism by looking at four and six dimensions in Section 3.3.

Progress has been slightly hampered in $d = 3$ because the blocks are not known in closed form. However, some headway has been made and we provide some analytical and numerical checks of the three dimensional formalism in Section 3.4.

In the latter parts of the chapter, we comment on what we can learn about Regge behaviour using alpha space in Section 3.5. We then discuss what constant Mellin amplitudes look like in alpha space in Section 3.6. Finally, we outline possible future directions in Section 3.7.

In Sections 3.1, 3.3 and 3.5.3, we allow for non-equal external scalars. For the rest of the chapter, we implicitly work with $\mathbf{a} = \mathbf{b} = 0$ and take the external operators to have scaling dimension Δ_ϕ.

3.1 General Alpha Space Transform

For general $d \geq 2$, the Sturm-Liouville procedure (once again over the Lorentzian interval $z, \bar{z} \in (0,1)$) begins by defining an inner product for two arbitrary functions f and g. In analogy with the $d = 1$ case, this is

$$\langle f, g \rangle \equiv \int_0^1 dz \int_0^1 d\bar{z}\, \mu(z,\bar{z}) f^*(z,\bar{z}) g(z,\bar{z}) \tag{3.1.1}$$

Self-adjointness of $\mathcal{D}$ requires the bracket to satisfy

$$\langle \mathcal{D}\, f, g\rangle - \langle f, \mathcal{D}\, g\rangle = 0 \tag{3.1.2}$$

up to boundary terms, where $\mathcal{D}(z,\bar{z})$ is the quadratic Casimir differential operator defined in Eq. (1.5.7).

Accordingly, the measure μ is found to be

$$\mu(z,\bar{z}) \equiv \left|\frac{\bar{z}-z}{z\bar{z}}\right|^{d-2} \mu(z)\mu(\bar{z}) \tag{3.1.3}$$

where the $d=1$ measure $\mu(z)$ was defined in Eq. (2.1.3).

The next step is to take linear combinations of eigenfunctions of $\mathcal{D}$ that are orthogonal with respect to Eq. (3.1.1). Our approach is to build a candidate for the transform kernel $\Psi_{\alpha,\bar{\alpha}}(z,\bar{z})$ by taking a linear combination of conformal blocks with coefficients chosen such that all of the $z,\bar{z}\to 1$ divergences are tamed. We use the general asymptotics of the blocks because $G_{\alpha,\bar{\alpha}}(z,\bar{z})$ is not known in a closed form for arbitrary dimension.

Taking z close to 0 and $\bar{z}$ close to 1, Eq. (1.5.10) tells us that the pure blocks behave asymptotically like

$$G^{\text{pure}}_{\alpha,\bar{\alpha}}(z,\bar{z}) \xrightarrow{z\to 0} \gamma(\alpha-\bar{\alpha}) z^{\alpha+\frac{d-1}{2}} Q(-\bar{\alpha})\Bigg((1-\bar{z})^{-(\mathbf{a}+\mathbf{b})}\Bigg(\frac{\bar{\alpha}}{\mathbf{a}+\mathbf{b}} + O\Big((1-\bar{z})\Big)\Bigg) + O\Big((1-\bar{z})^0\Big)\Bigg) \tag{3.1.4}$$

where the coefficient function $\gamma(\alpha)$ was defined in Eq. (1.5.11). As a reminder, a full block is the sum of two pure terms according to Eq. (1.5.9).

We can then take the linear combination of full blocks

$$\frac{1}{4}\Big(Q_1(\alpha,\bar{\alpha})G_{\alpha,\bar{\alpha}} + Q_2(\alpha,\bar{\alpha})G_{-\alpha,\bar{\alpha}} + Q_3(\alpha,\bar{\alpha})G_{\alpha,-\bar{\alpha}} + Q_4(\alpha,\bar{\alpha})G_{-\alpha,-\bar{\alpha}}\Big) \tag{3.1.5}$$

with four unknown Q-functions. Expanding using Eqs. (1.5.9) and (3.1.4), we can look at the coefficients of $z^{\pm\alpha}$, $z^{\pm\bar{\alpha}}$ and place constraints on the Q-functions by demanding that the $\bar{z}\to 1$ divergences drop out. Further limitations can be placed

by ensuring the $\alpha \leftrightarrow \bar{\alpha}$ symmetry and by expanding the blocks around $z, \bar{z} = 1$ to fix $\Psi_{\alpha,\bar{\alpha}}(1,1) = 1$.

This procedure uniquely determines $\Psi_{\alpha,\bar{\alpha}}$. By defining $Q(\alpha, \bar{\alpha})$ as

$$Q(\alpha,\bar{\alpha}) \equiv \left(\frac{2\Gamma(\frac{d}{2})\Gamma(\mathbf{a}+\mathbf{b}+\frac{d}{2})}{\Gamma(d-1)\Gamma(\mathbf{a}+\mathbf{b}+1)}\right) Q(\alpha)Q(\bar{\alpha})\gamma(\alpha+\bar{\alpha}) \tag{3.1.6}$$

the asymptotic behaviour of the blocks can be used to confirm that the linear combination

$$\boxed{\Psi_{\alpha,\bar{\alpha}} \equiv \frac{1}{4}\Big(Q(\alpha,\bar{\alpha})G_{\alpha,\bar{\alpha}} + Q(-\alpha,\bar{\alpha})G_{-\alpha,\bar{\alpha}} + Q(\alpha,-\bar{\alpha})G_{\alpha,-\bar{\alpha}} + Q(-\alpha,-\bar{\alpha})G_{-\alpha,-\bar{\alpha}}\Big)} \tag{3.1.7}$$

is perfectly well behaved as z or $\bar{z} \to 1$ and is normalised to $\Psi_{\alpha,\bar{\alpha}}(1,1) = 1$; this can moreover be checked numerically. This combination in Eq. (3.1.7) has been optimistically called $\Psi_{\alpha,\bar{\alpha}}$ and is assumed to be the correct Sturm-Liouville function for the time being. $\Psi_{\alpha,\bar{\alpha}}$ is a highly symmetric combination of pure blocks but it is not the standard conformal partial wave.

In fact, we can take an ansatz for $\Psi_{\alpha,\bar{\alpha}}(z,\bar{z})$ by expanding in non-negative integer powers of $1-z, 1-\bar{z}$. Plugging this in to the Casimir equations, we find that

$$\Psi_{\alpha,\bar{\alpha}}(z,\bar{z}) = 1 + \frac{4(\alpha^2+\bar{\alpha}^2) - d(d-2) - 2 + 8\mathbf{ab}}{4d + 8(\mathbf{a}+\mathbf{b})}(2-z-\bar{z}) + \dots \tag{3.1.8}$$

where the ellipses denote subleading $1-z, 1-\bar{z}$ terms. This is in perfect agreement with an expansion of Eq. (3.1.7).

The transform taking functions (that are square-normalisable with respect to Eq. (3.1.1) and symmetric under $z \leftrightarrow \bar{z}$) to alpha space for general d is then

$$\boxed{\hat{f}(\alpha,\bar{\alpha}) = \int_0^1 dz \int_0^1 d\bar{z}\, \mu(z,\bar{z})\, \Psi_{\alpha,\bar{\alpha}}(z,\bar{z}) f(z,\bar{z})} \tag{3.1.9}$$

the inverse of which is

$$\boxed{f(z,\bar{z}) = \int [d\alpha] \int [d\bar{\alpha}]\, \frac{\Psi_{\alpha,\bar{\alpha}}(z,\bar{z})\hat{f}(\alpha,\bar{\alpha})}{Q(\alpha,\bar{\alpha})Q(-\alpha,-\bar{\alpha})\gamma(\alpha-\bar{\alpha})\gamma(\bar{\alpha}-\alpha)}} \tag{3.1.10}$$

provided that our analysis is legitimate. As in $d = 2$, non-normalisable functions

$\alpha \to -\alpha$	$\Delta \to J + d - 1$ $J \to \Delta + 1 - d$
$\bar{\alpha} \to -\bar{\alpha}$	$\Delta \to 1 - J$ $J \to 1 - \Delta$
$\alpha \leftrightarrow \bar{\alpha}$	$J \to 2 - d - J$
$\alpha \to -\bar{\alpha}$ $\bar{\alpha} \to -\alpha$	$\Delta \to d - \Delta$

Table 3.1: This table shows some alpha space transformations and their equivalents in terms of dimension and spin. The first three are the standard $\mathbb{Z}_2$ symmetries of the Casimir eigenvalues. The fourth is a combination of the others and is known as a shadow-symmetry transformation.

can then be dealt with by deforming the contours and/or applying the Casimir.

The equalities relating $\alpha, \bar{\alpha}$ to the dimension and spin Δ, J are given in Eq. (1.4.8). For convenience, we reproduce them here:

$$\alpha = \frac{\Delta - J + 1 - d}{2} \qquad \Delta = \bar{\alpha} + \alpha + \frac{d}{2}$$
$$\bar{\alpha} = \frac{\Delta + J - 1}{2} \qquad J = \bar{\alpha} - \alpha + 1 - \frac{d}{2}$$

Analogously to the one-dimensional case, it is our hope that $\Psi_{\alpha,\bar{\alpha}}(z,\bar{z})$ acts like a delta-function along the imaginary axis. That is,

$$\int [d\beta] \int \left[d\bar{\beta}\right] \frac{\hat{f}(\beta,\bar{\beta}) \langle \Psi_{\alpha,\bar{\alpha}}, \Psi_{\beta,\bar{\beta}} \rangle}{Q(\alpha,\bar{\alpha}) Q(-\alpha,-\bar{\alpha}) \gamma(\alpha-\bar{\alpha}) \gamma(\bar{\alpha}-\alpha)} = \frac{\hat{f}(\alpha,\bar{\alpha}) + \text{`seven images'}}{8} \tag{3.1.11}$$

where once again the seven images are found from the three $\mathbb{Z}_2$ symmetries[1]. A selection of allowed transformations is listed in Table 3.1, where they are also expressed in terms of spin and dimension.

Using these symmetries, it can be shown that each term in Eq. (3.1.7) contributes equally to the inversion formula of Eq. (3.1.10) and so the split inverse transform is

$$f(z,\bar{z}) = \int [d\alpha] \int [d\bar{\alpha}] \frac{G_{\alpha,\bar{\alpha}}(z,\bar{z}) \hat{f}(\alpha,\bar{\alpha})}{Q(-\alpha,-\bar{\alpha}) \gamma(\alpha-\bar{\alpha}) \gamma(\bar{\alpha}-\alpha)} \tag{3.1.12}$$

For even d, the only poles in the right-hand α and $\bar{\alpha}$ planes come from $\hat{f}(\alpha,\bar{\alpha})$ and

[1] Together they generate the non-abelian dihedral group D_4.

so the explicit map between poles and blocks is then

$$G_{\beta,\bar{\beta}}(z,\bar{z}) \mapsto \left(\frac{Q(-\beta,-\bar{\beta})\gamma(\beta-\bar{\beta})\gamma(\bar{\beta}-\beta)}{2(\alpha-\beta)(\bar{\alpha}-\bar{\beta})} + \text{`seven images'} \right) \qquad (d \text{ even}) \tag{3.1.13}$$

However, when d is odd, the factor $1/\gamma\gamma$ has an infinite series of simple poles for physical spins (whenever $\bar{\alpha}-\alpha+1-\frac{d}{2}$ is a non-negative integer). As a result, the alpha space density must have single poles for operators (for example $\sim(\alpha-\beta)^{-1}$ rather than $\sim(\alpha-\beta)^{-1}(\bar{\alpha}-\bar{\beta})^{-1}$), as appropriate. This behaviour suggests that 'operator trajectories' may be more natural then simple poles, an idea that is investigated in Section 3.5. The fact that the integrand can automatically contain the physical spin poles within the $1/\gamma\gamma$ factor may have forced us to treat odd and even dimensions qualitatively differently. However, densities can often be re-written to include a factor of $\Gamma(-J)$, circumnavigating the problem. As a simple $d=2$ example with $\mathbf{a}=\mathbf{b}=0$, we have that the density for $(z\bar{z})^p$ is

$$\begin{aligned} &\frac{\Gamma(p-\frac{1}{2}\pm\alpha)\Gamma(p-\frac{1}{2}\pm\bar{\alpha})}{\Gamma^4(p)} = \\ &\quad \frac{\Gamma(1-p)\Gamma(p-\frac{1}{2}\pm\alpha)\Gamma(p-\frac{1}{2}+\bar{\alpha})\Gamma(1-\alpha+\bar{\alpha})\Gamma(\alpha-\bar{\alpha})}{4\Gamma^3(p)\Gamma(\frac{1}{2}\pm\alpha)\Gamma(\frac{3}{2}-p+\bar{\alpha})} + \text{`seven images'} \end{aligned} \tag{3.1.14}$$

where $\Gamma(\alpha-\bar{\alpha})=\Gamma(-J)$. This is an infinite series of poles for physical spins which mimics an odd-dimensional $1/\gamma\gamma$ factor.

So far, this analysis has relied heavily on one-dimensional intuition and it is not clear whether Eq. (3.1.10) is truly the inverse of Eq. (3.1.9) with $\Psi_{\alpha,\bar{\alpha}}$ defined in Eq. (3.1.7). Subsequent sections offer some substantiating evidence and check this claim on a case-by-case basis.

To conclude this section, it is interesting to consider $\Psi_{\alpha,\bar{\alpha}}$ with α and $\bar{\alpha}$ set to specific values. As an example, tuning to the stress tensor gives

$$\Psi_T(z,\bar{z}) \equiv \Psi_{-\frac{1}{2},\frac{d+1}{2}}(z,\bar{z})\Big|_{\mathbf{a}=\mathbf{b}=0} = \frac{1}{z}+\frac{1}{\bar{z}}-1 \tag{3.1.15}$$

which is independent of d.

3.1.1 General Split Kernel

As in the $d = 1$ case, a crossing kernel can be defined for arbitrary d by taking the crossing symmetry equation in Eq. (1.6.1) and going to alpha space using Eq. (3.1.9). The resulting integral equation is

$$\hat{\mathcal{G}}(\alpha, \bar{\alpha}) = \int [d\beta] \int \left[d\bar{\beta}\right] K_{\text{split}}(\alpha, \bar{\alpha}; \beta, \bar{\beta}|\Delta_i)\hat{\mathcal{G}}'(\alpha, \bar{\alpha}) \tag{3.1.16}$$

where the split kernel $K_{\text{split}}(\alpha, \bar{\alpha}; \beta, \bar{\beta}|\Delta_i)$ is defined to be

$$K_{\text{split}}(\alpha, \bar{\alpha}; \beta, \bar{\beta}|\Delta_i) = \tag{3.1.17}$$
$$\int_0^1 dz \int_0^1 d\bar{z}\, \frac{\mu(z, \bar{z})(z\bar{z})^{\frac{\Delta_1+\Delta_2}{2}}}{((1-z)(1-\bar{z}))^{\frac{\Delta_3+\Delta_2}{2}}} \frac{\Psi_{\alpha,\bar{\alpha}}(z, \bar{z})G'_{\beta,\bar{\beta}}(1-z, 1-\bar{z})}{Q'(-\beta, -\bar{\beta})\gamma(\beta-\bar{\beta})\gamma(\bar{\beta}-\beta)}$$

where $Q'(\alpha, \bar{\alpha})$ is equal to $Q(\alpha, \bar{\alpha})$ up to the redefinitions in Eq. (1.6.3). The split kernel in four dimensions is discussed in more detail in Section 3.3.1. There we show that it can be written in terms of $d = 1$ kernels.

3.1.2 Lorentzian Inversion Formula

The alpha space integral and its inverse in Eqs. (3.1.9) and (3.1.10) should be compared to Caron-Huot's Lorentzian inversion formula, which first appeared in [16] and is valid down to spin $J > 1$. In our α and $\bar{\alpha}$ variables, it is

$$c^{(t)}(\alpha, \bar{\alpha}) \equiv \frac{\Gamma(\frac{d}{2})}{2\Gamma(d-1)} \int_0^1 dz \int_0^1 d\bar{z}\, \mu(z, \bar{z})\, G_{-\alpha,\bar{\alpha}}(z, \bar{z})\, \text{dDisc}\left[\mathcal{G}(z, \bar{z})\right] \tag{3.1.18}$$

where the double discontinuity is defined as the stripped correlator minus two analytic continuations. Specifically,

$$\text{dDisc}\left[\mathcal{G}(z, \bar{z})\right] \equiv \cos(\pi(\mathbf{a}+\mathbf{b}))\mathcal{G}(z, \bar{z}) - \frac{1}{2}\left(e^{i\pi(\mathbf{a}+\mathbf{b})}\mathcal{G}^{\circlearrowleft}(z, \bar{z}) + e^{-i\pi(\mathbf{a}+\mathbf{b})}\mathcal{G}^{\circlearrowright}(z, \bar{z})\right) \tag{3.1.19}$$

and the arrows indicate the direction that $\bar{z}$ takes around 1. There is also an interesting interpretation of dDisc in terms of commutators. That is, the double discontinuity is equal to $-\frac{1}{2}\langle[\phi_2, \phi_3][\phi_1, \phi_4]\rangle$, which is non-negative in any quantum

field theory due to a Cauchy-Schwartz inequality used in conjunction with Rindler positivity [46].

The full density is then the sum of 't-channel' and 'u-channel' terms, each of which are analytic functions. That is,

$$c(\alpha,\bar{\alpha}) \equiv c^{(t)}(\alpha,\bar{\alpha}) + (-1)^{\bar{\alpha}-\alpha+1-\frac{d}{2}} c^{(u)}(\alpha,\bar{\alpha}) \tag{3.1.20}$$

and $c^{(u)}(\alpha,\bar{\alpha})$ differs from $c^{(t)}(\alpha,\bar{\alpha})$ through the exchange of operators 1 and 2.

The stripped correlator is then equal to

$$\mathcal{G}(z,\bar{z}) = 1 + \sum_{J=0}^{\infty} \int_{\frac{d}{2}-i\infty}^{\frac{d}{2}+i\infty} \frac{d\Delta}{2\pi i} \left. \frac{c(\alpha,\bar{\alpha})\, F_{\alpha,\bar{\alpha}}(z,\bar{z})}{\gamma(\alpha-\bar{\alpha})} \right|_{\alpha=\frac{\Delta-J+1-d}{2},\, \bar{\alpha}=\frac{\Delta+J-1}{2}} \tag{3.1.21}$$

which is the Euclidean inversion formula. It is worth keeping in mind that the s-channel identity operator shown in this expression will only actually be present if $\mathbf{a} = \mathbf{b} = 0$.

The conformal partial wave is

$$F_{\alpha,\bar{\alpha}}(z,\bar{z}) \equiv \frac{1}{2}\Big(\kappa(\alpha,\bar{\alpha}) G_{\alpha,\bar{\alpha}}(z,\bar{z}) + \kappa(-\bar{\alpha},-\alpha) G_{-\bar{\alpha},-\alpha}(z,\bar{z})\Big) \tag{3.1.22}$$

and

$$\kappa(\alpha,\bar{\alpha}) \equiv \frac{\Gamma(\frac{1}{2}+\bar{\alpha}\pm\mathbf{a})\Gamma(\frac{1}{2}+\bar{\alpha}\pm\mathbf{b})\Gamma(\bar{\alpha}+\alpha+\frac{d}{2}-1)}{2\pi^2\Gamma(2\bar{\alpha})\Gamma(2\bar{\alpha}+1)\Gamma(\bar{\alpha}+\alpha)} \tag{3.1.23}$$

The density in Eq. (3.1.18) differs from its definition in the original work in two regards. Firstly, the density here has been made shadow-symmetric and secondly, the blocks in this paper are normalised with a relative factor of γ, as detailed in Section 1.5.2. Similarly, the conformal partial wave is different here. For completeness, shadow-symmetry is invariance under the transformation $(\alpha \to -\bar{\alpha}, \bar{\alpha} \to -\alpha)$ such that $\Delta \to d - \Delta$ whilst the spin J remains unchanged.

The first undeniable advantage to Eq. (3.1.18) is that it has been rigorously derived directly from the well-established Euclidean formula by taking a series of analytic continuations. The second is that Eq. (3.1.21) explicitly includes a sum over J. In contrast, the fact that spin is necessarily restricted to the non-negative integers is

obscured in the alpha space formalism because we have a double contour integral. However, this perhaps is the strength of Eq. (3.1.10) because analyticity in both spin and dimension is more emphatic.

To gain some insight into how our density differs from Eq. (3.1.20), we conclude this section by considering a simple example in $d = 2$ with $\mathbf{a} = \mathbf{b} = 0$. The alpha space density is

$$\left(\frac{z\bar{z}}{(1-z)(1-\bar{z})}\right)^p \mapsto \hat{f}(\alpha,\bar{\alpha}) = \frac{\Gamma^2(1-p)\Gamma(p-\frac{1}{2}\pm\alpha)\Gamma(p-\frac{1}{2}\pm\bar{\alpha})}{\Gamma^2(p)\Gamma(\frac{1}{2}\pm\alpha)\Gamma(\frac{1}{2}\pm\bar{\alpha})} \tag{3.1.24}$$

whereas the density from Eq. (3.1.18) is

$$c^{(t)}(\alpha,\bar{\alpha}) = -\frac{\pi^2\,\Gamma^2(1-p)}{\Gamma^2(p)}\left(\frac{\alpha\bar{\alpha}\,Q(\alpha)Q(-\bar{\alpha})\,\Gamma(p-\frac{1}{2}-\alpha)\Gamma(p-\frac{1}{2}+\bar{\alpha})}{\Gamma(\frac{3}{2}-p-\alpha)\Gamma(\frac{3}{2}-p+\bar{\alpha})}\right) \tag{3.1.25}$$

Therefore, for this example we have that

$$\Big(c^{(t)}(\alpha,\bar{\alpha})Q(-\alpha)Q(\bar{\alpha}) + (\alpha\to-\alpha)\Big) + (\bar{\alpha}\to-\bar{\alpha}) = 4\sin^2(\pi p)\hat{f}(\alpha,\bar{\alpha}) \tag{3.1.26}$$

That is, Caron-Huot's density can be thought of (in this case at least) as a split version of our alpha space density.

3.2 Generalised Free Fields

A generalised free field ϕ is defined to have a stripped correlator equal to a sum of Wick contractions. That is,

$$\langle\phi\phi\phi\phi\rangle = \frac{\mathcal{G}_{\text{GFF}}(z,\bar{z})}{x_{12}^{\Delta_\phi}x_{34}^{\Delta_\phi}} \qquad \mathcal{G}_{\text{GFF}}(z,\bar{z}) \equiv 1 + (z\bar{z})^{\Delta_\phi} + \left(\frac{z\bar{z}}{(1-z)(1-\bar{z})}\right)^{\Delta_\phi} \tag{3.2.1}$$

Since the operator product expansion (OPE) coefficients are known, the corresponding alpha space density $\hat{\mathcal{G}}_{\text{GFF}}(\alpha,\bar{\alpha})$ can be reverse-engineered. We found that

$$\hat{\mathcal{G}}_{\text{GFF}}(\alpha,\bar{\alpha}) = \tag{3.2.2}$$
$$\left(1 - \frac{\cos(\pi\alpha)\cos(\pi\bar{\alpha})}{\sin(\pi\Delta_\phi)\sin(\pi(\Delta_\phi-\frac{d}{2}))}\right)\frac{\Gamma(d-1)\Gamma(\Delta_\phi-\frac{d-1}{2}\pm\alpha)\Gamma(\Delta_\phi-\frac{d-1}{2}\pm\bar{\alpha})}{\Gamma^2(\Delta_\phi)\Gamma^2(\Delta_\phi+1-\frac{d}{2})}$$

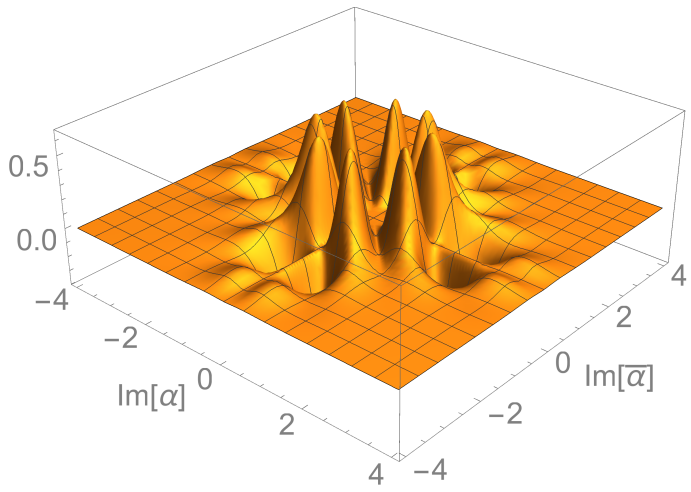

Figure 3.1: Plotted is the $d = 4$ integrand in Eq. (3.2.7) against imaginary α and $\bar{\alpha}$ for $\Delta_\phi = \frac{11}{5}$, $z = \frac{1}{3}$ and $\bar{z} = \frac{1}{4}$. Numerically integrating under this graph gives 1, in support of the hypothesised alpha space density for $(z\bar{z})^{\Delta_\phi}$, which is the first term in Eq. (3.2.2). Note that Δ_ϕ has been chosen to be large enough to ensure that the contours along the imaginary axes separate left- and right-running sequences of poles without the need for any deformations.

which can be inverted using Eq. (3.1.10) to give

$$\mathcal{G}_{\text{GFF}}(z,\bar{z}) = 1 + \sum_{\substack{m,n=0 \\ m\geq n}} \text{Res}\left(\frac{2\,\hat{\mathcal{G}}_{\text{GFF}}(\alpha,\bar{\alpha})}{Q(-\alpha,-\bar{\alpha})\gamma(\alpha-\bar{\alpha})\gamma(\bar{\alpha}-\alpha)}\right)\Bigg|_{\substack{\alpha=\alpha_n \\ \bar{\alpha}=\bar{\alpha}_m}} G_{\alpha_n,\bar{\alpha}_m}(z,\bar{z}) \tag{3.2.3}$$

where

$$\alpha_n \equiv \Delta_\phi - \frac{d-1}{2} + n \qquad \bar{\alpha}_m \equiv \Delta_\phi - \frac{1}{2} + m \tag{3.2.4}$$

Eq. (3.2.3) is true for arbitrary $d \geq 2$. Note that although $\hat{\mathcal{G}}_{\text{GFF}}(\alpha,\bar{\alpha})$ has poles at unphysical spins when d is odd, these are cancelled by zeros in $1/\gamma\gamma$. As an example of this, $\hat{\mathcal{G}}_{\text{GFF}}(\alpha,\bar{\alpha})$ for $d = 3$ has right-running poles for $\alpha, \bar{\alpha} = \Delta_\phi - 1 + \mathbb{N}$. These would naively imply half-integer spins because of how $\alpha, \bar{\alpha}$ are related to Δ, J through Eq. (1.4.8). However, the factor $(\gamma(\alpha-\bar{\alpha})\gamma(\bar{\alpha}-\alpha))^{-1}$ has zeros at these points. In fact,

$$\frac{1}{\gamma(\alpha-\bar{\alpha})\gamma(\bar{\alpha}-\alpha)}\bigg|_{d=3} = \frac{\pi\,\Gamma(\frac{1}{2} \pm (\bar{\alpha}-\alpha))}{\Gamma(\pm(\bar{\alpha}-\alpha))} \tag{3.2.5}$$

so this term is the source of the physical poles as well as the necessary zeros.

As a quick consistency check for the generalised free field density, α and $\bar{\alpha}$ can be tuned to the stress tensor values such that $\Psi_{\alpha,\bar{\alpha}}$ is given by Eq. (3.1.15). The integral taking the function $(z\bar{z})^{\Delta_\phi}$ to alpha space can then be done explicitly to give

$$2\int_0^1 \frac{d\bar{z}}{\bar{z}^2}\int_0^{\bar{z}} \frac{dz}{z^2}\left(\frac{\bar{z}-z}{z\bar{z}}\right)^{d-2}(z\bar{z})^{\Delta_\phi}\left(\frac{1}{z}+\frac{1}{\bar{z}}-1\right)=\frac{2\Delta_\phi\Gamma(d-1)\Gamma(\Delta_\phi-d)}{(2\Delta_\phi-d)\Gamma(\Delta_\phi)} \tag{3.2.6}$$

which matches the first term in Eq. (3.2.2) for $\alpha=-\frac{1}{2},\bar{\alpha}=\frac{d+1}{2}$.

Fig. 3.1 plots the $d=4$ integrand

$$\left.\frac{\Psi_{\alpha,\bar{\alpha}}(z,\bar{z})\Gamma(d-1)\Gamma(\Delta_\phi-\frac{d-1}{2}\pm\alpha)\Gamma(\Delta_\phi-\frac{d-1}{2}\pm\bar{\alpha})}{(2\pi)^2Q(\alpha,\bar{\alpha})Q(-\alpha,-\bar{\alpha})\gamma(\alpha-\bar{\alpha})\gamma(\bar{\alpha}-\alpha)\Gamma^2(\Delta_\phi)\Gamma^2(\Delta_\phi+1-\frac{d}{2})(z\bar{z})^{\Delta_\phi}}\right|_{d=4} \tag{3.2.7}$$

against imaginary α and $\bar{\alpha}$. Numerically integrating this tells us that the area under the plot is equal to 1, in support of the alpha space density in Eq. (3.2.2). One obvious feature of this figure is the eight-fold symmetry from the three $\mathbb{Z}_2$ symmetries.

3.3 Four and Six Dimensions

In even dimensions, the conformal blocks are known in closed form in terms of hypergeometric functions. The $d=4$ and $d=6$ blocks were given in Eqs. (1.5.16) and (1.5.17) respectively.

3.3.1 Four Dimensions

In four dimensions, the definition in Eq. (3.1.7) gives $\Psi_{\alpha,\bar{\alpha}}(z,\bar{z})$ as a symmetrised sum over four blocks. A $d=4$ block can be written in terms of one-dimensional blocks and we found that it is possible to express $\Psi_{\alpha,\bar{\alpha}}(z,\bar{z})$ in terms of one-dimensional Ψ-functions. Explicitly,

$$\Psi_{\alpha,\bar{\alpha}}(z,\bar{z})=\left(\frac{z\bar{z}}{\bar{z}-z}\right)\frac{\Psi_\alpha(z)\Psi_{\bar{\alpha}}(\bar{z})-\Psi_\alpha(\bar{z})\Psi_{\bar{\alpha}}(z)}{\alpha^2-\bar{\alpha}^2}(1+\mathbf{a}+\mathbf{b}) \tag{3.3.1}$$

The benefit of writing $\Psi_{\alpha,\bar{\alpha}}$ like this is that the $d = 1$ orthogonality relation in Eq. (2.1.11) can used to quickly confirm that Eq. (3.1.11) holds for $d = 4$. The derivation starts by noting that

$$\langle \Psi_{\alpha,\bar{\alpha}}, \Psi_{\beta,\bar{\beta}} \rangle = \frac{2(1+\mathbf{a}+\mathbf{b})^2}{(\alpha^2-\bar{\alpha}^2)(\beta^2-\bar{\beta}^2)} \Big(\langle \Psi_\alpha, \Psi_\beta \rangle \langle \Psi_{\bar{\alpha}}, \Psi_{\bar{\beta}} \rangle - \langle \Psi_{\bar{\alpha}}, \Psi_\beta \rangle \langle \Psi_\alpha, \Psi_{\bar{\beta}} \rangle \Big) \quad (3.3.2)$$

such that

$$\begin{aligned} &\int [d\beta] \int \left[d\bar{\beta}\right] \frac{\hat{f}(\beta,\bar{\beta}) \langle \Psi_{\alpha,\bar{\alpha}}, \Psi_{\beta,\bar{\beta}} \rangle}{Q(\alpha,\bar{\alpha}) Q(-\alpha,-\bar{\alpha}) \gamma(\alpha-\bar{\alpha}) \gamma(\bar{\alpha}-\alpha)} \qquad (3.3.3) \\ &\quad = \int [d\beta] \int \left[d\bar{\beta}\right] \left(\frac{2(\alpha^2-\bar{\alpha}^2)\hat{f}(\beta,\bar{\beta})}{\beta^2-\bar{\beta}^2} \right) \frac{\langle \Psi_\alpha, \Psi_\beta \rangle \langle \Psi_{\bar{\alpha}}, \Psi_{\bar{\beta}} \rangle - \langle \Psi_{\bar{\alpha}}, \Psi_\beta \rangle \langle \Psi_\alpha, \Psi_{\bar{\beta}} \rangle}{Q(\alpha) Q(\bar{\alpha}) Q(-\alpha) Q(-\bar{\alpha})} \\ &\quad = \int [d\beta] \, (\alpha^2-\bar{\alpha}^2) \left[\frac{\langle \Psi_\alpha, \Psi_\beta \rangle}{Q(\alpha)Q(-\alpha)} \left(\frac{\hat{f}(\beta,\bar{\alpha}) + \hat{f}(\beta,-\bar{\alpha})}{2(\beta^2-\bar{\alpha}^2)} \right) \right. \\ &\qquad\qquad \left. - \frac{\langle \Psi_{\bar{\alpha}}, \Psi_\beta \rangle}{Q(\bar{\alpha})Q(-\bar{\alpha})} \left(\frac{\hat{f}(\beta,\alpha) + \hat{f}(\beta,-\alpha)}{2(\beta^2-\alpha^2)} \right) \right] \\ &\quad = \frac{\hat{f}(\alpha,\bar{\alpha}) + \text{`seven images'}}{8} \end{aligned}$$

Therefore Eq. (3.1.10) is indeed the inverse of the alpha space transform in Eq. (3.1.9), at least in this number of dimensions.

A second benefit of this representation is that the split kernel of Eq. (3.1.17) can be written in terms of $d = 1$ kernels. This is done by starting with the definition of the kernel in Eq. (3.1.17) and substituting in Eqs. (1.5.16) and (3.3.1). All in all, we found that

$$\begin{aligned} &K_{\text{split}}(\alpha,\bar{\alpha};\beta,\bar{\beta}|\Delta_i) = \qquad (3.3.4) \\ &\quad -\frac{1}{2} \left(\frac{1+\mathbf{a}+\mathbf{b}}{1+\mathbf{a}'+\mathbf{b}'} \right) \left(\frac{\beta^2-\bar{\beta}^2}{\alpha^2-\bar{\alpha}^2} \right) K_{\text{split}}(\alpha;\beta|\Delta_i-1) K_{\text{split}}(\bar{\alpha};\bar{\beta}|\Delta_i-1) + (\alpha \leftrightarrow \bar{\alpha}) \end{aligned}$$

The shorthand $\Delta_i - 1$ here means that each external dimension has been reduced by 1 with respect to the kernel in Section 2.6.1. That is,

$$K_{\text{split}}(\alpha;\beta|\Delta_i-1) = \frac{2}{Q'(-\beta)} \int_0^1 dz \, \mu(z) \frac{z^{\frac{\Delta_1-1+\Delta_2-1}{2}}}{(1-z)^{\frac{\Delta_3-1+\Delta_2-1}{2}}} \Psi_\alpha(z) G'_\beta(1-z) \quad (3.3.5)$$

Eq. (3.3.4) is arguably the most important result in this work. It gives the $d = 4$

split crossing kernel in terms of gamma and analytic Wilson functions, after using Eq. (2.6.25) to rewrite $K_{\text{split}}(\alpha;\beta|\Delta_i - 1)$. We can integrate a density against the kernel in Eq. (3.3.4) to determine the crossed-channel density.

Performing a calculation analogous to the one in Section 2.6.2, we found that the leading $d = 4$ asymptotic correction to the anomalous dimension of $\phi\partial^J\Box^n\phi$ due to a single t-channel operator is

$$-\frac{\lambda_{\beta,\bar{\beta}}}{(J/2)^{2\beta+3}}\left(\frac{Q(-\bar{\beta})\Gamma^2(\Delta_\phi)\Gamma^2(\Delta_\phi-1)}{(\bar{\beta}-\beta)\Gamma^2(\Delta_\phi-\beta-\frac{3}{2})}\right)\left(\frac{n!\,\text{ɥ}_n(\bar{\beta},\Delta_\phi-1)}{\Gamma(2\Delta_\phi-3+n)}\right) \tag{3.3.6}$$

Once again, there is a suppression in spin to the power of twist. Since Eqs. (2.6.46) and (3.3.6) are so similar, we tentatively hypothesise the d-dimensional result as

$$-\frac{\lambda_{\beta,\bar{\beta}}}{(J/2)^{2\beta+d-1}}\left(\frac{Q(-\bar{\beta})\Gamma^2(\Delta_\phi)\Gamma^2(\Delta_\phi+1-\frac{d}{2})\gamma(\beta-\bar{\beta})}{\Gamma^2(\Delta_\phi-\beta-\frac{d-1}{2})}\right)\left(\frac{n!\,\text{ɥ}_n(\bar{\beta},\Delta_\phi+1-\frac{d}{2})}{\Gamma(2\Delta_\phi+1-d+n)}\right) \tag{3.3.7}$$

For $n = 0$, this matches the literature [12]. When comparing our work to the citation, please remember that we include a factor of $\gamma(\beta-\bar{\beta})$ which comes from the normalisation conventions set out in Section 1.5.2.

3.3.2 Six Dimensions

As in four dimensions, the $d = 6$ version of $\Psi_{\alpha,\bar{\alpha}}(z,\bar{z})$ can be massaged into a representation composed of $d = 1$ functions. We found that

$$\Psi_{\alpha,\bar{\alpha}}(z,\bar{z}) = \Bigg(-\frac{3\Psi_\alpha(z)}{2\bar{\alpha}(\bar{\alpha}^2-\alpha^2)}\left(\frac{z\bar{z}}{\bar{z}-z}\right)^3\left(\frac{(2\bar{\alpha}-1)\Psi_{\bar{\alpha}-1}(\bar{z})}{(\bar{\alpha}-1)^2-\alpha^2}+\frac{(2\bar{\alpha}+1)\Psi_{\bar{\alpha}+1}(\bar{z})}{(\bar{\alpha}+1)^2-\alpha^2}\right) + (z\leftrightarrow\bar{z})\Bigg) + (\alpha\leftrightarrow\bar{\alpha}) \tag{3.3.8}$$

where **a** and **b** have been set to zero to ease notation, as in Eq. (1.5.17) where the $d = 6$ block was defined.

Analogously to the derivation in Eq. (3.3.3), the $d = 6$ representation of $\Psi_{\alpha,\bar{\alpha}}(z,\bar{z})$ in terms of $d = 1$ functions can be used to prove the orthogonality relation of Eq. (3.1.11).

3.4 Three Dimensions

Unfortunately, the alpha space formalism set out in Section 3.1 is not as easy to implement in odd dimensions. In essence, this is because the blocks $G_{\alpha,\bar{\alpha}}(z,\bar{z})$ are not known in a closed form. Therefore, we cannot write Eq. (3.1.7) in terms of a finite[2] sum of hypergeometric functions, which would have allowed us to calculate some alpha space densities in the usual manner.

However, the function $\Psi_{\alpha,\bar{\alpha}}(z,\bar{z})$ can still be expressed as a series expansion around $z,\bar{z}=1$. With Eqs. (3.3.1) and (3.3.8) in mind, a sensible ansatz for $d=3$ is

$$\Psi_{\alpha,\bar{\alpha}}(z,\bar{z}) = \sum_{n,m=0}^{\infty} a(n,m) \left(\frac{z-1}{z}\right)^n \left(\frac{\bar{z}-1}{\bar{z}}\right)^m \tag{3.4.1}$$

where the coefficients are symmetric in $m \leftrightarrow n$ and the function is normalised to 1 at $z=\bar{z}=1$. That is,

$$a(n,m) = a(m,n) \qquad a(0,0) = 1 \tag{3.4.2}$$

The quadratic and quartic Casimir equations in Eqs. (1.5.6) and (1.5.8) can then be used to derive recursion relations for $a(n,m)$. With $d=3$, the function $\Psi_{\alpha,\bar{\alpha}}(z,\bar{z})$ satisfies

$$\mathcal{D}\Psi_{\alpha,\bar{\alpha}} = \left(\bar{\alpha}^2 + \alpha^2 - \frac{5}{4}\right)\Psi_{\alpha,\bar{\alpha}} \tag{3.4.3}$$

and

$$\left(\frac{z\bar{z}}{z-\bar{z}}\right)(D_z - D_{\bar{z}})\left(\frac{z-\bar{z}}{z\bar{z}}\right)(D_z - D_{\bar{z}})\,\Psi_{\alpha,\bar{\alpha}}(z,\bar{z}) = \left(\alpha^4 + \bar{\alpha}^4 - \frac{\alpha^2+\bar{\alpha}^2}{2} - 2\alpha^2\bar{\alpha}^2 + \frac{1}{16}\right)\Psi_{\alpha,\bar{\alpha}}(z,\bar{z}) \tag{3.4.4}$$

with

$$\mathcal{D}(z,\bar{z}) \equiv D_z + D_{\bar{z}} + \left(\frac{z\bar{z}}{z-\bar{z}}\right)\left((1-z)\frac{\partial}{\partial z} - (1-\bar{z})\frac{\partial}{\partial \bar{z}}\right) \tag{3.4.5}$$

Plugging the ansatz from Eq. (3.4.1) into these differential equations, we found that

[2] It might be possible to write $\Psi_{\alpha,\bar{\alpha}}(z,\bar{z})$ for $d=3$ as an *infinite* sum over hypergeometrics using the results of [47]. That paper used dimensional reduction to write d-dimensional blocks as infinite sums over $(d-1)$-dimensional blocks.

n \ m	0	1	2	3
0	1	-5	9	-5
1	-5	6	-3	0
2	9	-3	0	0
3	-5	0	0	0

Table 3.2: This table gives the values of $a(n,m)$ appearing in the $d=3$ ansatz sum for $\Psi_{\alpha,\bar{\alpha}}$ (Eq. (3.4.1)) for the case of $\alpha=-\frac{1}{2}$, $\bar{\alpha}=4$. These values of α and $\bar{\alpha}$ correspond to the spin-4 conserved current. The sum terminates in this case and these are the only non-zero terms.

$a(n,m)$ satisfies

$$\begin{aligned} a(n,0) = &\left(\frac{(2n-1)(8n(n-1)+5-4(\alpha^2+\bar{\alpha}^2))}{4n^2(2n+1)}\right)a(n-1,0) \\ &-\left(\frac{4(n-1+\alpha)(n-1-\alpha)(n-1+\bar{\alpha})(n-1-\bar{\alpha})}{n^2(4n^2-1)}\right)a(n-2,0) \end{aligned} \tag{3.4.6}$$

and

$$\begin{aligned} a(n,m) = \frac{1}{4m^2}\Bigg(&\Big(4(m+n+1)(m-n-2)\Big)a(n+1,m-1) \\ &+\Big(4m(m-1)+4n(n+2)+5-4(\alpha^2+\bar{\alpha}^2)\Big)a(n,m-1) \\ &+\Big(4(n+2)^2\Big)a(n+2,m-2) \\ &-\Big(4m(m-2)+4n(n+3)+13-4(\alpha^2+\bar{\alpha}^2)\Big)a(n+1,m-2)\Bigg) \end{aligned} \tag{3.4.7}$$

These are slightly unwieldy but no worse than the usual recursion relations for the $d=3$ conformal block. Fig. 3.2 plots a finite number of terms from the ansatz sum with $z=\bar{z}$ to check that it converges to the true function.

In fact, we found that Eqs. (3.4.6) and (3.4.7) can be solved with α and $\bar{\alpha}$ suitably tuned. As a first example, for values corresponding to the spin $J\in\mathbb{Z}^{\geq 1}$ conserved current we found that the sum truncates to

$$\begin{aligned} &\Psi_{-\frac{1}{2},J}(z,\bar{z}) = \\ &\sum_{\substack{m,n=0\\ m+n<J}} \frac{(-4)^{n+m}(J+n+m)!\,\Gamma(n+\frac{1}{2})\Gamma(m+\frac{1}{2})}{J\pi\, n!\, m!\,\Gamma(J-n-m)\Gamma(2(1+n+m))}\left(\frac{z-1}{z}\right)^n\left(\frac{\bar{z}-1}{\bar{z}}\right)^m \end{aligned} \tag{3.4.8}$$

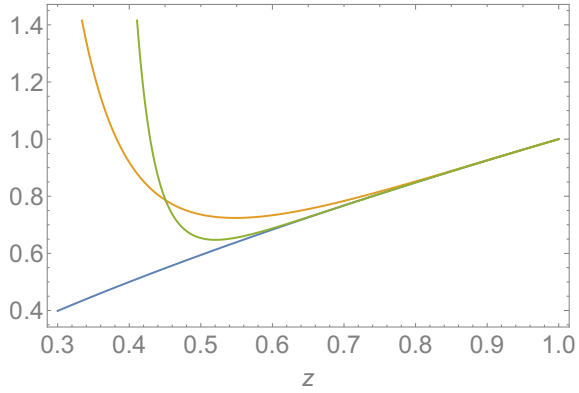

Figure 3.2: This figure plots the ansatz sum in Eq. (3.4.1) up to $n, m = 2$ (orange) and $n, m = 6$ (green) against z with $\bar{z} = z$, $\alpha = \frac{1}{3}$, $\bar{\alpha} = \frac{1}{5}$. As more terms are kept, the sum converges to the true function $\Psi_{\alpha,\bar{\alpha}}(z, z)$ (blue) which we know from Eqs. (1.5.18) and (3.1.7).

Table 3.2 shows all of the non-zero coefficients $a(n, m)$ for $\Psi_{-\frac{1}{2},4}(z, \bar{z})$, which corresponds to the spin-4 conserved current.

As a second example, we found that the recursion relations can be solved when α and $\bar{\alpha}$ are tuned to scalar values. In this case, $\Psi_{\alpha,\bar{\alpha}}$ becomes

$$\Psi_{\frac{\Delta-2}{2},\frac{\Delta-1}{2}}(z,\bar{z}) = \sum_{n,m=0}^{\infty} \frac{\sqrt{\pi}(n+m)!\Gamma(n+\frac{\Delta}{2})\Gamma(n+\frac{3-\Delta}{2})\Gamma(m+\frac{\Delta}{2})\Gamma(m+\frac{3-\Delta}{2})}{2(n!)^2(m!)^2\Gamma(n+m+\frac{3}{2})\Gamma^2(\frac{3-\Delta}{2})\Gamma^2(\frac{\Delta}{2})} \left(\frac{z-1}{z}\right)^n \left(\frac{\bar{z}-1}{\bar{z}}\right)^m \tag{3.4.9}$$

which is significant because a closed-form expression for the scalar block itself is not known. Interestingly, this simplifies to

$$\Psi_{\frac{\Delta-2}{2},\frac{\Delta-1}{2}}(z,1) = {}_2F_1\left(\frac{3-\Delta}{2}, \frac{\Delta}{2}; \frac{3}{2}; -\frac{1-z}{z}\right) \tag{3.4.10}$$

for[3] $\bar{z} = 1$.

3.4.1 Tests for $d = 3$

Here we present some tests of the $d = 3$ alpha space transform, its inverse and the recursion relations for $\Psi_{\alpha,\bar{\alpha}}$. Whilst none conclusively prove the validity of

[3] Intriguingly, this is equal to the $d = 1$ alpha space function $z^{\mathbf{a}}\Psi_\alpha(z)$ with $\mathbf{a} = \mathbf{b} = \frac{1}{4}$ and $\alpha = \frac{2\Delta-3}{4}$. This reminds us of work done on the crosscap [48] and it would be interesting to further understand how this phenomenon emerges at the boundary $\bar{z} = 1$.

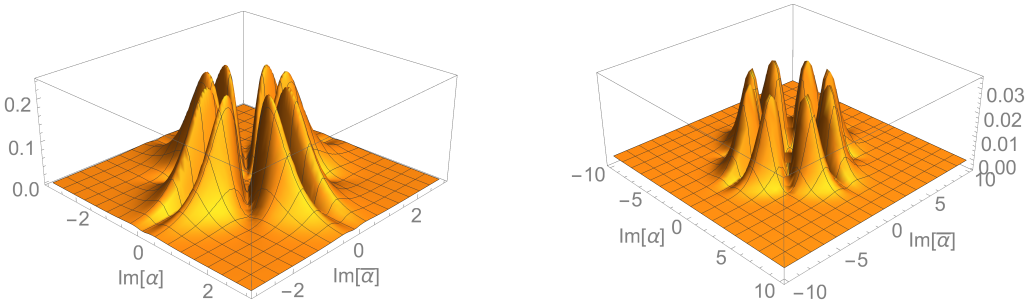

(a) $(z\bar{z})^p$: $z = \bar{z} = \frac{8}{9}$, $p = \frac{5}{4}$. (b) $\frac{\partial^3 (z\bar{z})^p}{\partial z^2 \partial \bar{z}}$: $z = \bar{z} = 1$, $p = \frac{9}{4}$.

Figure 3.3: Plotted are two inverse alpha space integrands, normalised by the apposite position space terms. Fig. 3.3a is for $(z\bar{z})^p$ on the diagonal, where we use an exact expression for $\Psi_{\alpha,\bar{\alpha}}(z,z)$ using Eqs. (1.5.18) and (3.1.7). Fig. 3.3b is for $\frac{\partial^3 (z\bar{z})^p}{\partial z^2 \partial \bar{z}}$ at $z = \bar{z} = 1$ where we use $\frac{\partial^3 \Psi_{\alpha,\bar{\alpha}}(z,\bar{z})}{\partial z^2 \partial \bar{z}}\Big|_{z=\bar{z}=1}$, equal to $2(a(2,1) - a(1,1))$. The recursion relations in Eqs. (3.4.6) and (3.4.7) are used to find $a(n,m)$. Numerically integrating, we found that the area under each graph is 1, in support of the inverse alpha space transform of Eq. (3.1.9).

Eqs. (3.1.9) and (3.1.10), they are at least pleasing and reassuring.

Exact Check

As an exact check, we note that the recursion relations of Eqs. (3.4.6) and (3.4.7) can be solved exactly for the conserved currents where $J \in \mathbb{Z}^{\geq 1}$ and the ansatz sum terminates to Eq. (3.4.8). Therefore, we can exactly perform the integral

$$2\int_0^1 \frac{d\bar{z}}{\bar{z}^2} \int_0^{\bar{z}} \frac{dz}{z^2} \left(\frac{\bar{z}-z}{z\bar{z}}\right) (z\bar{z})^p \, \Psi_{-\frac{1}{2},J}(z,\bar{z}) = \frac{2\Gamma(p-1\pm J)}{\Gamma^2(p)(2p-3)} \tag{3.4.11}$$

which is in exact agreement with the density for $(z\bar{z})^p$ given by the first term in Eq. (3.2.2) after replacing Δ_ϕ with p.

Numerical Checks

A couple of numerical checks are plotted in Fig. 3.3. The plots show two normalised inverse alpha space integrands in the imaginary $\alpha, \bar{\alpha}$ plane. The area under each graph is equal to 1, as predicted by the inverse alpha space transform of Eq. (3.1.9).

Notice that once again the eight-fold $\mathbb{Z}_2$ symmetry is present in the plots and this makes the numerical integration less computationally expensive.

3.5 Regge Behaviour

In Section 3.1, we noticed that the $1/\gamma\gamma$ factor in the inverse alpha space integral of Eq. (3.1.10) has poles at values corresponding to physical spins for odd dimensions. Furthermore, we mentioned that this hints that operator trajectories may be more natural than isolated poles. In this section, we make this statement more precise in three dimensions. We then hypothesis what Regge trajectories [49] look like in alpha space in Section 3.5.1 before asking what we can learn about the Regge limit in Section 3.5.2.

Consider a $d = 3$ alpha space density of the form

$$\hat{f}(\alpha, \bar{\alpha}) = \hat{f}(\bar{\alpha}) \left(\frac{1}{\alpha - \beta(\bar{\alpha})} - \frac{1}{\alpha + \beta(\bar{\alpha})} \right) + (\alpha \leftrightarrow \bar{\alpha}) \tag{3.5.1}$$

where we assume that $\hat{f}(\bar{\alpha})$ and $\beta(\bar{\alpha})$ are both analytic and even functions. We also assume that the equation $\bar{\alpha} = \beta(\bar{\alpha}) + \frac{1}{2} + n$ has a unique solution for $n \in \mathbb{N}$, which we call $\bar{\alpha}_n$ with $\beta_n \equiv \beta(\bar{\alpha}_n)$. The picture that we have in mind is drawn schematically in Fig. 3.4.

Plugging this density into the inverse alpha space integral, splitting in the usual manner and closing the α and $\bar{\alpha}$ contours to the right gives

$$\sum_{n=0}^{\infty} \frac{2(1+2n)(2\beta_n + n)\gamma(-(2\beta_n + n))f(\beta_n + \frac{1}{2} + n)}{Q(-(\beta_n + \frac{1}{2} + n))Q(-\beta_n)} G_{\beta_n, \beta_n + \frac{1}{2} + n}(z, \bar{z}) \tag{3.5.2}$$

as the position space analogue of $\hat{f}(\alpha, \bar{\alpha})$. This is a sum over operators lying on a trajectory and approaching constant twist β_∞. This is known as a Regge trajectory.

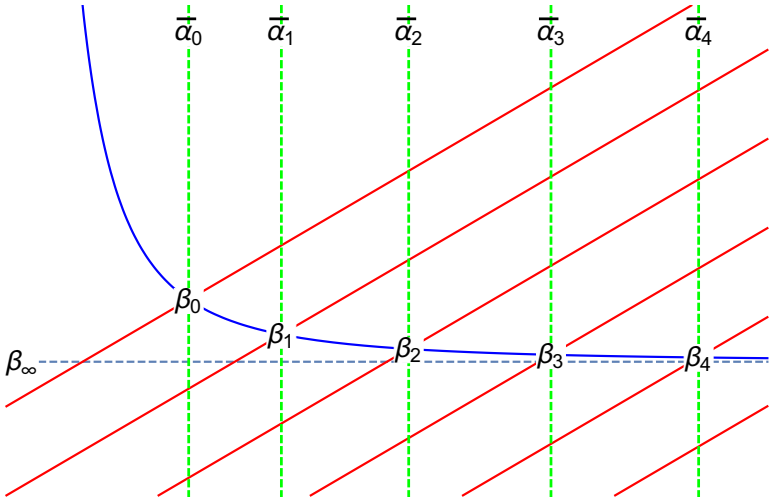

Figure 3.4: Plotted is a schematic for β (blue line) as a function of $\bar{\alpha}$. The equation $\bar{\alpha} = \beta(\bar{\alpha}) + \frac{1}{2} + n$ has a unique solution for $n \in \mathbb{N}$, which we call $\bar{\alpha}_n$ with $\beta_n \equiv \beta(\bar{\alpha}_n)$. The topmost red line corresponds to $n = 0$, the next is $n = 1$ and so on. The green lines mark the intersection points and asymptote to have integer spacing as n becomes large. This defines a Regge trajectory in $d = 3$, as discussed in the text of Section 3.5.

3.5.1 Analyticity and Regge Trajectories

In Fig. 3.5, we hypothesis analytic structure in alpha space by drawing Regge trajectories in the real α, $\bar{\alpha}$ plane. We only draw them from a physical pole off to constant twist as we are unsure how or if individual trajectories will match up. If we can smoothly deform a physical pole along a line of constant spin from the 'GFF-like' picture of Fig. 3.5a to Fig. 3.5b then the trajectory should presumably go on to turn and asymptote to the blue dashed line once again, as we have plotted.

In Fig. 3.5c, the original pole has been shifted to such an extent that it has left the physical zone. In our picture, the image that it exchanges with becomes the physical pole and we have marked this in blue. Importantly, this allows for the image of one operator to lie on the Regge trajectory of some other physical operator. This phenomenon has been commented on before [50].

Finally, we remark upon the curious case of Fig. 3.5d. Here, the deformation has been tuned so that one of the images is physical. It would be interesting to understand whether or not this situation could be realised in a conformal field theory.

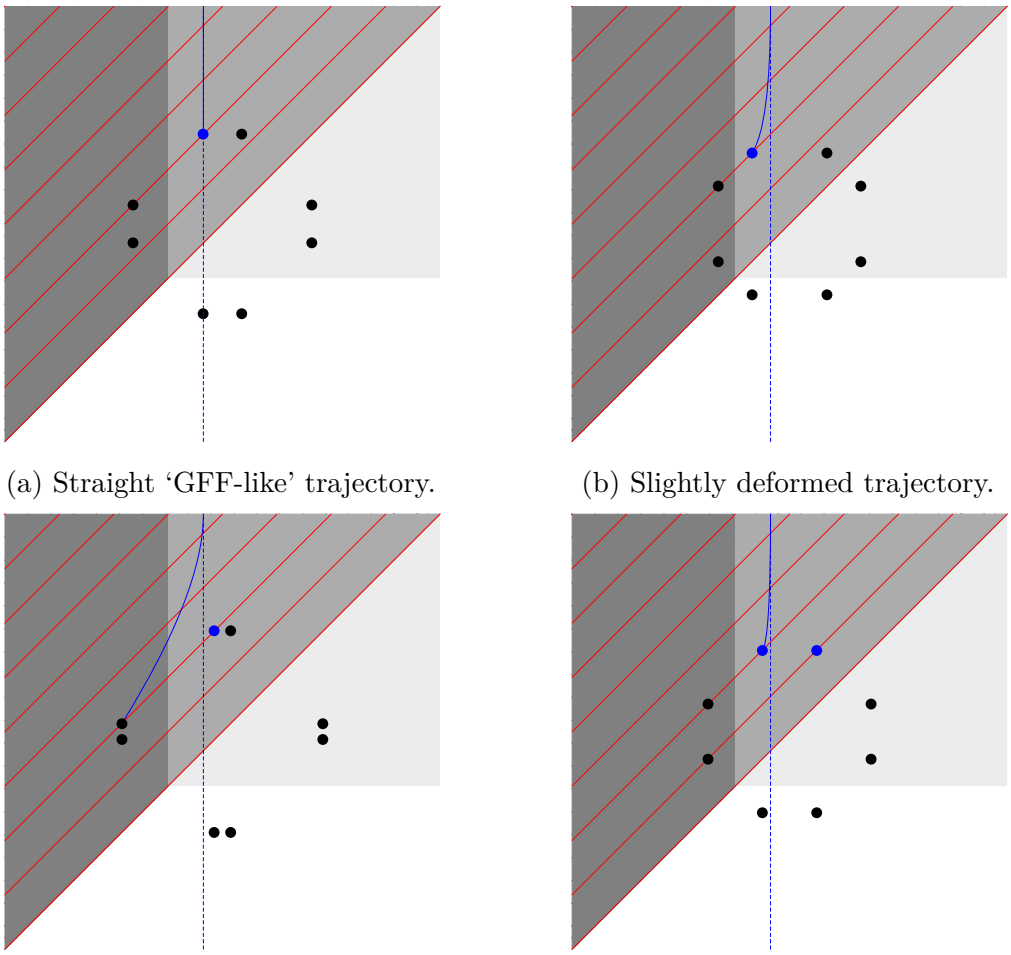

(a) Straight 'GFF-like' trajectory.

(b) Slightly deformed trajectory.

(c) Leaving the physical triangle.

(d) Fine-tuning.

Figure 3.5: Here we plot a hypothesised picture of an operator and its shadows in the real α, $\bar{\alpha}$ plane. The physical pole is marked in blue and the black dots are its images. The pole is part of a Regge trajectory (blue line) that tends to a constant twist. The light grey box denotes the region where the dimension is greater than zero and the dark grey triangle marks the positive spin zone. The medium-tone grey overlap is then where physical operators can live, although images may also be present here. Integer spins are marked by the red lines, the right-most one being the spin-zero line. The individual plots themselves are discussed in Section 3.5.1. This plot is for $d = 2$ but other dimensions only differ by shifts of the physical zones.

3.5.2 Regge Limit and Alpha Space

The Regge limit of a stripped correlator is defined by taking $\bar{z}$ counter-clockwise around the branch point at 1 and then bringing both z and $\bar{z}$ to 0 with $z/\bar{z}$ held finite. In this limit, the asymptotics are conjectured to be dominated by the leading Regge trajectory. That is, the tower of operators that tends to the smallest twist value.

The t-channel identity operator offers a simple test of conformal Regge theory. In this case, the analytic continuation around $\bar{z} = 1$ simply introduces a phase of $e^{-2\pi i \Delta_\phi}$ and so the Regge limit is equivalent to the familiar s-channel limit. Using the density in Eq. (3.2.2), the twist n contribution is then $O(z^{2(\Delta_\phi + n)})$. That is, the leading twist tower dominates in the Regge limit as conjectured. This is admittedly a very simple example with straight trajectories, however many good justifications of conformal Regge theory can be found in the literature; see for instance [51].

Taking the inverse alpha space transform of Eq. (3.1.10), we might naively say that we cannot access the Regge limit because $\Psi_{\alpha,\bar{\alpha}}(z,\bar{z})$ does not have a branch point to encircle at $\bar{z} = 1$. This apparent paradox is resolved by the understanding that we must keep track of the contours themselves during the analytic continuation. If the integral's region of convergence moves away from the imaginary axes then the contours must shift accordingly.

Indeed, we found that the contours tend to make half-rotations as $\bar{z}$ is taken around 1. This reveals to us an inconvenient truth. As the contours rotate, they necessarily pick up the poles along the real-axes. That is, we are forced to sum up the blocks and analytically continue the resulting function. Unfortunately, we have not found a short-cut around this issue. Even if the α integral is split and the contour closed to pick up the leading Regge pole, the remaining $\bar{\alpha}$ contour still rotates as we analytically continue the integrand.

Eq. (5.20) of [51] hypothesised the leading Regge behaviour as an integral parallel to the imaginary Δ-axis. It would be interesting to understand whether or not their

contour suffers the same fate as ours as the integrand is analytically continued.

3.5.3 Ising Model in Three Dimensions

In this section, we invite the reader to engage in some astrology by looking for patterns in the incomplete 'dot-to-dot' puzzle of Fig. 3.6. The figure plots a portion of the $\mathbb{Z}_2$-even spectrum [37] for the $d = 3$ Ising model with α and $\bar{\alpha}$ increasing to the east and north respectively. Although it is believed that Regge trajectories should tend to 'GFF-like' straight lines, the behaviour around the origin is more complicated. It is unclear how the trajectories join (if at all), if they can leave the plane altogether and whether or not all physical operators must lie on one.

3.6 Mellin Space

In this section, we briefly comment on the feasibility of going between Mellin and alpha space by way of a simple example.

A stripped correlator $\mathcal{G}(z, \bar{z})$ can be written in terms of a Mellin space integral like

$$\mathcal{G}(z,\bar{z}) = \int [ds] \int [dt]\, \frac{M(s,t)\,(z\bar{z})^{t/2}}{((1-z)(1-\bar{z}))^{(s+t)/2}} \Gamma^2\Big(\Delta_\phi - \frac{t}{2}\Big)\,\Gamma^2\Big(-\frac{s}{2}\Big)\,\Gamma^2\Big(\frac{s+t}{2}\Big) \tag{3.6.1}$$

where $M(s,t)$ is called the Mellin amplitude. There are a number of reasons why this is a sensible thing to do [38, 39, 40]. One is that the OPE causes $M(s,t)$ to factorise in some sense. Another is that Mellin space offers a natural language for AdS/CFT correlators. In particular, contact Witten diagrams have constant Mellin amplitudes.

In four dimensions, we can use the expression for $\Psi_{\alpha,\bar{\alpha}}$ in Eq. (3.3.1) along with Eq. (2.1.21) and the fact that $z^p(1-z)^{-q} = \sum_{n=0}^{\infty}(q)_n z^{p+n}/n!$ to determine that

$$\frac{(z\bar{z})^p}{((1-z)(1-\bar{z}))^q} \mapsto \hat{f}_{p,q}(\alpha,\bar{\alpha}) \equiv 2\left(\frac{\hat{f}_{p-1,q}(\alpha)\hat{f}_{p,q}(\bar{\alpha}) - \hat{f}_{p-1,q}(\bar{\alpha})\hat{f}_{p,q}(\alpha)}{\alpha^2 - \bar{\alpha}^2}\right) \quad (d=4) \tag{3.6.2}$$

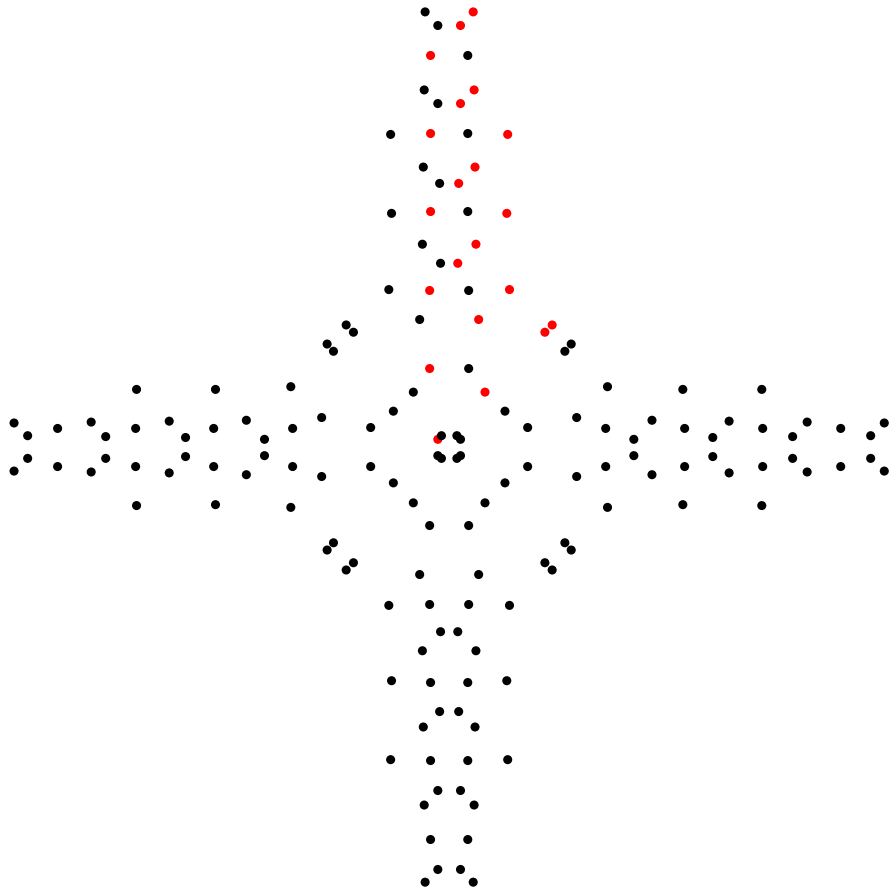

Figure 3.6: Plotted is a portion of the $\mathbb{Z}_2$-even spectrum for the $d = 3$ Ising model with α and $\bar{\alpha}$ increasing to the east and north respectively. We invite the reader to engage in some astrology and complete the 'dot-to-dot' puzzle by drawing some Regge trajectory candidates. Common belief is that they should tend to straight lines, as we see for generalised free fields. The trajectories may pass through both physical (red) and image (black) poles. We have chosen not to dress this diagram with the lines of positive integer spin or with the physical wedge as we did in Fig. 3.5. However, they can both be imagined by looking at how the red poles fall. The raw data is from [37].

where $\hat{f}_{p,q}(\alpha)$ is the $d=1$ density for $z^p(1-z)^{-q}$ that was calculated in [1]. That is,

$$z^p(1-z)^{-q} \mapsto \hat{f}_{p,q}(\alpha) \equiv \frac{\Gamma(p-\frac{1}{2}\pm\alpha)}{\Gamma^2(p)}\ {}_3F_2\left(\begin{matrix} p-\frac{1}{2}+\alpha, p-\frac{1}{2}-\alpha, q \\ p, p \end{matrix}; 1\right) \tag{3.6.3}$$

Therefore, the $d=4$ alpha space density for a contact Witten diagram is proportional to

$$\hat{\mathcal{G}}_{\text{contact}}(\alpha,\bar{\alpha}) = \int [ds] \int [dt]\, \hat{f}_{\frac{t}{2},\frac{s+t}{2}}(\alpha,\bar{\alpha}) \Gamma^2\Big(\Delta_\phi - \frac{t}{2}\Big)\Gamma^2\Big(-\frac{s}{2}\Big)\Gamma^2\Big(\frac{s+t}{2}\Big) \tag{3.6.4}$$

As usual, the spectrum can be determined by looking at the divergences. Varying $\alpha, \bar{\alpha}$ does not pinch the s-contour and so we can focus on the t-integral. The t-poles from $\hat{f}_{\frac{t}{2},\frac{s+t}{2}}(\alpha,\bar{\alpha})$ are left-running and so can pinch the contour against some of the right-running poles from the factor $\Gamma^2\big(\Delta_\phi - \frac{t}{2}\big)$. Therefore, we can safely tune α and $\bar{\alpha}$ after pulling the contour through enough of the $t = 2(\Delta_\phi + \mathbb{N})$ poles. As an example, the lowest lying operator is the scalar of dimension $2\Delta_\phi$. For this, we only need the residue at $t = 2\Delta_\phi$. Taking this, expanding around $\alpha = \Delta_\phi - \frac{3}{2}, \bar{\alpha} = \Delta_\phi - \frac{1}{2}$ and evaluating the resulting integral in s, we found the leading divergence to be

$$\hat{\mathcal{G}}_{\text{contact}}(\alpha,\bar{\alpha}) \sim -\frac{2\Gamma(2\Delta_\phi-1)}{4\Delta_\phi(\Delta_\phi-2)+3}\left(\frac{1}{(\alpha-(\Delta_\phi-\frac{3}{2}))^2(\bar{\alpha}-(\Delta_\phi-\frac{1}{2}))}\right) \tag{3.6.5}$$

Getting a general expression is a bit tricky as multiple poles get pinched. However, alpha space has provided a simple algorithm for finding any of the residues.

3.7 Future Directions

In this chapter, we have extended the alpha space formalism of [1] beyond two dimensions. We have hypothesised an invertible integral transform in Eq. (3.1.9) based on the Sturm-Liouville intuition that we established for $d=1$ in Chapter 2.

There are many potential directions that future work can take. Primarily, we believe that it will be important to more rigorously underpin the alpha space construction. This may perhaps be achieved by formalising Section 3.1.2 through a more complete

comparison between our transform and the Lorentzian inversion formula of Caron-Huot [16]. In addition, it should be possible to extend the formalism to accommodate for spinning external operators without too much difficulty.

Conformal partial waves can be written as a conformally invariant integral over the product of two three-point functions, enabling them to be interpreted as $6j$ symbols [52]. An attractive thought is that $\Psi_{\alpha,\bar{\alpha}}(z,\bar{z})$ also can be written and interpreted in a similar manner. The work done on representation theory and Wilson functions in [53] leaves us optimistic.

Thereafter, it will be interesting to understand how we may place constraints on crossing-symmetric conformal field theories using alpha space. The integral equation of Eq. (3.1.16) provides an interesting kernel but it is unclear whether or not we can perform any useful bootstrap-style calculations as yet. Future work should perhaps also improve our slightly nebulous discussion on the exponentiation of poles by using doubly-split kernels, which tend to lead to better convergence.

Chapter 4

Truncated Conformal Space

In this chapter, we address several questions about perturbative renormalisation from the Hamiltonian perspective. Our main interest in this method is its importance for the truncated conformal space approach (TCSA) of Yurov and Zamolodchikov [2]. We go on to illustrate our general results with the ϕ^4 theory in d dimensions.

The TCSA is the Rayleigh-Ritz method adapted to quantum field theory. The main idea is to truncate the discrete Hilbert space of a field theory on a compact spatial manifold to a certain finite-dimensional vector space. This in particular truncates the Hamiltonian to a finite-dimensional matrix, which one then proceeds to diagonalise numerically to obtain an estimate of the field theory spectrum. In practical computations one is confronted with an exponential growth in the number of states which necessitates improvements to this 'bare' procedure in order to obtain meaningful results. One such an improvement is to add counterterms to the Hamiltonian in order to approximately take into account the effect of states above the cut-off. This idea was introduced first in [54] and implemented and refined in several other works: see [55, 56, 57, 58, 59] and more recently [60] (which includes a review of earlier works) and [61, 62, 63, 64, 65]; a recent review is [66].

Our first question concerns the connection between the anomalous dimensions of composite operators in the plane, and the eigenvalues of the Hamiltonian on the cylinder. For conformal field theories (CFTs), the state-operator correspondence

dictates that these ought to be completely equivalent, and whilst this is easily verified at first order in perturbation theory (see e.g. [8, Chapter 5]), it becomes less straightforward at the next order. Here, we find the explicit relation up to third order using an argument which is easily extendable to higher orders. In Section 4.1, we explain that the precise connection is provided by using conformal perturbation theory on the plane, rather than the usual Feynman diagrams. In Section 4.3, we use these newfound equations to compute the anomalous dimensions at the Wilson-Fisher fixed points to second order in the epsilon expansion. This computation is remarkably straightforward and avoids the evaluation of (two-loop) Feynman diagrams. It would be interesting to investigate if this relative simplicity persists at higher orders and/or for other classes of theories.

Our second question is 'precisely what is allowed in the counterterm action?'. As usual, this is intricately related to the nature of the cut-off and the symmetries that it preserves. Implementing a TCSA cut-off is a non-local operation, and correspondingly the counterterm action could feature non-local terms as well [60]. Clearly, an arbitrarily non-local counterterm action could be disastrous for the viability of the Hamiltonian truncation method, but fortunately the non-localities are suppressed by powers of the cut-off. In Section 4.2, we use crossing symmetry to analyse the structure of the leading-order divergence. At subleading orders we cannot use any general theorems, but for the ϕ^4 theory we can make progress by analysing a particular summand; this we do in detail in Section 4.3. This allows us to demonstrate the necessity of non-local counterterms at second order, as well as tensorial counterterms that in principle could break Lorentz invariance.

Lastly, with an eye towards numerical work we consider the perturbative determination of the coefficients of the counterterm action for the ϕ^4 theory at second order. When a counterterm is marginally relevant, this may be of limited relevance for practical numerical computations because in such cases the counterterms receive corrections at all orders in perturbation theory and numerical tuning will be required to obtain finite answers in the large cut-off limit. However, when the counterterms

are strictly relevant, they receive only a finite number of pertubative contributions and the determination of these coefficients is directly useful for numerical studies. We provide precise expressions in Section 4.3.2, including non-divergent subleading terms which can be used to improve the Hamiltonian in numerical studies.

4.1 Anomalous Dimensions from Infinite Matrix Diagonalisation

In this section we explain how the perturbative computation of the anomalous dimensions of composite operators is related to the diagonalisation of the infinite, tree-level matrix of operator product expansion (OPE) coefficients. We start with a CFT in d dimensions and deform it by a relevant operator that we call $\sigma(x)$, with dimension Δ_σ. We work perturbatively in the corresponding coupling constant g.

4.1.1 The Hamiltonian Perspective

The Hamiltonian procedure starts by putting the d-dimensional ultraviolet (UV) CFT on the cylinder $\mathbb{R} \times S^{d-1}_R$ where, by virtue of the state-operator correspondence, the Hamiltonian is simply the dilation operator:

$$H_{\text{CFT}}|\mathcal{O}_i\rangle = \frac{\Delta_i}{R}|\mathcal{O}_i\rangle\,. \tag{4.1.1}$$

where R is the cylinder radius and we label states by their corresponding local operator $\mathcal{O}_i(x)$. A relevant deformation of the CFT by an operator σ with coupling g modifies the Hamiltonian to

$$H = H_{\text{CFT}} + R^{d-1}\int_{S^{d-1}} d\mathbf{n}\, g\, \sigma(\tau, \mathbf{n}) + H_{\text{ct}}, \tag{4.1.2}$$

where $\mathbf{n}$ is a unit vector in $\mathbb{R}^d$ which parametrises S^{d-1}. We will be consistent in writing operators in the cylinder picture with two arguments (a 'time' component and a unit vector in $\mathbb{R}^d$) whereas flat space operators will be given one argument (a

vector in $\mathbb{R}^d$). H_{ct} is the counterterm Hamiltonian, which we assume starts at order g^2.

We can compute the matrix elements of the Hamiltonian in the UV basis by transforming to flat space and using the standard CFT OPE introduced in Section 1.4, which here takes the form

$$\sigma(x)\mathcal{O}_j(0) = \sum_k \frac{\lambda_{\sigma j}{}^k}{|x|^{\Delta_\sigma+\Delta_{jk}}}\mathcal{O}_k(0) + \dots \tag{4.1.3}$$

with the dots here representing non-scalar operators (and so $\mathcal{O}_k$ may or may not be primary). Also, we define $\Delta_{ij} \equiv \Delta_i - \Delta_j$. Then, in terms of

$$V_i{}^j \equiv S_d R^{d-\Delta_\sigma} g \lambda_{\sigma i}{}^j \tag{4.1.4}$$

we find that

$$H|\mathcal{O}_i\rangle = \frac{1}{R}\left(\Delta_i \delta_i^j + V_i{}^j + W_i{}^j\right)|\mathcal{O}_j\rangle \tag{4.1.5}$$

where $R^{-1}W_i{}^j$ are the matrix elements of H_{ct} in the CFT basis. Here, $S_d \equiv 2\pi^{d/2}/\Gamma(d/2)$ is the volume of the unit radius sphere embedded in d dimensions. In this chapter, we are careful to differentiate between $\lambda_{ij}{}^k$ and λ_{ijk} because we later introduce the Gram matrix which raises and lowers indices.

In order to find the spectum of the deformed theory, we need to diagonalise the Hamiltonian matrix. To second order in the coupling g, we find the eigenvalues

$$E_i = \frac{1}{R}\left(\Delta_i + V_i{}^i + \sum_{j\neq i}\frac{V_i{}^j V_j{}^i}{\Delta_{ij}} + W_i{}^i + \dots\right) \tag{4.1.6}$$

where the index i is not summed over and we only keep the second-order term in $W_i{}^i$. For this equation to be valid we need to request that $V_i{}^j$ is diagonal in the finite-dimensional subspace of operators with the same Δ_i, and that any degeneracies are broken by the second-order correction. If these conditions are not met, we need to resort to the usual methods of degenerate perturbation theory to find the correct eigenvalues.

Since the energies are supposed to be finite, the role of the counterterms at second

order is to make finite the expression

$$\sum_{k\neq i} \frac{V_i{}^k V_k{}^j}{\Delta_{ik}} + W_i{}^j \tag{4.1.7}$$

for $i = j$. Notice that it is not necessary for the counterterms to also make this expression finite when $i \neq j$ and we comment further on this below. For later reference, we note that the third-order corrections also take a well-known form and are given by

$$\frac{1}{R}\left(\sum_{k\neq i}\sum_{j\neq i} \frac{V_i{}^j V_j{}^k V_k{}^i}{\Delta_{ij}\Delta_{ik}} - \sum_{j\neq i} \frac{V_i{}^i V_i{}^j V_j{}^i}{\Delta_{ij}^2} + \sum_{k\neq i} \frac{W_i{}^k V_k{}^i}{\Delta_{ik}} + \sum_{j\neq i} \frac{V_i{}^j W_j{}^i}{\Delta_{ij}} + W_i{}^i\right) \tag{4.1.8}$$

where each instance of the counterterm Hamiltonian W is taken at the appropriate order.

4.1.2 The Lagrangian Perspective

In the Lagrangian approach, or more precisely in conformal perturbation theory, we compute the perturbative renormalisation of $\mathcal{O}_i$ by introducing the renormalised operator

$$[\mathcal{O}]_i(x) \equiv Z_i{}^j \mathcal{O}_j(x) \tag{4.1.9}$$

and perturbatively evaluating correlation functions of the form

$$\mathcal{G}_i \equiv \langle \ldots [\mathcal{O}]_i(0)\rangle_g \equiv \langle \ldots \exp\left(-\int d^d x\, (g\,\sigma(x) + L_{\rm ct}(x))\right) Z_i{}^j \mathcal{O}_j(0)\rangle \tag{4.1.10}$$

now evaluated on flat $\mathbb{R}^d$. Here the ellipses signify a string of operators inserted away from the origin and the expectation values on the right-hand side are those of the undeformed theory. Our aim is to compute the matrix of anomalous dimensions

$$\Gamma_i{}^j \equiv -\,\mu\frac{\partial}{\partial\mu}\log Z_i{}^j\Big|_{g_B} \tag{4.1.11}$$

where the partial derivative is taken with the bare (dimensionful) coupling g_B held fixed. We assume that the counterterms start at $O(g^2)$ and we work to second order in g. We shall also assume that the dimension Δ_σ of the perturbing operator is

nearly marginal,

$$\Delta_\sigma = d - \epsilon \tag{4.1.12}$$

and that ϵ is small, which essentially amounts to working in dimensional regularisation. As usual, we ignore power law divergences and focus on the poles in ϵ.

The expansions

$$\begin{aligned} Z_i{}^j &= \delta_i^j + g Z_i^{(1)j} + g^2 Z_i^{(2)j} + \dots \\ \mathcal{G}_i &= \mathcal{G}_i^{(0)} + g\,\mathcal{G}_i^{(1)} + g^2\,\mathcal{G}_i^{(2)} + \dots \\ L_{\text{ct}} &= g^2 L_{\text{ct}}^{(2)} + \dots \end{aligned} \tag{4.1.13}$$

then give

$$\begin{aligned} \mathcal{G}_i^{(0)} &= \langle \dots \mathcal{O}_i(0) \rangle \\ \mathcal{G}_i^{(1)} &= \langle \dots \left(- \int d^d x\, \sigma(x) \delta_i^j + Z_i^{(1)j} \right) \mathcal{O}_j(0) \rangle \\ \mathcal{G}_i^{(2)} &= \langle \dots \Big(\frac{1}{2} \int d^d x \int d^d y\ \sigma(x)\sigma(y)\delta_i^j - \int d^d x\, L_{\text{ct}}^{(2)}(x)\delta_i^j \\ &\qquad - \int d^d x\, \sigma(x) Z_i^{(1)j} + Z_i^{(2)j} \Big) \mathcal{O}_j(0) \rangle \end{aligned} \tag{4.1.14}$$

In calculating $Z_i{}^j$ we may focus on some neighbourhood of $\mathcal{O}_i$, where the pertinent divergences appear. Therefore we limit all spatial integrals to a spherical region of radius R, away from the other operator insertions. For definiteness, one may think of this procedure as the perturbative computation of one-point functions on the ball given by $|x| < R$, but in practice such a physical picture is not important for the computations of the renormalisation constants.

Upon substitution of the OPE (Eq. (4.1.3) into Eq. (4.1.14)), we find divergences which we can make finite using dimensional regularisation. Collecting the first-order terms, we find that

$$\begin{aligned} &Z_i^{(1)j} - \int_{|x|<R} d^d x\, \frac{\lambda_{\sigma i}{}^j}{|x|^{\Delta_\sigma + \Delta_{ij}}} = \\ &Z_i^{(1)j} - \frac{S_d \lambda_{\sigma i}{}^j R^{\epsilon - \Delta_{ij}}}{\epsilon - \Delta_{ij}} \end{aligned} \tag{4.1.15}$$

should be finite. We see that there are divergences only when $\Delta_{ij} = O(\epsilon)$. What's

more, since R is a scale which is set far away from the operator insertion, locality dictates that $Z_i{}^j$ cannot depend on R. We therefore need to introduce a renormalisation scale μ. Altogether, we therefore set

$$Z_i^{(1)j} = \begin{cases} \dfrac{S_d \lambda_{\sigma i}{}^j \mu^{-\epsilon+\Delta_{ij}}}{\epsilon - \Delta_{ij}} & \text{if } \Delta_{ij} = O(\epsilon) \\ 0 & \text{otherwise} \end{cases} \tag{4.1.16}$$

Now we need a little discussion about $\lambda_{\sigma i}{}^j$. As observed in [60], there is a clear problem if $\Delta_{ij} = \epsilon$, since in that case the integral would not be rendered finite by dimensional regularisation. Therefore $\lambda_{\sigma i}{}^j$ must vanish precisely for these cases, at least for every theory that is made finite by dimensional regularisation. (This was also explicitly shown to be the case in the ϕ^4 theories in [60].) In fact, if $\Delta_{ij} = \kappa_{ij}\epsilon$ with κ_{ij} finite as $d \to 4$, then $\lambda_{\sigma i}{}^j = 0$ unless $\kappa_{ij} = 0$. Furthermore, since operators are orthogonal unless $\Delta_{ij} = 0$ for all d,[1] it follows that we can pick an orthogonal basis in the space of operators where both the tree-level scaling dimensions are diagonalised for all d and also $\lambda_{\sigma i}{}^j$ is *diagonal* on every finite-dimensional subspace of operators whose scaling dimensions coincide for $d \to 4$. (Of course, outside of this subspace it can have all kinds of off-diagonal terms.) In this basis, we find the simpler structure

$$Z_i^{(1)j} = \begin{cases} \dfrac{S_d \lambda_{\sigma i}{}^i \mu^{-\epsilon}}{\epsilon} & \text{if } \mathcal{O}_i = \mathcal{O}_j \\ 0 & \text{otherwise} \end{cases} \tag{4.1.17}$$

and, again in this basis, the leading order anomalous dimensions are then simply

$$\Gamma_i{}^i = g\mu^{-\epsilon} S_d \lambda_{\sigma i}{}^i + O(g^2) \tag{4.1.18}$$

where we used that $g_B = g + O(g^2)$. This expression agrees precisely with the Hamiltonian picture discussed previously, which is Eq. (4.1.6) to first order in the coupling. This first-order computation can also be found in the textbook [8].

[1] To clarify: here we use the fact that we can track operators $\mathcal{O}_i$ in the free theory whilst varying d, so their dimensions Δ_i then become simple functions of d. The claimed orthogonality then follows from the *ϕ-type* selection rule in [67].

At second order, we find some new structures. For now, we assume that the counterterm Lagrangian is given by a simple renormalisation of the coupling,

$$g^2 L_{\rm ct}^{(2)} = g^2 \mu^{-\epsilon} S_d X^\sigma \sigma(x) \tag{4.1.19}$$

with the dimensionless coefficient X^σ tuned to make the second-order results finite. (In subsequent sections, we allow for other operators to appear in the counterterm action.) For future reference, we mention that with this counterterm the bare coupling is

$$g_B(g,\mu) = g + g^2 \mu^{-\epsilon} S_d X^\sigma + O(g^3)\,. \tag{4.1.20}$$

Using then that $\frac{1}{2}\int d^dx \int d^dy\, \sigma(x)\sigma(y) = \int d^dx \int_{|y|<|x|} d^dy\, \sigma(x)\sigma(y)$ to make sure the OPE expansion is valid, we find

$$\begin{aligned}\mathcal{G}_i^{(2)} = \Big(&\frac{\lambda_{\sigma i}{}^k \lambda_{\sigma k}{}^j S_d^2 R^{2\epsilon-\Delta_{ij}}}{(\epsilon-\Delta_{ik})(2\epsilon-\Delta_{ij})} - \frac{Z_i^{(1)k}\lambda_{\sigma k}{}^j S_d R^{\epsilon-\Delta_{kj}}}{\epsilon-\Delta_{kj}} \\ &+ Z_i^{(2)j} - \frac{X^\sigma \lambda_{\sigma i}{}^j S_d^2 \mu^{-\epsilon} R^{\epsilon-\Delta_{ij}}}{(\epsilon-\Delta_{ij})}\Big)\langle \dots \mathcal{O}_j(0)\rangle\end{aligned} \tag{4.1.21}$$

and therefore the term in parentheses should be finite. We see that possible divergences can arise through the sum over intermediate operators k, but also through small denominators, for example when $\Delta_{ij} = O(\epsilon)$. The latter divergences are cancelled by setting

$$Z_i^{(2)j} = \begin{cases} -\frac{\lambda_{\sigma i}{}^k \lambda_{\sigma k}{}^j S_d^2 \mu^{-2\epsilon+\Delta_{ij}}}{(\epsilon-\Delta_{ik})(2\epsilon-\Delta_{ij})} + \frac{Z_i^{(1)k}\lambda_{\sigma k}{}^j S_d \mu^{-\epsilon+\Delta_{kj}}}{\epsilon-\Delta_{kj}} + \frac{X^\sigma \lambda_{\sigma i}{}^j S_d^2 \mu^{-2\epsilon+\Delta_{ij}}}{(\epsilon-\Delta_{ij})} & \text{if } \Delta_{ij} = O(\epsilon) \\ 0 & \text{otherwise} \end{cases} \tag{4.1.22}$$

This cancellation is not entirely obvious since there are double poles, but upon substituting the lower-order result from Eq. (4.1.16), one finds that all of the divergences are indeed removed. Let us now choose the aforementioned basis of operators, where

we find the simpler expression:

$$Z_i^{(2)j} = \begin{cases} \frac{S_d^2\mu^{-2\epsilon}}{\epsilon}\left(-\frac{\lambda_{\sigma i}{}^k\lambda_{\sigma k}{}^i}{2(\epsilon-\Delta_{ik})}+\frac{\lambda_{\sigma i}{}^i\lambda_{\sigma i}{}^i}{\epsilon}+X^\sigma\lambda_{\sigma i}{}^i\right) & \text{if } \mathcal{O}_i=\mathcal{O}_j \\ 0 & \text{otherwise} \end{cases} \tag{4.1.23}$$

Using this expression to compute the matrix of anomalous dimensions, we find that the double poles cancel precisely and that

$$\Gamma_i{}^i = V_i{}^i + \sum_{k\neq i}\frac{V_i{}^kV_k{}^i}{\Delta_{ik}-\epsilon} + W_i{}^i + O(g^3) \tag{4.1.24}$$

where now

$$V_i{}^j = S_d\mu^{-\epsilon}g\lambda_{\sigma i}{}^j\,, \qquad W_i{}^i = S_d^2\mu^{-2\epsilon}X^\sigma\lambda_{\sigma i}{}^i\,. \tag{4.1.25}$$

At an IR fixed point the Γ_i^i will be the anomalous dimensions of the composite operators, so the coefficient X^σ should be chosen such that these are finite for all i. That this can be done at all is of course a consequence of perturbative renormalisability.

The third-order correction can be found in the same manner. We will not spell out the details of the tedious but straightforward computation and instead quote the result:

$$\left(\sum_{k\neq i,m\neq i}\frac{V_i{}^kV_k{}^mV_m{}^i}{(\Delta_{ik}-\epsilon)(\Delta_{im}-2\epsilon)} - V_i{}^i\sum_{k\neq i}\frac{V_i{}^kV_k{}^i}{(\Delta_{ik}-\epsilon)(\Delta_{ik}-2\epsilon)} + \sum_{k\neq i}\frac{(W_i{}^kV_k{}^i+V_i{}^kW_k{}^i)}{\Delta_{ik}-\epsilon} + W_i{}^i\right) \tag{4.1.26}$$

where we work in the basis discussed above and the third-order counterterm action is assumed to take the form

$$g^2L_{\text{ct}}^{(3)} = g^3\mu^{-2\epsilon}S_d^2Y^\sigma\sigma(x) \tag{4.1.27}$$

for some (divergent) c-number Y^σ.

From the renormalisation of composite operators, we can work out the beta function

to one higher order using a familiar trick. Consider

$$\langle \dots \exp\left(-g_B(g,\mu)\int d^dx\,\sigma(x)\right)\rangle \tag{4.1.28}$$

away from any operator insertions, and with the bare coupling $g_B(g,\mu) = g + g^2\mu^{-\epsilon}S_dX^\sigma + g^3\mu^{-2\epsilon}S_d^2Y^\sigma + O(g^4)$, which ensures that the result is finite. Taking a derivative with respect to g, we produce an extra insertion of σ. This is still finite, so we conclude that

$$\langle \dots \exp\left(-g_B(g)\int d^dx\,\sigma(x)\right)\frac{\partial g_B}{\partial g}\sigma(0)\rangle \tag{4.1.29}$$

is also finite. But then we can choose

$$Z_\sigma{}^\sigma = \frac{\partial g_B}{\partial g}\,. \tag{4.1.30}$$

for the renormalisation of the operator $\sigma(x)$. Using that

$$\beta(g) \equiv \mu\frac{\partial g}{\partial \mu}\bigg|_{g_B} \tag{4.1.31}$$

and doing a little rewriting, we find the familiar relation between the anomalous dimension and the derivative of the beta function:

$$\frac{\partial\beta}{\partial g} = \Gamma_\sigma{}^\sigma \tag{4.1.32}$$

Below, we use this to find the beta function at order g^3 from the renormalisation factor $Z_\sigma{}^\sigma$ at order g^2.

4.1.3 Comparing the Hamiltonian and Lagrangian Approaches

We now have an abstract way to compute two sets of observables to third order in the deforming operator g: the spectrum of the theory on the cylinder expressed in Eqs. (4.1.6) and (4.1.8), and the matrix of anomalous dimensions in Eqs. (4.1.24) and (4.1.26). Both expressions are similar and become equivalent if we ignore the

additional ϵ in the denominators and identify R and μ^{-1}.[2]

Altogether, we can view the perturbative computation of anomalous dimensions in a new light: not as the diagonalisation of the finite-dimensional matrices $\Gamma_i{}^j$ whose elements we need to compute order by order in perturbation theory, but rather as the perturbative diagonalisation of the infinite-dimensional matrix $V_i{}^j$ whose elements are just those of the unperturbed theory.

We should stress that the two pictures do not always have to agree. In fact, they agree if two conditions are met. First of all, the perturbing operator should be marginal or marginally (ir)relevant. Indeed, if this condition is not met there are (generically) no logarithmic divergences, there is no renormalisation scale μ, and the matrix of anomalous dimensions vanishes. In our computations, this shows up because we need poles in ϵ in the Lagrangian computation but not in the Hamiltonian one. Secondly, the theory should remain conformal or flow to a nearby IR (or UV) fixed point. Only in this case can we use the Callan-Symanzik equation to relate $\Gamma_i{}^j$ to scheme-independent observables like the anomalous dimensions of local operators, and of course the state-operator map to relate these scaling dimensions to the spectrum of the theory on the cylinder.

Both of the conditions discussed above are met in Wilson-Fisher type fixed points, to which we turn our attention in Section 4.3. This will also allow us to investigate the counterterm action $W_i{}^j$ in more detail. To do so we however first need to improve our understanding of the generally infinite sum in Eq. (4.1.6), which we discuss in the next section.

[2]Ignoring the ϵ factors in the denominators is not obviously allowed, since the whole sum is divergent and, after defining it through analytic continuation, has a pole at $\epsilon = 0$. Nevertheless, we find in the next subsection that the finite part is unmodified by the presence of the additional ϵ in the denominator. Similar cancellations are presumably required for the Hamiltonian and Lagrangian perspectives to agree also at higher orders, but we have not investigated this in detail.

4.2 Divergences with the TCSA cut-off

In a nutshell, the TCSA procedure of Yurov and Zamolodchikov [2] amounts to truncating the Hamiltonian matrix by ignoring all states (in the UV basis) with dimensions larger than a cut-off value $\Delta_{\max}$. The resulting matrix can then be diagonalised numerically, which for sufficiently small couplings (made dimensionless by using powers of R) ought to give an accurate representation of the spectrum of the deformed theory.

On the cylinder $\mathbb{R} \times S^{d-1}$ this truncation procedure preserves the rotations $SO(d)$ and time translations $\mathbb{R}$, so in principle the regularisation prescription does not break more symmetries than the background geometry, which itself serves as an infrared regulator. The counterterms that we find will therefore preserve these symmetries, but a priori one may not recover a full Lorentz symmetry as we send the sphere radius to infinity. Another issue is that the truncation of the Hilbert space breaks locality on the sphere, so locality of the counterterm action is no longer guaranteed. The two issues of non-Lorentz invariant counterterms and non-local counterterms were raised before in [60].

In the radial quantisation picture, we can mimic the cut-off in the TCSA by sandwiching the insertions of the perturbing operator between a Hilbert space projector

$$\mathcal{P} \equiv \sum_{\Delta_n \leq \Delta_{\max}} |\mathcal{O}_n\rangle\langle\mathcal{O}_n| \tag{4.2.1}$$

which removes intermediate states of weight greater than $\Delta_{\max}$. Notice that this amounts to a cut-off in energies with associated scale $\Lambda = \Delta_{\max}/R$, with R the radius of the sphere where we insert $\mathcal{P}$. This cut-off breaks locality on these spatial spheres (but not in the radial 'time' direction), as well as covariance under translations on the plane.

To take the new cut-off into account we need to modify the analysis in the preceding section as follows. First of all, we need to more carefully keep track of power law divergences and not just the poles as $\epsilon \to 0$ in dimensional regularisation. This

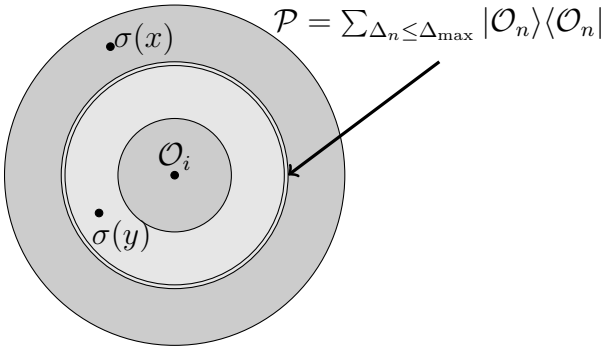

Figure 4.1: A Hilbert space projector $\mathcal{P}$ is placed between the two σ operators, removing intermediate states of weight greater than $\Delta_{\max}$ and regulating contact divergences.

implies that, compared to Section 4.1, we need to modify the counterterm action to

$$g^2 L^{(2)}_{\rm ct}(x) = g^2 \mu^{-\epsilon} S_d X^k \mathcal{O}_k(x) + g^2 \mu^{-\epsilon} S_d X^\sigma \sigma(x) \tag{4.2.2}$$

with some operators $\mathcal{O}_k(x)$ and coefficients X^k and X^σ. We expect $L_{\rm ct}$ to include $\Delta_{\max}$ divergent counterterms defined to cancel divergences arising from the hard truncation of the Hilbert space, as well as $1/\epsilon$ divergent counterterms associated with the same coupling renormalisation. In terms of the double limit, we should technically take $\Delta_{\max} \to \infty$ with ϵ finite prior to taking $\epsilon \to 0$. However, we only analyse the $\Delta_{\max}$ divergences, which suffices to get a finite answer at fixed ϵ, so e.g. at $\epsilon = 1$ for the ϕ^4 theory in $d = 3$.[3]

The coefficients X^k and X^σ are non-trivial functions of the cut-off, and are fixed by the requirement that physical observables are finite. In the Hamiltonian perspective (to second order), this concretely means that there should be no divergences in

$$\sum_{\substack{k \neq i \\ \Delta_k \leq \Delta_{\max}}} \frac{\lambda_i{}^k \lambda_k{}^i}{\Delta_{ik}} + X^k \lambda_{ki}{}^i + X^\sigma \lambda_{\sigma i}{}^i \tag{4.2.3}$$

as we send $\Delta_{\max} \to \infty$. Clearly, in order to determine the counterterms, we need to have some amount of control over the asymptotics of the sum. To start with,

[3]Notice that we should also be able to renormalise the second-order divergences for $\epsilon < 0$; there is a suitable counterterm action for the ϕ^4 theory for any d to any finite order in perturbation theory.

we focus on the behaviour of the summand as a function of the dimension of the intermediate operator. That is, we consider the object

$$\sum_{k:\Delta_k=\Delta} \lambda_{\sigma i}{}^{k}\lambda_{\sigma k}{}^{j} \tag{4.2.4}$$

as a function of Δ (and i and j).

In this section, we review the analysis in [60], which uses crossing symmetry and a Tauberian theorem to constrain the large Δ behaviour in full generality. In Section 4.3.2, we then apply the results to the free scalar theory, and show that there we can obtain better results than those rigorously proven by the Tauberian theorem.

4.2.1 Tauberian Theorem

In an attempt to estimate the divergences in Eq. (4.2.3), we introduce the four-point function studied in [60]:

$$\mathcal{F}_{ji}(\tau) \equiv e^{\tau(\Delta_\sigma+\Delta_{ij}/2)}\langle \mathcal{O}_j(\infty)\int_{S^{d-1}} d\mathbf{n}\int_{S^{d-1}} d\mathbf{n}'\,\sigma(e^{\tau/2}\mathbf{n})\sigma(e^{-\tau/2}\mathbf{n}')\mathcal{O}_i(0)\rangle \tag{4.2.5}$$

where $\tau > 0$ and $\mathcal{O}(\infty) \equiv \lim_{|x|\to\infty}|x|^{2\Delta_\mathcal{O}}\mathcal{O}(x)$. The exponential pre-factor is pulled out for later convenience. Evaluating this gives

$$\mathcal{F}_{ji}(\tau) = S_d^2 e^{\tau(d-\epsilon+\Delta_i)}\sum_k e^{-\tau\Delta_k}\lambda_{\sigma i}{}^{k}\lambda_{\sigma kj} \tag{4.2.6}$$

with $\lambda_{\sigma kj} = \sum_l \lambda_{\sigma k}{}^{l}\mathrm{G}_{lj}$, where G_{lj} is the Gram matrix (which will drop out from all our relevant results below). As in Section 4.1, the sum is over intermediate scalars only, because of the spherical integrals. We can try to get an idea of the asymptotic behaviour of the sum by using an inverse Laplace transform. For example, if the behaviour near $\tau = 0$ is of the form

$$\mathcal{F}_{ji}(\tau) = c_\alpha \tau^{-\alpha}(1 + O(\tau)) \tag{4.2.7}$$

with $\alpha > 0$, then we would roughly speaking expect that

$$\sum_{k\,:\,\Delta_k=\Delta} \lambda_{\sigma i}{}^{k}\lambda_{\sigma kj} \sim \frac{c_\alpha \Delta^{\alpha-1}}{\Gamma(\alpha)} \qquad \text{as } \Delta\to\infty, \tag{4.2.8}$$

simply because

$$\int_0^\infty \Delta^{\alpha-1} e^{-\Delta\tau} d\Delta = \Gamma(\alpha)\tau^{-\alpha} \tag{4.2.9}$$

and the non-analytic behaviour in τ originates from the large Δ part of the integral.

Of course, the preceding claim cannot be exactly true, for the simple reason that the left-hand side of Eq. (4.2.8) is not a smooth function of Δ. The precise statement follows from the Hardy-Littlewood Tauberian theorem, which states that this holds only in an aggregrate sense. The version that we need is the one explained in [68] and proven, for example, in [69]: take a (positive) measure $d\mu(\Delta)$ such that $\int_a^b d\mu(\Delta)$ is finite for every finite a and b. Now if

$$F(\tau) = \int_0^\infty e^{-\tau\Delta} d\mu(\Delta) \tag{4.2.10}$$

behaves for small τ as

$$F(\tau) \sim \tau^{-\rho} \tag{4.2.11}$$

with $\rho > 0$, then

$$\int^{\Delta_{\max}} d\mu(\Delta) \sim \frac{\Delta_{\max}^\rho}{\Gamma(\rho+1)} \tag{4.2.12}$$

for large $\Delta_{\max}$. Here $a \sim b$ means that $a/b \to 1$ in the relevant limit.

Unfortunately, without further assumptions we can say little useful about the subleading terms. For example, if we try to subtract the leading term from $d\mu(\Delta)$, then it is generally no longer positive and the theorem ceases to apply.

4.2.2 Using Crossing Symmetry

To estimate the small τ behaviour of Eq. (4.2.5), we expand in the crossed channel by first fusing the two σ operators, as indicated in Fig. 4.2. Taking z and $\bar{z}$ as the standard cross-ratios introduced in Eq. (1.3.2), we then obtain

$$\mathcal{F}_{ji}(\tau) = \int_{S^{d-1}} d\mathbf{n} \int_{S^{d-1}} d\mathbf{n}' \sum_{\hat{k}} \frac{\lambda_{\sigma\sigma}{}^{\hat{k}} \lambda_{\hat{k}ij}}{(\mathbf{n} - e^{-\tau}\mathbf{n}')^{2\Delta_\sigma}} G^{(\ell_{\hat{k}})}_{\Delta_{\hat{k}}}(z, \bar{z}) \tag{4.2.13}$$

$$= S_d S_{d-1} \sum_{\hat{k}} \int_0^\pi d\theta \frac{\sin(\theta)^{d-2} \lambda_{\sigma\sigma}{}^{\hat{k}} \lambda_{\hat{k}ij}}{(1 + e^{-2\tau} - 2e^{-\tau}\cos\theta)^{d-\epsilon}} G^{(\ell_{\hat{k}})}_{\Delta_{\hat{k}}}(z, \bar{z}) \tag{4.2.14}$$

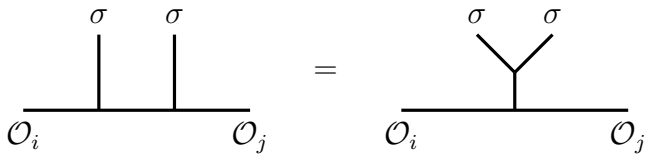

Figure 4.2: Crossing symmetry allows us to equate fusion channels. This is integral in the arguments of Section 4.2 and Section 4.3 which explain why counterterms are made up from the local operators in the $\sigma \times \sigma$ OPE, dressed with dilation operators.

with $\cos(\theta) = \mathbf{n} \cdot \mathbf{n}'$ and with

$$z\bar{z} = (\mathbf{n} - e^{-\tau}\mathbf{n}')^2 = 1 + e^{-2\tau} - 2e^{-\tau}\cos\theta \qquad (1-z)(1-\bar{z}) = e^{-2\tau} \tag{4.2.15}$$

This time, the sum is over all of the *primaries* in the theory, which we have indicated with a hatted index $\hat{k}$. The conformal blocks are fixed by conformal symmetry and encode the contribution of the descendants, as discussed in Section 1.5. As always, the blocks implicitly depend on Δ_{ij}. For the decomposition, we set $x_1 = e^{\tau/2}\mathbf{n}$, $x_2 = e^{-\tau/2}\mathbf{n}'$, $x_3 = 0$ and $x_4 = \infty$ and we follow the familiar conventions of Dolan and Osborn [31]. This OPE expansion is not strictly valid across the whole integration domain because the operator at the origin sits midway between the two σ operators when they are at antipodal points. However, we are only interested in the non-analytic part as $\tau \to 0$, which comes from the σ OPE region where $\cos(\theta)$ is close to 1, and in this region the sum converges.

A conformal block can be expanded [70] as a sum of Gegenbauer polynomials:

$$G_{\Delta}^{(l)}(z,\bar{z}) = |z|^{\Delta} \sum_{n,m=0}^{\infty} c_{n,m}|z|^n \frac{m!}{(d-2)_m} C_m^{d/2-1}(\cos(\arg(z))) \tag{4.2.16}$$

The coefficients $c_{n,m}$ depend on Δ_{ij}, l, d and Δ. In Appendix B, we review how to determine $c_{n,m}$ recursively from the Casimir equation.

Notice that we use a more traditional notation and normalisation for the blocks in this chapter. To convert between the two representations used in this work, use the

equivalence

$$G_{\Delta}^{(J)}(z,\bar{z}) = \left.\frac{G_{\alpha,\bar{\alpha}}(z,\bar{z})}{\gamma(\alpha-\bar{\alpha})}\right|_{\alpha=\frac{\Delta-J+1-d}{2}\,\bar{\alpha}=\frac{\Delta+J-1}{2}} \tag{4.2.17}$$

for $\gamma(\alpha)$ defined in Eq. (1.5.11).

The complex cross-ratio in our conventions is given by

$$z = 1 - e^{-\tau+i\theta} \tag{4.2.18}$$

and therefore

$$|z|^2 = 1 + e^{-2\tau} - 2e^{-\tau}\cos\theta \qquad \cos(\arg z) = \frac{1-e^{-\tau}\cos\theta}{\sqrt{1+e^{-2\tau}-2e^{-\tau}\cos\theta}} \tag{4.2.19}$$

This leads us to define the integrals:

$$I_{\alpha}^{(m)}(\tau) := S_d S_{d-1}\int_0^{\pi} d\theta \frac{\sin(\theta)^{d-2}}{(1+e^{-2\tau}-2e^{-\tau}\cos\theta)^{d-\epsilon-\alpha/2}} C_m^{d/2-1}(\cos\arg z) \tag{4.2.20}$$

which have small τ behaviour of the form, for example,

$$\begin{aligned} I_{\alpha}^{(0)}(\tau) &= \tau^{-(d+1-\alpha-2\epsilon)} S_d^2 \left(\xi(\alpha) + O(\tau)\right) \\ I_{\alpha}^{(1)}(\tau) &= \tau^{-(d+1-\alpha-2\epsilon)} S_d^2 \left(-(d-2)\xi(\alpha-1) + O(\tau)\right) \\ I_{\alpha}^{(2)}(\tau) &= \tau^{-(d+1-\alpha-2\epsilon)} S_d^2 \left(\frac{(d-2)(d-\alpha-2\epsilon)}{1+d-\alpha-2\epsilon}\xi(\alpha-2) + O(\tau)\right) \end{aligned} \tag{4.2.21}$$

where we have introduced

$$\xi(\alpha) \equiv \frac{\Gamma(\frac{d}{2})\Gamma(\frac{d+1-\alpha}{2}-\epsilon)}{2\sqrt{\pi}\Gamma(d-\frac{\alpha}{2}-\epsilon)} \tag{4.2.22}$$

The integral of a conformal block is then an infinite sum of these integrals:[4]

$$\mathcal{I}_{\Delta}^{(\ell)}(\Delta_{ij};\tau) \equiv \sum_{n,m=0}^{\infty} c_{n,m}\frac{m!}{(d-2)_m} I_{\Delta+n}^{(m)}(\tau) \tag{4.2.23}$$

and now we can efficiently write

$$\mathcal{F}_{ji}(\tau) = \sum_{\hat{k}} \lambda_{\sigma\sigma}{}^{\hat{k}}\lambda_{\hat{k}ij}\mathcal{I}_{\Delta_{\hat{k}}}^{(\ell_{\hat{k}})}(\Delta_{ij};\tau) \tag{4.2.24}$$

[4]In practice we expand this expression around $\tau = 0$, which means we restrict ourselves to only the leading terms in this sum. We are therefore not worried about convergence of the sum.

For concreteness, an integrated scalar block looks like

$$\begin{aligned}\mathcal{I}^{(0)}_{\Delta}(\Delta_{ij};\tau) = I^{(0)}_{\Delta}(\tau) &+ \frac{\Delta_{ij}+\Delta}{2(d-2)} I^{(1)}_{\Delta+1}(\tau) \\ &+ \frac{(2+\Delta)(\Delta_{ij}+\Delta)(2+\Delta_{ij}+\Delta)}{4d(d-2)(1+\Delta)} I^{(2)}_{\Delta+2}(\tau) \\ &- \frac{(d-2-\Delta)(d-2-\Delta-\Delta_{ij})(\Delta_{ij}+\Delta)}{4d(d-2(1+\Delta))} I^{(0)}_{\Delta+2}(\tau) + \dots \end{aligned} \tag{4.2.25}$$

which we can subsequently expand for small τ using the previous expressions.

The leading term in the σ self-OPE corresponds to the identity operator. Its entire contribution to $\mathcal{F}_{ji}(\tau)$ is

$$\begin{aligned}\mathcal{F}_{ji}(\tau) \supset \lambda_{\sigma\sigma}{}^{\mathbf{1}} \mathrm{G}_{ij} \mathcal{I}^{(0)}_{0}(\Delta_{ij};\tau) &= \lambda_{\sigma\sigma}{}^{\mathbf{1}} \mathrm{G}_{ij} I^{(0)}_{0}(\tau) \\ &= \lambda_{\sigma\sigma}{}^{\mathbf{1}} \mathrm{G}_{ij} \tau^{-(d+1-2\epsilon)} S_d^2 \xi(0)\,(1+O(\tau)) \end{aligned} \tag{4.2.26}$$

If we set $j = i$ to ensure positivity, we find that the Hardy-Littlewood Tauberian theorem rigorously applies and therefore (with no sum over i)

$$\sum_{k\,:\,\Delta_k \le \Delta_{\max}+d-\epsilon+\Delta_i} \lambda_{\sigma i}{}^{k} \lambda_{\sigma k}{}^{i} \sim \frac{\lambda_{\sigma\sigma}{}^{\mathbf{1}} \Delta_{\max}^{d+1-2\epsilon}}{\Gamma(d+2-2\epsilon)} \left(\xi(0) + \dots\right) \tag{4.2.27}$$

where the offset in the sum on the left-hand side (which is actually subleading here) originates from the shift in the exponent in Eq. (4.2.6).

Eq. (4.2.27) is as far as rigorous results can carry us [68]. However, in Section 4.3.2 we show that we can do much better by following [60] and inverse Laplace transforming the subleading terms in τ to estimate the subleading terms in the $\Delta_{\max}$ expansion. Below, we use the closed-form OPE coefficients for the ϕ^k operators in the free scalar theory to illustrate this procedure in detail.

4.3 Scalar Theory

In this section, we exemplify the abstract computations of Section 4.1 and Section 4.2 by considering the second-order corrections in a theory of an interacting scalar field $\phi(x)$ in d dimensions. We perturb the free massless theory by the operator $\phi^k(x)$

and investigate the anomalous dimensions of the subset of operators $\phi^l(x)$ with $l \in \{1, 2, 3, \ldots\}$. As in Eq. (1.2.4), the scalar is normalised such that

$$\langle \phi(x)\phi(0)\rangle = \frac{1}{|x|^{2\Delta_\phi}} \tag{4.3.1}$$

in the unperturbed theory. Here $\Delta_\phi = (d-2)/2$.

We now compute, using Wick contractions, the following OPE:

$$\begin{aligned}\int_{S^{d-1}} d\mathbf{n}\, \phi^k(x)\phi^l(0) &= \sum_p p! \binom{k}{p}\binom{l}{p} \int_{S^{d-1}} d\mathbf{n}\, |x|^{-2p\Delta_\phi} : \phi^{k-p}(x)\phi^{l-p}(0) : \\ &= S_d \sum_p p! \binom{k}{p}\binom{l}{p} \sum_{n=0}^{\infty} \frac{|x|^{2(n-p\Delta_\phi)}}{2^{2n} n! (d/2)_n} \phi^{l-p}\Box^n \phi^{k-p}(0)\end{aligned} \tag{4.3.2}$$

where the integral serves to project onto scalar operators, $(a)_n \equiv \Gamma(a+n)/\Gamma(a)$ is the usual Pochhammer symbol and we use colons to explicitly mark normal ordered operators only when there is a potential ambiguity. $\binom{l}{p}$ is the usual binomial coefficient. The OPE coefficients can then be read off:

$$\lambda_{\phi^k\ \phi^l}{}^{\phi^{l-p}\Box^n\phi^{k-p}} = \binom{k}{p}\binom{l}{p} \frac{p!}{2^{2n} n! (d/2)_n} \tag{4.3.3}$$

and a similar computation yields, for $n \geq 0$ and $r = k - p + \frac{l-q}{2} \in \mathbb{Z}$,

$$\lambda_{\phi^k\ \phi^{l-p}\Box^n\phi^{k-p}}{}^{\phi^q} = \sum_m r! \binom{k}{r}\binom{k-p}{m}\binom{l-p}{r-m} 2^{2n} (m\Delta_\phi)_n ((m-1)\Delta_\phi)_n \tag{4.3.4}$$

Notice in particular that

$$\lambda_{\phi^4\ \phi^l}{}^{\phi^l} = 6l(l-1), \qquad \lambda_{\phi^3\ \phi^l}{}^{\phi^l} = 0, \tag{4.3.5}$$

which we use below.

We can now compute the corrections to the cylinder energies by summing them as in Eq. (4.1.6), and we therefore consider

$$\Xi_{k\,l}{}^{q} \equiv \sum_{n=0}^{\infty} \sum_{p=0}^{\min(k,l)} \frac{\lambda_{\phi^k\ \phi^l}{}^{\phi^{l-p}\Box^n\phi^{k-p}} \lambda_{\phi^k\ \phi^{l-p}\Box^n\phi^{k-p}}{}^{\phi^q}}{l\Delta_\phi - (l+k-2p)\Delta_\phi - 2n} \tag{4.3.6}$$

It is remarkable that we can find a simple closed-form expression for this sum where every intermediate operator is clearly identifiable. As we show below, this offers us

a unique playground to test the ideas introduced in the previous sections without having to resort to any numerical approximations.

The sum in Eq. (4.3.6) is infinite and we will regularise it in three different ways. Our first regularisation procedure is the familiar dimensional regularisation, which will allow us to check our computations and recover the perturbative anomalous dimensions at the Wilson-Fisher fixed points.

4.3.1 Dimensional Regularisation and Wilson-Fisher Fixed Points

For each p, the infinite sums in Eq. (4.3.6) turn out to be of a ${}_3F_2$ hypergeometric nature, and after using some hypergeometric identities we can perform the required analytic continuation in ϵ. Collecting all the factors and the lower-order terms as in Eq. (4.1.6), we find that the second-order energies on the cylinder are given by

$$\begin{aligned} RE_{\phi^l} &= l + 6l(l-1)gR^{-\epsilon}S_d \\ &+ \left(-\frac{216}{\epsilon}l(l-1) - 68l^3 + 132l^2 - 52l + 6X^\sigma l(l-1) + O(\epsilon)\right) g^2 R^{-2\epsilon} S_d^2 + O(g^3). \end{aligned} \tag{4.3.7}$$

In the Lagrangian perspective we are supposed to perform as in Eq. (4.1.24), which differs from Eq. (4.3.6) by an additional ϵ in the denominator of the sum. This happens to make the sum slightly easier since we get just ${}_2F_1$ hypergeometric sums, and we find that the resulting small ϵ expansion up to $O(\epsilon)$ is exactly the same. So,

$$\begin{aligned} \Gamma_{\phi^l}{}^{\phi^l} &= 6l(l-1)gR^{-\epsilon}S_d \\ &+ \left(-\frac{216}{\epsilon}l(l-1) - 68l^3 + 132l^2 - 52l + 6X^\sigma l(l-1) + O(\epsilon)\right) g^2 R^{-2\epsilon} S_d^2 + O(g^3) \end{aligned} \tag{4.3.8}$$

This result is in agreement with the above discussion: the Lagrangian and Hamiltonian perspectives match for small ϵ. That is, $RE_{\phi^l} = l + \Gamma_{\phi^l}{}^{\phi^l} + O(\epsilon)$ up to second order in g.

Finding the counterterm action is straightforward, as X^σ is the only counterterm coefficient that we can tune. Notice that it should remove the divergences for every l, but this works out perfectly and all anomalous dimensions (or cylinder energies in Eq. (4.3.7)) are finite if we set

$$X^\sigma = \frac{36}{\epsilon}\,. \tag{4.3.9}$$

It is worthwhile to work out the details a bit further and get the two-loop anomalous dimensions. For $l = 4$, we find

$$\Gamma_{\phi^4}{}^{\phi^4} = 72 S_d g \mu^{-\epsilon} - 2448 S_d^2 g^2 \mu^{-2\epsilon} \tag{4.3.10}$$

and therefore

$$Z_{\phi^4}{}^{\phi^4} = 1 + \frac{72}{\epsilon} S_d g \mu^{-\epsilon} + 72 \left(\frac{36}{\epsilon^2} - \frac{17}{\epsilon}\right) S_d^2 g^2 \mu^{-2\epsilon} + O\left(g^3\right) \tag{4.3.11}$$

which we can integrate once more with respect to g to see that

$$g_B(g,\mu) = g + \frac{36}{\epsilon} S_d g^2 \mu^{-\epsilon} + 24 \left(\frac{36}{\epsilon^2} - \frac{17}{\epsilon}\right) S_d^2 g^3 \mu^{-2\epsilon} + O\left(g^4\right) \tag{4.3.12}$$

The leading term already agrees with the counterterm we found above, but we now also have the next-order counterterm at our disposal. Similarly, the quantum beta function for the dimensionful coupling is $\beta(g) = 36 S_d g^2 \mu^{-\epsilon} - 816 S_d^2 g^3 \mu^{-2\epsilon} + O(g^4)$ from integrating $\Gamma_{\phi^4}{}^{\phi^4}$ and so the dimensionless coupling $\tilde{g} \equiv g\mu^{-\epsilon}$ has a beta function of the form

$$\tilde{\beta}(\tilde{g}) = -\epsilon \tilde{g} + 36 S_d \tilde{g}^2 - 816 S_d^2 \tilde{g}^3 + O(\tilde{g}^4) \tag{4.3.13}$$

The fixed point is located at

$$\tilde{g}^* = \left(\frac{\epsilon}{36} + \frac{17\epsilon^2}{972}\right) / S_d \tag{4.3.14}$$

resulting in the fixed-point anomalous dimensions:

$$\Gamma^*_{\phi^l}{}^{\phi^l} = \frac{\epsilon l(l-1)}{6} - \frac{\epsilon^2 l(47 + l(17l - 67))}{324}\,. \tag{4.3.15}$$

Plugging in $l = 1, 2, 3, 4$ then gives the familiar results

$$\Gamma^*_{\phi} = \epsilon^2/108 \qquad \Gamma^*_{\phi^2} = \epsilon/3 + 19\epsilon^2/162$$
$$\Gamma^*_{\phi^3} = \epsilon + \epsilon^2/108 \qquad \Gamma^*_{\phi^4} = \beta'(g^*) = \epsilon - 17\epsilon^2/27 \tag{4.3.16}$$

The similarity between Γ^*_{ϕ} and $\Gamma^*_{\phi^3}$ arises due to the fact that the conformal multiplets of ϕ^3 and ϕ recombine at the Wilson-Fisher fixed point, according to the equation of motion.

In exactly the same manner we find the following results for the ϕ^3 theory in $d = 6 - 2\epsilon$:

$$\Gamma_{\phi^l}{}^{\phi^l} = 3l(6-5l)g^2 S_d^2 \mu^{-2\epsilon} \tag{4.3.17}$$

Notice that $\lambda_{\phi^3\,\phi^l}{}^{\phi^l} = 0$ and therefore the operators do not 'see' the ϕ^3 counterterm. This implies that the sums in $\Gamma_{\phi^l}{}^{\phi^l}$ have to come out finite, as indeed they do. We deduce:

$$\tilde{\beta}(\tilde{g}) = -\epsilon\tilde{g} - 27S_d^2 g^3 \tag{4.3.18}$$

and find a (non-unitary) fixed point at $g^* S_d = \sqrt{-\epsilon/27}$, leading to the anomalous dimensions

$$\Gamma^*_{\phi} = -\epsilon/9 \quad \Gamma^*_{\phi^2} = 8\epsilon/9 \quad \Gamma^*_{\phi^3} = 3\epsilon \quad \Gamma^*_{\phi^4} = \beta'(g^*) = 56\epsilon/9 \tag{4.3.19}$$

and this time the first two are related precisely such that $\Delta_{\Box\phi} = \Delta_{\phi^2}$, as expected by the equation of motion. Notice that we did not use the wave function renormalisation counterterm here.

4.3.2 TCSA Cut-Off

We have seen that the sum in Eq. (4.3.6) can be regulated by dimensional regularisation, which allowed us to find a somewhat novel way to extract the correct second-order anomalous dimensions. Our main focus in this paper is however the TCSA cut-off introduced in Section 4.2. In this section, we use this cut-off to regularise the sum in Eq. (4.3.6).

Determination of the Counterterm Action

Section 4.2.1 instructs us to consider the four-point function $\mathcal{F}_{ji}(\tau)$, which is schematically $\langle j| \int \sigma \int \sigma |i\rangle$. In our case $\sigma(x) = \phi^4(x)$ and we take $\mathcal{O}_j$ to be ϕ^k and $\mathcal{O}_i$ to be ϕ^l. Terms in the self-OPE of the ϕ^4 operator like

$$\phi^4(x)\phi^4(0) \supset \frac{24}{|x|^{8\Delta_\phi}}\mathbf{1} + \frac{96}{|x|^{6\Delta_\phi}}\left(\phi^2(0) + \text{desc.}\right) + \frac{72}{|x|^{4\Delta_\phi}}\left(\phi^4(0) + \text{desc.}\right) + \dots \tag{4.3.20}$$

and similarly for the stress tensor T, lead to small τ behaviour dictated by the expansion

$$\mathcal{F}^j{}_i(\tau) \supset 24\delta_i^j \mathcal{I}_0^{(0)}(\tau) + 96\lambda_{\phi^2}{}_i{}^j \mathcal{I}_{2\Delta_\phi}^{(0)}(\tau) + 72\lambda_{\phi^4}{}_i{}^j \mathcal{I}_{4\Delta_\phi}^{(0)}(\tau) + \lambda_{\phi^4\phi^4}{}^T \lambda_T{}_i{}^j \mathcal{I}_d^{(2)}(\tau) + \dots \tag{4.3.21}$$

which concretely leads to small τ behaviour of the form

$$\begin{aligned} S_d^{-2}\mathcal{F}^j{}_i(\tau) = 24\delta_i^j \tau^{3\epsilon-5}\xi(0) &\left(\underbrace{1}_{\#1} + \underbrace{(4-2\epsilon)\tau}_{\#2} + \frac{1}{6}(2-\epsilon)(23-12\epsilon)\tau^2 + \dots\right) \\ + 96\lambda_{\phi^2}{}_i{}^j \tau^{2\epsilon-3}\xi(2-\epsilon) &\left(\underbrace{1}_{\#2} + \left(4-2\epsilon+\frac{\Delta_{ij}}{2}\right)\tau + \text{horrid}\,\tau^2 + \dots\right) \\ + 72\lambda_{\phi^4}{}_i{}^j \tau^{\epsilon-1}\xi(4-2\epsilon) &\left(1 + \left(4-2\epsilon+\frac{\Delta_{ij}}{2}\right)\tau + \dots\right) \\ + \lambda_{\phi^4\phi^4}{}^T \lambda_T{}_i{}^j \tau^{2\epsilon-1}\xi(4-\epsilon) &\left(-\frac{2\epsilon}{4-3\epsilon} + \dots\right) \end{aligned} \tag{4.3.22}$$

where

$$\text{horrid} = \frac{3\Delta_{ij}^2\epsilon - 12\Delta_{ij}(\epsilon-2)(2\epsilon-1) + 2(\epsilon-2)(\epsilon(24\epsilon-59)+24)}{12(2\epsilon-1)} \tag{4.3.23}$$

and also

$$\lambda_{\phi^4\phi^4}{}^T \lambda_T{}_{\phi^l}{}^{\phi^k} = 24l(2-\epsilon)^2\delta_k^l\,. \tag{4.3.24}$$

In which sense does this predict the leading behaviour of the squared OPE coefficients? If we inverse Laplace transform the very leading coefficient, which is the

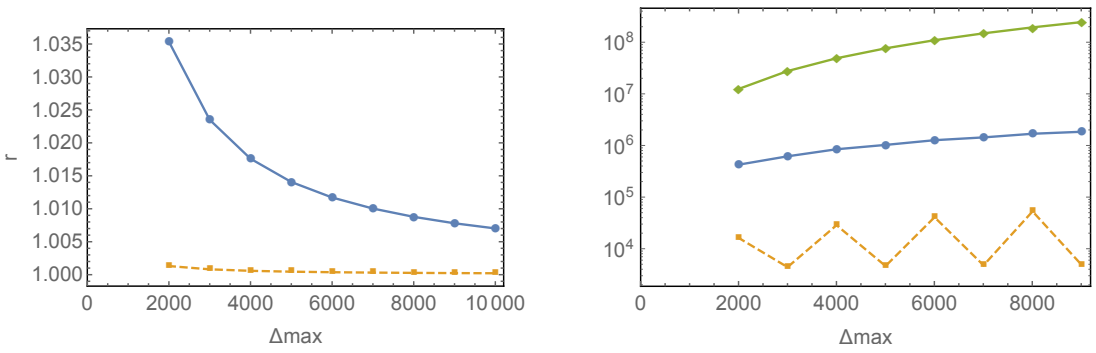

Figure 4.3: Tests of the approximation in Eq. (4.3.25) with $l = k = 2$ and $\epsilon = 1$ so $d = 3$. As a function of $\Delta_{\max}$, we plot on the left the ratio r between the left-hand side and the right-hand side (solid line) as well as an improved estimate obtained by including on the right-hand side also the two terms labelled #2 (dashed line). On the right, we log-plotted (from top to bottom) first the value of the left-hand side and then the values obtained by subtracting the terms #1 and the terms #1 and #2, respectively.

term labelled #1, then we find that

$$\sum_{m:\Delta_m \leq \Delta_{\max}+d-\epsilon+l\Delta_\phi} \lambda_{\phi^4\,\phi^l}{}^m \lambda_{\phi^4 m}{}^{\phi^k} \sim 48\delta_l^k \frac{\Delta_{\max}^{5-3\epsilon}}{\Gamma(6-3\epsilon)}\xi(0) \tag{4.3.25}$$

For $k = l$ this estimate should be correct by the Tauberian theorem quoted above. This is confirmed for $\epsilon = 1$ and $l = k = 2$ by the top line in Fig. 4.3, where we plot the ratio r between the left-hand side and just the leading term on the right-hand side – the ratio converges to one as expected.

Let us now investigate the subleading terms. At $\epsilon = 1$, the first subleading terms arise from the terms labelled #2 above. If we add the inverse Laplace transform of these terms on the right-hand side of Eq. (4.3.25), we find the improved convergence behaviour shown by the dashed line on the left in Fig. 4.3. Although this might look encouraging, the applicability of this result is limited. After all, we are actually not interested in the *ratio* between the two terms but in rather in their *difference* since we are trying to estimate the correct counterterm action. On the right in Fig. 4.3 we see that the leading term #1 subtracts a nice chunk of the value of the sum. We do even better by including #2. However, at the next order we would run into

trouble: there are visible subleading oscillations which do not decrease in size. Our approximations are based on keeping only a few terms in a power series in τ, which (inverse) Laplace transform to a smooth function of Δ. It is therefore simply not possible to reproduce such oscillating behaviour within our framework. We address this issue below, but for the remainder of this subsection we simply sidestep it by considering the summand itself.

To do so, let us first discuss how the summand

$$\lambda_{\phi^4\,\phi^k}{}^{m}\lambda_{\phi^4\,m}{}^{\phi^l}|_{\Delta_m=\Delta} \tag{4.3.26}$$

admits a natural analytical continuation in Δ. The OPE coefficients in Eqs. (4.3.3) and (4.3.4) are smooth functions of n, for fixed k and p . For each p, we thus obtain a smooth function of n, which we can trade for Δ_m (and hence Δ) by simply setting $\Delta_m = (l+4-2p)\Delta_\phi + 2n$. We then perform the finite sum over p to obtain the desired continuation. We evaluate this function (for now) at the shifted value $\Delta \to \Delta + d - \epsilon + k\Delta_\phi$ to take into account the extra τ dependence in the prefactor in Eq. (4.2.6), just as we did in Eq. (4.2.27).

The analytic continuation admits a simple asymptotic power series expansion. We find

$$\begin{aligned}
&\lambda_{\phi^4\,\phi^l}{}^{m}\lambda_{\phi^4\,m}{}^{\phi^k}|_{\Delta_m=\Delta+d-\epsilon+l\Delta_\phi} \\
&= 48\delta_l^k\Delta^{4-3\epsilon}\xi(0)\left(\frac{1}{\Gamma(5-3\epsilon)}+\frac{4-2\epsilon}{\Gamma(4-3\epsilon)}\Delta^{-1}+\frac{(2-\epsilon)(23-12\epsilon)}{6\Gamma(3-3\epsilon)}\Delta^{-2}+\dots\right) \\
&+192\lambda_{\phi^2\phi^l}{}^{\phi^k}\Delta^{2-2\epsilon}\xi(2-\epsilon)\left(\frac{1}{\Gamma(3-2\epsilon)}+\frac{4-2\epsilon+\frac{(l-k)(2-\epsilon)}{4}}{\Gamma(2-2\epsilon)}\Delta^{-1}+\frac{\text{horrid}}{\Gamma(1-2\epsilon)}\Delta^{-2}+\dots\right) \\
&+2\lambda_{\phi^4\phi^4}{}^{T}\lambda_{T\,\phi^l}{}^{\phi^k}\Delta^{-2\epsilon}\xi(4-\epsilon)\left(\frac{2\epsilon}{(3\epsilon-4)\Gamma(1-2\epsilon)}+\dots\right) \\
&+144\lambda_{\phi^4\phi^l}{}^{\phi^k}\xi(4-2\epsilon)\Delta^{-\epsilon}\left(\frac{1}{\Gamma(1-\epsilon)}+\dots\right)
\end{aligned} \tag{4.3.27}$$

As far as we checked, both the powers and coefficients in this expansion *precisely* match those predicted by the inverse Laplace transform of the leading terms in

$\mathcal{F}^{\phi^k}{}_{\phi^l}(\tau)$, with an extra factor 2 arising only because the Δ's that contribute to the sum are spaced in units of two (since the Laplacian operator has dimension 2). In equations, we can say that to every order in the small τ and large Δ expansion:

$$\mathcal{L}^{-1}\left[S_d^{-2}\mathcal{F}^{\phi^k}{}_{\phi^l}(\tau);\tau\to\Delta\right]=\frac{1}{2}\lambda_{\phi^4\,\phi^l}{}^{m}\lambda_{\phi^4\,m}{}^{\phi^k}|_{\Delta_m=\Delta+d-\epsilon+l\Delta_\phi} \tag{4.3.28}$$

with the inverse Laplace transform obeying

$$\mathcal{L}^{-1}\left[\tau^{-\rho};\tau\to\Delta\right]=\frac{\Delta^{\rho-1}}{\Gamma(\rho)} \tag{4.3.29}$$

and the right-hand side considered as an analytic function in Δ. We have checked this claim for the identity operator (which reproduces the $\Delta^{4-3\epsilon}$ terms) to second subleading order, for the ϕ^2 operator and the stress tensor (the $\Delta^{2-2\epsilon}$ and $\Delta^{-2\epsilon}$ terms) together also to second subleading order, and finally to leading order for the ϕ^4 operator (the $\Delta^{-\epsilon}$ terms). Altogether, this shows that the subleading terms in the large Δ expansion would be captured perfectly by the subleading terms in $\mathcal{F}_{ji}(\tau)$, were it not for the fact that we sum rather than integrate over the intermediate operators.

Ignoring (still) the issue of the oscillations, we can use the subleading terms in $\mathcal{F}_{ji}(\tau)$ to compute the counterterms to high subleading orders. The counterterm Hamiltonian will then look like this:

$$H_{\rm ct}=g^2S_dR^{2(d-\Delta_\sigma)-1}\int_{S^{d-1}}d\mathbf{n}\left(\mathbf{1}X_{\mathbf{1}}+R^{\Delta_\phi^2}\phi^2X_{\phi^2}+R^dT_{\tau\tau}X_T+R^{\Delta_\phi^4}\phi^4X_{\phi^4}\right) \tag{4.3.30}$$

with dimensionless $X_{\mathcal{O}}$ coefficients which are roughly speaking determined by the inverse Laplace transform of $\mathcal{F}_{ji}(\tau)$ given in Eq. (4.3.27). If we set $\Lambda=\Delta_{\rm max}/R$, then it follows from a dimensional analysis argument that $X_{\mathcal{O}}\sim\Delta_{\rm max}^{2\Delta_\sigma-d-\Delta_{\mathcal{O}}}$ to leading order. There are however several subtleties that we need to address before we can use Eq. (4.3.27) to obtain the explicit form of the $X_{\mathcal{O}}$. Let us discuss them one at a time.

Offset in $\Delta_{\rm max}$ Our first subtlety is the extra prefactor $\exp\left(\tau(d-\epsilon+\Delta_i)\right)$ in

Eq. (4.2.6) which leads to a small imperfection in the relation between the inverse Laplace transform of $\mathcal{F}_{ji}(\tau)$ and the sum of squared OPE coefficients. This is reflected in the offset on the left-hand side of Eq. (4.3.27). This will have to be taken into account by *non-local* counterterms of the form already written down in [60]:

$$W \supset g^2 R^{2\epsilon} \left(\frac{\Delta_{\max}}{R}\right)^{d-\Delta_k} \left(\int_{S_R^{d-1}} d\mathbf{n}\, \mathcal{O}_k\right) \left(\frac{RH_{\text{CFT}}}{\Delta_{\max}}\right)^n \tag{4.3.31}$$

which leads to matrix elements of the form:

$$RW_i{}^j \supset g^2 R^{2\epsilon} S_d \Delta_{\max}^{d-\Delta_k-n} \Delta_i^n \lambda_{ki}{}^j \tag{4.3.32}$$

These operators can be made Hermitian by instead considering anti-commutators, for example $\{O_k, H_{\text{CFT}}\}$. The *commutators* that this introduces are discussed further on.

Since H_{CFT} is the integral of a local density but not a local operator itself, it follows that the counterterm is not local (unless $O_k = \mathbf{1}$ and $n = 1$). In practice, we get finitely many non-local counterterms because we keep only finitely many terms in the $\Delta_{\max}$ expansion.

The Denominator and the Integral In our analysis we have seen that $\mathcal{F}_{ji}(\tau)$ provides a good approximation of the sum of squared OPE coefficients $\lambda_{\sigma i}{}^k \lambda_{\sigma kj}$ but we need to still add the denominator $(\Delta_i - \Delta)$ in Eq. (4.1.6) and integrate over Δ. The Δ_i dependence in the denominator translates into yet another non-locality of the same type as dicussed in our previous point. Altogether, we can take into account both the offset and the denominator by the following replacement rule: any Δ^α in the inverse Laplace transform of $\mathcal{F}_{ji}(\tau)$ – so in Eq. (4.3.27) – needs to be replaced by

$$\begin{aligned} \Delta^\alpha \to \widehat{\Delta^\alpha_{\max}} &\equiv \int^{\Delta_{\max}} d\Delta \frac{(\Delta - d + \epsilon - RH_{\text{CFT}})^\alpha}{RH_{\text{CFT}} - \Delta} \\ &= \Delta_{\max}^\alpha \left(-\frac{1}{\alpha} + \Delta_{\max}^{-1}\left(RH_{\text{CFT}} + \frac{\alpha(d-\epsilon)}{\alpha - 1}\right) + O(\Delta_{\max}^{-2})\right) \end{aligned} \tag{4.3.33}$$

If we keep only finitely many terms in the Δ-expansion, then the counterterm will

be polynomial in $RH_{\rm CFT}$.

Δ_{ij} Dependence in the Blocks For non-identical operators, the conformal blocks depend on the difference Δ_{ij} in operator dimensions. This is a generic property, and in our case this shows up in the subleading terms in the expansion of $\mathcal{F}_{ji}(\tau)$ given above in Eq. (4.3.22). By their very nature, these terms only show up in the off-diagonal elements in sums like Eq. (4.1.6), so in the terms with $i \neq j$. These terms are unimportant for the computation of second-order energies, and therefore we can set to zero the Δ_{ij} terms in the inverse Laplace transform of the blocks. We give a more elaborate discussion of this below.

With this notation in place our counterterms take the form:

$$
\begin{aligned}
X_{\mathbf{1}} &= -24\,\xi(0)\left(\frac{\widehat{\Delta_{\max}^{4-3\epsilon}}}{\Gamma(5-3\epsilon)} + \frac{(4-2\epsilon)\widehat{\Delta_{\max}^{3-3\epsilon}}}{\Gamma(4-3\epsilon)} + \frac{(2-\epsilon)(23-12\epsilon)\widehat{\Delta_{\max}^{2-3\epsilon}}}{6\Gamma(3-3\epsilon)} + \dots\right)\\
X_{\phi^2} &= -96\,\xi(2-\epsilon)\left(\frac{\widehat{\Delta_{\max}^{2-2\epsilon}}}{\Gamma(3-2\epsilon)} + \frac{(4-2\epsilon)\widehat{\Delta_{\max}^{1-2\epsilon}}}{\Gamma(2-2\epsilon)} + \frac{\text{horrid}\,\widehat{\Delta_{\max}^{-2\epsilon}}}{\Gamma(1-2\epsilon)} + \dots\right)\\
X_{\mathbf{T}} &= -{\lambda_{\phi^4\phi^4}}^{T}\,\xi(4-\epsilon)\left(\frac{2\epsilon\widehat{\Delta_{\max}^{-2\epsilon}}}{(3\epsilon-4)\Gamma(1-2\epsilon)} + \dots\right)\\
X_{\phi^4} &= -72\,\xi(4-2\epsilon)\left(\frac{\widehat{\Delta_{\max}^{-\epsilon}}}{\Gamma(1-\epsilon)} + \dots\right)
\end{aligned}
\tag{4.3.34}
$$

with all-important minus signs because they are supposed to *cancel* divergences, and with $\Delta_{ij} \to 0$ also in 'horrid' as given in Eq. (4.3.23). The preceding equation is the main result of this section, and few more comments are in order.

First of all, as noticed already in [60], the counterterm action has certain non-localities. Of course, a completely arbitrary non-local counterterm action would be worrying. However in this case, the non-locality enters in a mild and prescribed way, namely only through the substitution in Eq. (4.3.33). Unfortunately, at higher orders things appear less benign, for example in [64] a counterterm $:\int\phi^2\int\phi^4:$ was introduced. The restoration of locality in the continuuum limit therefore hinges on the irrelevance (in the technical sense) of these non-local counterterms. For the examples considered in the literature this seems to work well, but for less relevant

(in the technical sense) perturbations this may become an issue.

Secondly, the conformal block decomposition of the four-point function organises the counterterms also in conformal multiplets. More precisely, we only need to add the conformal primary $\mathcal{O}_k(x)$ as an explicit operator in the counterterm Hamiltonian, and can then take into account descendants (i.e. subleading terms in the block expansion) by improving its coefficient X^k. Notice that if we want finite energies at second order then we can extract the necessary counterterms from only those four-point functions $\mathcal{F}_{ji}(\tau)$ with $j = i$, so the Δ_{ij} terms that appear in a general conformal block can be ignored. We are again supposing here that all degeneracies have been resolved and therefore that $\lambda_{\sigma i}{}^{j}$ has been diagonalised within small blocks as explained above.

Thirdly, manifestly Lorentz-violating counterterms can only arise from other Lorentz-violating primary operators in the OPE expansion. Such counterterms are clearly *allowed* as long as the vectorial indices point in the τ direction to preserve rotational invariance on the spacelike sphere, and then they are also *expected* since they do not break more symmetries than our regulator. The need for tensorial counterterms had been noticed in [60], but in the examples considered in that paper they were subleading and not worked out in detail. Of course the integral of $T_{\tau\tau}$ is special since it is just the Hamiltonian again and, despite appearances, it does not break Lorentz invariance. We believe that the corresponding counterterm can be interpreted as wave function renormalisation, which would be absent with a local Lorentz-invariant cut-off but does show up here. Notice also that it has the same matrix element as the subleading term proportional to H_{CFT} in the expansion of the identity counterterm. However they appear with very different powers of $\Delta_{\max}$, so they are certainly different counterterms, and our analysis rigorously establishes the appearance of both.

Our fourth and last comment concerns the off-diagonal elements in Eq. (4.1.6). These terms are equally divergent and we would like to ask whether the counterterm action is expected to make the terms with $i \neq j$ finite as well. As we have discussed, this is

not necessary to have renormalised energies at second order. In fact, because of the Δ_i in the denominator the sum in Eq. (4.1.6) is not even Hermitian (real symmetric in this case) so there is no Hermitian counterterm that can make that expression finite to arbitrary subleading order. One may of course try to modify the expression to e.g.

$$\frac{V_i{}^k V_k{}^j}{\frac{1}{2}(\Delta_i + \Delta_j) - \Delta_k} \tag{4.3.35}$$

but the question then arises what the motivation would be for these ad hoc replacements.

An issue that is very much related to the issue of off-diagonal elements is the existence of counterterms that arise from commutator operators like

$$[H_{\mathrm{CFT}}, \dots [H_{\mathrm{CFT}}, \mathcal{O}]] \sim \partial_t \dots \partial_t \mathcal{O} \tag{4.3.36}$$

whose matrix elements between states $\langle j|$ and $|i\rangle$ are proportional to Δ_{ij}, to an arbitrary power. These counterterms are compatible with the residual symmetries of the cylinder and so can in principle be added; one might in fact be tempted to do so at subleading orders when there is Δ_{ij} dependence in the blocks. However, to maintain a real symmetric Hamiltonian one can only add terms with even powers of Δ_{ij}, and we have already seen that the blocks contain terms linear in Δ_{ij} above.

We believe the question of the off-diagonal term could be addressed by going one order higher and looking at the third-order correction. This is because, for a *local* cut-off at least, we may expect the third-order counterterm to be completely local. If we look at Eq. (4.1.8), this for example implies that divergences arising in the limit[5] $j \to \infty$ for fixed but finite k ought to be cancelled automatically by the counterterms in the latter two sums rather than by the third-order counterterm, which is the last term in Eq. (4.1.8). One could for example speculate that $W_i{}^j$ for a local cut-off instead makes finite an expression of the form

$$U_i{}^j := W_i{}^i + \frac{V_i{}^k V_k{}^i}{\Delta_{ik}} \qquad \text{when } i = j$$

[5]More precisely, the analogue limit in the case of a local cut-off.

$$U_i{}^j := W_i{}^j + \frac{V_i{}^k V_k{}^j}{2}\left(\frac{1}{\Delta_{ik}} + \frac{1}{\Delta_{jk}} - \frac{\Delta_i + \Delta_j}{\Delta_{ik}\Delta_{jk}}\right) \qquad \text{when } i \neq j \tag{4.3.37}$$

Indeed, in terms of these new matrices, Eq. (4.1.8) becomes

$$\frac{1}{R}\left(\frac{U_i{}^j V_j{}^i + V_i{}^j U_j{}^i}{\Delta_{ij}} + W_i{}^i\right) \tag{4.3.38}$$

and, provided the divergences take a local form, the diagonal elements of $W_i{}^i$ may now also be fixed to a local expression.

Unfortunately, the TCSA cut-off is not local, so the reasoning of the previous paragraph does not obviously apply and it remains an interesting question to what extent we can use locality of third-order counterterms to gain insight in the off-diagonal terms at second order. For example, in [65] non-local counterterms of the schematic form $\int \phi^2 \int \phi^4$ were introduced at third order, and it would be interesting to work out how second-order off-diagonal counterterms like those in Eq. (4.3.36) would modify the coefficient of that counterterm.

Oscillations and a Smoothly Varying Projector

Eq. (4.3.27) relates the *summand* in Eq. (4.3.6) order-by-order to a simple asymptotic power series. The oscillations in Fig. 4.3 exemplify how the full sum can only be replicated on average by an integral of the series. Up to now, we have flagrantly ignored these subleading oscillations, which arise inevitably from the discreteness of spectrum. One may wonder if there exists a more sophisticated counterterm action that takes into account these oscillations. For example, we can make the coefficients $X_{\mathcal{O}}$ in Eq. (4.3.34) more complicated functions of Δ_{max} which also oscillate and then precisely cancel the oscillating sum. This is not a straightforward task and may drastically increase the non-locality of the counterterm action. In this section we therefore suggest how the issue can be mitigated by using a smoothed-out cut-off, centered around Δ_{max}. Concretely, we replace the TCSA projector $\mathcal{P}$ introduced above with a projector that smooths out the hard truncation at Δ_{max}. This leads to a new version of the replacement rule in Eq. (4.3.33), but otherwise the counterterms

are unchanged.

Specifically, we consider a smoothly varying projector which flips from 1 to 0 around $\Delta_{\rm max}$ with a transition width growing slower than $\Delta_{\rm max}$. For example,

$$\mathcal{P} \to \mathcal{P}_f := \sum_{\Delta} |\Delta\rangle f(\Delta, \Delta_{\rm max}) \langle\Delta| \tag{4.3.39}$$

with

$$f(\Delta, \Delta_{\rm max}) \equiv \frac{1}{2}\left(1 - \tanh\left(\frac{\Delta - \Delta_{\rm max}}{\sqrt{\Delta_{\rm max}}}\right)\right) \tag{4.3.40}$$

Asymptotically, we have that (for $\alpha > 0$)

$$\int^{\infty} d\Delta\, f(\Delta, \Delta_{\rm max}) \Delta^{\alpha-1} \sim \frac{f_\alpha(\Delta_{\rm max})\, \Delta_{\rm max}^{\alpha}}{\alpha} \tag{4.3.41}$$

where

$$f_\alpha(\Delta_{\rm max}) \equiv \sum_{k=0}^{\lfloor\alpha\rfloor} 2(-1)^k (1 - 2^{2k-1}) \left(\frac{\pi}{8}\right)^k \frac{B_{2k}}{(2k)!} \frac{\Delta_{\rm max}^{-k}}{(1+\alpha)_{-2k}} \tag{4.3.42}$$

and B_n is the $n^{\rm th}$ Bernoulli number. This implies that the reincarnation of Eq. (4.3.33) with the smoothed cut-off should be

$$\begin{aligned} \Delta^\alpha \to \widehat{\widehat{\Delta^\alpha_{\rm max}}} &\equiv \int^{\infty} d\Delta \frac{(\Delta - d + \epsilon - RH_{\rm CFT})^\alpha}{RH_{\rm CFT} - \Delta} f(\Delta, \Delta_{\rm max}) \\ &= \Delta^\alpha_{\rm max}\left(-\frac{f_\alpha(\Delta_{\rm max})}{\alpha} + \frac{f_{\alpha-1}(\Delta_{\rm max})}{\Delta_{\rm max}}\left(RH_{\rm CFT} + \frac{\alpha(d-\epsilon)}{\alpha - 1}\right) + ...\right) \end{aligned} \tag{4.3.43}$$

Each singly hatted $\Delta_{\rm max}$ in Eq. (4.3.34) can be replaced with a doubly hatted one, and this gives the counterterms within the smoothly truncated theory.

Fig. 4.4 provides evidence that these smooth counterterms work in the ϕ^4 theory. The oscillations that arose due to the discreteness of the spectrum get trampled and we end up with a convergent sum.

Example: Three Dimensions

As an explicit example in an integer dimension, Eq. (4.3.34) with $\epsilon = 1$ becomes

$$\begin{aligned} X_{\mathbf{1}} &= -6\widehat{\Delta_{\max}} - 12\widehat{\Delta^0_{\max}} \\ X_{\phi^2} &= -48\widehat{\Delta^0_{\max}} \end{aligned} \tag{4.3.44}$$

where each singly hatted $\Delta_{\max}$ is replaced with a doubly hatted one in the smooth theory.

Some care must be taken at this stage, since the replacement rules have to be extended to include logarithmic divergences:

$$\begin{aligned} \widehat{\Delta_{\max}} &= -\Delta_{\max} + 2\log\Delta_{\max} + \dots \\ \widehat{\Delta^0_{\max}} &= -\log\Delta_{\max} + \dots \end{aligned} \tag{4.3.45}$$

To this order, $\widehat{\widehat{\Delta_{\max}}} = \widehat{\Delta_{\max}}$ and $\widehat{\widehat{\Delta^0_{\max}}} = \widehat{\Delta^0_{\max}}$.

Fig. 4.5 shows how these counterterms nicely regularise the $d = 3$ variant of Eq. (4.2.3).

Decaying Counterterms

The $d = 3$ counterterms can be extended to include some decaying contributions, in an attempt to improve convergence. Taking the first decaying term,

$$\begin{aligned} X_{\mathbf{1}} &= -6\widehat{\Delta_{\max}} - 12\widehat{\Delta^0_{\max}} \\ X_{\phi^2} &= -48\widehat{\Delta^0_{\max}} \\ X_{\phi^4} &= -36\widehat{\Delta^{-1}_{\max}} \end{aligned} \tag{4.3.46}$$

where

$$\begin{aligned} \widehat{\Delta_{\max}} &= -\Delta_{\max} + 2\log\Delta_{\max} - 2RH_{\mathrm{CFT}}\,\Delta^{-1}_{\max} + ... \\ \widehat{\Delta^0_{\max}} &= -\log\Delta_{\max} + RH_{\mathrm{CFT}}\,\Delta^{-1}_{\max} + ... \\ \widehat{\Delta^{-1}_{\max}} &= \Delta^{-1}_{\max} + ... \end{aligned} \tag{4.3.47}$$

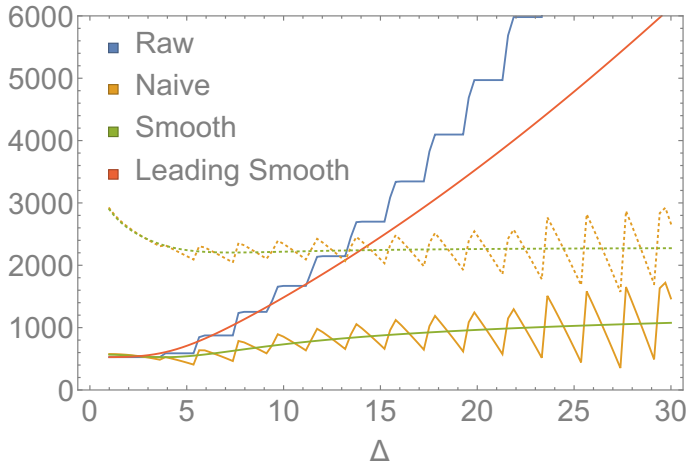

Figure 4.4: The negative of Eq. (4.2.3) in ϕ^4 theory is plotted as a function of Δ_{max} for $\mathcal{O}_i = \mathcal{O}_j = \phi^2$ and $\epsilon = 1/5$, so that $d = 3.8$. The blue line is the raw data and the orange line incorporates the naive counterterms in Eq. (4.3.34). The red line displays the same sum but with the smooth projector in Eq. (4.3.39), and it includes the leading correction. Finally, the green line utilises all smooth counterterms. The dashed lines are discussed in the 'Decaying Counterterms' part of Section 4.3.2.

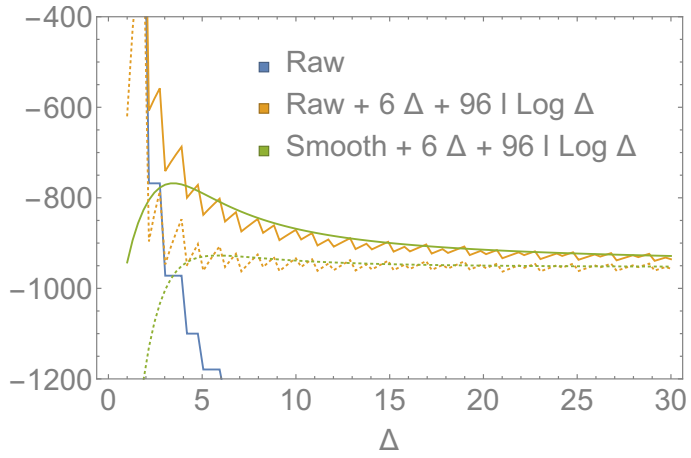

Figure 4.5: Eq. (4.2.3) in ϕ^4 theory is plotted as a function of Δ_{max} for $\mathcal{O}_i = \mathcal{O}_j = \phi^2$ $(l = 2)$ and $\epsilon = 1$, so that $d = 3$. The blue line is the raw data, whereas the orange line includes the addition of the naive counterterms and the green line is the regularised smoothed data. The oscillation amplitude appears to stay finite for this special case. The dashed lines are discussed in the 'Decaying Counterterms' part of Section 4.3.2.

To this order, we have some discrepancy between singly and doubly hatted counterterms:

$$\begin{aligned}\widehat{\Delta_{\max}} &= \widehat{\widehat{\Delta_{\max}}} + \frac{\pi^2}{12\,\Delta_{\max}} \\ \widehat{\Delta^0_{\max}} &= \widehat{\widehat{\Delta^0_{\max}}} - \frac{\pi^2}{24\,\Delta_{\max}}\end{aligned} \tag{4.3.48}$$

The dashed lines in Fig. 4.5 show how including these decaying counterterms can significantly improve convergence. Also note that the analogous dashed lines in Fig. 4.4, which indicate a massive improvement in convergence that arises because the first correction is increasingly large as $\epsilon \to 0$; that is as ϕ^4 becomes marginal.

4.3.3 TCSA-Inspired Cutoffs for the Scalar Theory

The TCSA offers a natural and universally implementable cut-off. For the scalar theory we can however consider more customised cut-offs which would be suitable for perturbative computations.

A particularly natural perturbative cut-off to consider would be a spatial momentum-space cut-off on the cylinder. In terms of canonical quantisation, this amounts to setting to zero all the creation operators with large momentum on the sphere. This would be a local cut-off in the sense that any momentum-space cut-off is local: it morally corresponds to discretising space to a lattice.[6] The state-operator correspondence maps these high-momentum modes to operators with many derivatives, and therefore it amounts to setting to zero operators with more than, say, $n_{\max}$ derivatives per ϕ. This cut-off is however not easily implemented for our sum ${\Xi_{kl}}^q$ in Eq. (4.3.6), because we would then have to work out the Laplacians in the intermediate operator $\phi^{l-p}\Box^n\phi^{k-p}$ and keep only those operators with less than $n_{\max}$ derivatives per ϕ.

A somewhat related perturbative cut-off would be to limit the *total* spatial mo-

[6] This cut-off would exactly correspond to a spatial lattice if the spatial manifold was a torus. For the sphere, we are not aware of an explicit lattice that would truncate the spherical harmonic expansion, but see [71] for an attempt at a lattice formulation of radial quantisation.

mentum on the cylinder. Again through the state-operator correspondence, this cut-off amounts to a bound on the total number of derivatives in a given composite operator. For our sum ${\Xi_{kl}}^q$ given in Eq. (4.3.6), this truncation is simply:

$$n \leq N_{\max} \tag{4.3.49}$$

and the UV cut-off scale is $\Lambda = 2N_{\max}/R$. This cut-off does not appear to be local: for example, for a two-particle state the momentum of one particle is constrained in terms of the momentum of the other.

It is important to realise that the energy of a state (or the scaling dimension of an operator) can grow very large not only by taking large momentum (or many derivatives in the operator) but also by taking many particles (or many fundamental fields in the operator). Since we did not truncate the latter, any possible divergences arising from arbitrarily-many-particle states are not regulated by these cut-offs. Although this implies that these cut-offs are problematic non-perturbatively, such divergences are absent at any finite order in perturbation theory, since at every order a ϕ^k interaction adds only up to k (i.e. finitely many) extra fields. This is why the momentum cut-offs work only in perturbation theory.

Let us consider the ϕ^4 theory again, now with the cut-off in total spatial momentum of Eq. (4.3.49). Analysing the large n behaviour of the summand is simple, both at the level of the integrand and using some simple modifications of the results in the previous section. The dimension of the intermediate operator in ${\Xi_{4l}}^q$ is given by

$$\Delta = (l + k - 2p)\Delta_\phi + 2n \tag{4.3.50}$$

and so to leading order the cut-off in n essentially agrees with a cut-off in Δ. We therefore propose the same leading-order counterterms. At subleading orders, there are small modifications. These are not interesting enough to write down explicitly,

except that structurally we observe that with the cut-off of Eq. (4.3.49):

$$\begin{aligned}\Xi_{k\,l}{}^{q} &= N_{\max}^{4-3\epsilon}(\#\delta_l^q + O(1/N_{\max})) \\ &+ N_{\max}^{2-2\epsilon}(\#\lambda_{\phi^2\phi^l}{}^{\phi^q} + \#(l-q+6-12\epsilon)N_{\max}^{-1}\lambda_{\phi^2\phi^l}{}^{\phi^q} + O(1/N_{\max}^2)) \\ &+ N_{\max}^{-\epsilon}(\#\lambda_{\phi^4\phi^l}{}^{\phi^q} + \#(l-q-4-4\epsilon)N_{\max}^{-1}\lambda_{\phi^4\phi^l}{}^{\phi^q} + O(1/N_{\max}^2))\end{aligned} \tag{4.3.51}$$

where the coefficients # are unimportant functions of ϵ only.

We can offer two interesting observations about this cut-off. The first pertains to the oscillations discussed in the previous subsection. We observe that for the diagonal elements with $l = q$ the dependence on l in Eq. (4.3.51) is fully captured by the OPE coefficients. This means that there exists non-trivial counterterm coefficients $X_{\mathcal{O}}$, functions of $\Delta_{\max}$ and ϵ only, which can get rid of the oscillations in $\Xi_{k\,l}{}^{q}$ completely. The question that arises now is whether this holds for arbitrary external operators – in that case we could claim that this cut-off allows us to get rid of the oscillations without introducing drastic new non-localities.

Our second observation concerns the off-diagonal matrix elements. In Eq. (4.3.51), we observe subleading off-diagonal terms, only one power down in the $N_{\max}$ expansion, with non-trivial dependence on l and q, so the naive counterterms do not make the full matrix $\Xi_{4\,l}{}^{q}$ finite. In fact, as we pointed out before, the divergences are not Hermitian and so no reasonable counterterm action can cancel them.

Things marginally improve once we symmetrise the denominator as in Eq. (4.3.35): in that case we find that Eq. (4.3.51) gets modified so that only even powers of $(l-q)$ appear, with the leading appearance one power further down. Remarkably, this is precisely the kind of subleading divergence that can in principle be addressed with Hermitian counterterms of the form $\partial_t^2\phi^2$ and $\partial_t^2\phi^4$. However, without a third-order analysis along the lines sketched in Section 4.3.2 we cannot be sure whether we need to add them.

Finally, passing to the more sophisticated Eq. (4.3.37) we observe that, with the $N_{\max}$ cut-off, there is an additional non-trivial l-dependence in the analogue of Eq. (4.3.51), and we need to either include non-local counterterms or new operators to cancel

these terms. It follows that (with this cut-off) the naive counterterm action does not make Eq. (4.3.37) finite. The subleading terms again have even powers of $(l-q)$ beginning at one power further down than in Eq. (4.3.51).

4.4 TCSA Conclusions

The TCSA has proven to be a very useful numerical method for a wide variety of field theories. One of its main virtues is its simplicity, relying only on a simple Hamiltonian perspective that is familiar from quantum mechanics. In this work, we studied the TCSA cut-off in the framework of perturbative renormalisation and discussed some of its less attractive features like non-localities, non-covariant counterterms, and oscillations that are not easily cancelled. Fortunately, these effects are all suppressed by powers of the cut-off, and the suppression becomes stronger for more strongly relevant deformations. Morally speaking then, our results support the usual lore that the TCSA is at its most useful for strongly relevant deformations.

There are several possible future directions that naturally arise from this work. Firstly, we have seen that the conformal perturbation theory framework replaces the usual Feynman integrals with sums over computable free-field OPE coefficients. This offered us a remarkably simple way to compute second-order anomalous dimensions at the Wilson-Fisher fixed points. It would be interesting to see how this approach compares in difficulty to the Feynman diagram expansion in more general theories and/or at higher orders. How would the computational cost compare with the Feynman diagram expansion? Also, we have seen how the Hamiltonian viewpoint leads to an unconventional picture where anomalous dimensions arise from the diagonalisation of a single infinite matrix. We would be interested in learning the analogous picture for gauge theories and in particular integrable theories like planar $\mathcal{N}=4$ SYM.

In numerical work, the focus has been on finding a counterterm action that approximates well the full matrix in Eq. (4.1.6) (for reasons that are explained in [60]). In

perturbation theory, we only care about diagonal elements in these kind of sums and there are subleading divergences in the off-diagonal terms that are not obviously cancelled by the counterterm action. In the future it would be interesting to understand these differences further. To do so one could for example work out the third-order correction for a local cut-off, which we expect to give us more information about the off-diagonal divergences at second order. Related to this, one could analyse the dependence of non-local divergences at third order (with the TCSA cut-off) on the details of the second-order counterterm action.

Finally, our work can provide a stepping stone for the numerical TCSA, in particular for the ϕ^4 theories in three dimensions. We have provided the explicit second-order counterterm action in the 'Three Dimensions' part of Section 4.3.2 above. This counterterm action should suffice to get finite numerical results. However, to get *accurate* results one may need to add further improvement terms, similar to those obtained in two dimensions in [65, 64], and perhaps a smoother cut-off like the one introduced above may be necessary to deal with any remaining oscillations. It would be very interesting to see if this will suffice to get accurate predictions from the TCSA in three spacetime dimensions.

Appendix A

Discontinuity Trick

In this appendix, we explain how to go from expansions of alpha space densities which are valid for large imaginary values to asymptotic discontinuities across the real axis. This is the trick that allows for the replacement in Eq. (2.6.35).

Consider a density $\hat{f}(\alpha)$ that asymptotically goes like

$$\hat{f}(\alpha) = (-\alpha^2)^p \Big(1 + O(\alpha^{-2})\Big) \tag{A.0.1}$$

at large imaginary α. We then claim that on average

$$\text{disc}_\alpha \hat{f}(\alpha) = -\frac{\alpha^{2p}}{\Gamma(p)\Gamma(1-p)} \Big(1 + O(\alpha^{-2})\Big) \tag{A.0.2}$$

where the discontinuity is across the real axis and is defined in Eq. (2.6.23). By average, we mean in the integrated sense of the Hardy-Littlewood Tauberian theorem discussed in Section 4.2.1. Explicitly, we mean that

$$\int^\infty d\alpha\, e^{-s\alpha}\, \text{disc}_\alpha \hat{f}(\alpha) = -\frac{\Gamma(2p+1)}{s^{2p+1}\Gamma(p)\Gamma(1-p)} \Big(1 + O(s^2)\Big) \tag{A.0.3}$$

This is a consequence of a dispersion relation proved[1] nicely in the appendices of

[1] The really nice aspect of this proof is that it is for a *complex* Tauberian theorem. Therefore, the authors have better control over the subleading terms.

[72] (in a slightly different context). As a knavish justification, we note that

$$\hat{f}(\alpha) - \frac{\Gamma(p+\frac{1}{2}\pm\alpha)}{\Gamma(\frac{1}{2}\pm\alpha)} = (-\alpha^2)^p\Big(O(\alpha^{-2})\Big) \tag{A.0.4}$$

That is, the two densities are equivalent to leading order in the large imaginary α limit. The Laplace transform of the latter density is

$$\begin{aligned}\int_0^\infty ds\, e^{-s\alpha}\,\mathrm{disc}_\alpha\left(\frac{\Gamma(p+\frac{1}{2}\pm\alpha)}{\Gamma(\frac{1}{2}\pm\alpha)}\right) &= -\frac{e^{-sp}(1-e^{-s})^{-2p}}{e^{s/2}-e^{-s/2}}\left(\frac{\Gamma(2p+1)}{\Gamma(p)\Gamma(1-p)}\right) \\ &= -\frac{\Gamma(2p+1)}{s^{2p+1}\Gamma(p)\Gamma(1-p)}\Big(1+O(s^2)\Big)\end{aligned} \tag{A.0.5}$$

and so we can call upon Eqs. (A.0.4) and (A.0.5) to partially legitimise Eq. (A.0.3).

Appendix B

Block Recursion Relations

Conformal blocks obey a quadratic Casimir equation [73]:

$$\mathcal{D}G_{\Delta}^{(J)} = \mathcal{C}_{\Delta}^{(J)}G_{\Delta}^{(J)} \tag{B.0.1}$$

with the eigenvalue equal to

$$\mathcal{C}_{\Delta}^{(J)} = \frac{\Delta(\Delta - d) + J(J + d - 2)}{2} \tag{B.0.2}$$

The differential operator is given by

$$\mathcal{D}(z, \bar{z}) = D_z + D_{\bar{z}} + (d-2)\frac{z\bar{z}}{z - \bar{z}}\Big((1-z)\partial_z - (1-\bar{z})\partial_{\bar{z}}\Big) \tag{B.0.3}$$

where

$$D_z = z^2(1-z)\partial_z^2 - (\mathbf{a} + \mathbf{b} + 1)z^2\partial_z - \mathbf{ab}z \tag{B.0.4}$$

and

$$\mathbf{a} = -\frac{1}{2}\Delta_{12} \qquad \mathbf{b} = \frac{1}{2}\Delta_{34} \tag{B.0.5}$$

We can expand the conformal block as a sum of Gegenbauer polynomials [70]:

$$G_{\Delta}^{(J)} = \sum_{n,m=0}^{\infty} c_{n,m}\mathcal{G}_{\Delta}^{(J)}(n,m) = |z|^{\Delta}\sum_{n,m=0}^{\infty} c_{n,m}|z|^n \frac{m!}{(2\nu)_m}C_m^{\nu}(\cos(\arg(z))) \tag{B.0.6}$$

where we have defined $\nu \equiv d/2 - 1$ and, in general, $c_{n,m}$ depends on $\mathbf{a}, \mathbf{b}, J, d$ and Δ.

A Gegenbauer polynomial is a particular type of Jacobi polynomial. The latter was

introduced in Eq. (2.1.25). Explicitly,

$$C_n^{\alpha}(z) = \frac{(2\alpha)_n}{(\alpha+\frac{1}{2})_n} P_n^{(\alpha-\frac{1}{2},\alpha-\frac{1}{2})}(z) \tag{B.0.7}$$

Defining

$$x = |z| \qquad y = \cos(\arg(z)) = \frac{z+\bar{z}}{2|z|} \tag{B.0.8}$$

we have that

$$\begin{aligned}
\mathcal{D} &= \frac{1}{2}\Big(\mathcal{D}_0 + \mathcal{D}_1 + \mathcal{D}_{\text{ext}}\Big) \qquad (B.0.9)\\
\mathcal{D}_0 &= x^2\partial_x^2 - (1-y^2)\partial_y^2 - (2\nu+1)(x\partial_x - y\partial_y)\\
\mathcal{D}_1 &= x\left(-x^2 y\partial_x^2 + y(1-y^2)\partial_y^2 + 2x(1-y^2)\partial_x\partial_y - xy\partial_x - (2\nu+y^2)\partial_y\right)\\
\mathcal{D}_{\text{ext}} &= -2x(\mathbf{a}+\mathbf{b})(xy\partial_x - (1-y^2)\partial_y) - 4xy\mathbf{ab}
\end{aligned}$$

Using some Gegenbauer identities, we see that these operators act nicely on our summand:

$$\begin{aligned}
\mathcal{D}_0\mathcal{G}_{\Delta}^{(J)}(n,m) &= \mathcal{C}_{\Delta+n}^{(m)}\mathcal{G}_{\Delta}^{(J)}(n,m) \qquad (B.0.10)\\
\mathcal{D}_1\mathcal{G}_{\Delta}^{(J)}(n,m) &= -\gamma_{n,m}^{(+)}\mathcal{G}_{\Delta}^{(J)}(n+1,m+1) - \gamma_{n,m}^{(-)}\mathcal{G}_{\Delta}^{(J)}(n+1,m-1)\\
\mathcal{D}_{\text{ext}}\mathcal{G}_{\Delta}^{(J)}(n,m) &= -\eta_{n,m}^{(+)}\mathcal{G}_{\Delta}^{(J)}(n+1,m+1) - \eta_{n,m}^{(-)}\mathcal{G}_{\Delta}^{(J)}(n+1,m-1)
\end{aligned}$$

where

$$\gamma_{n,m}^{(+)} = \frac{(m+2\nu)(\Delta+n+m)^2}{2(m+\nu)} \qquad \gamma_{n,m}^{(-)} = \frac{m(\Delta+n-m-2\nu)^2}{2(m+\nu)} \tag{B.0.11}$$

and

$$\begin{aligned}
\eta_{n,m}^{(+)} &= \frac{(m+2\nu)\left((\mathbf{a}+\mathbf{b})(\Delta+n+m)+2\mathbf{ab}\right)}{m+\nu} \qquad (B.0.12)\\
\eta_{n,m}^{(-)} &= \frac{m\left((\mathbf{a}+\mathbf{b})(\Delta+n-m-2\nu)+2\mathbf{ab}\right)}{m+\nu}
\end{aligned}$$

from which we find the following recursion relation:

$$c_{n,m}\left(\mathcal{C}_{\Delta+n}^{(m)} - \mathcal{C}_{\Delta}^{(l)}\right) = c_{n-1,m-1}\xi_{n-1,m-1}^{(+)} + c_{n-1,m+1}\xi_{n-1,m+1}^{(-)} \tag{B.0.13}$$

where $\xi^{(+/-)}_{n,m} = \gamma^{(+/-)}_{n,m} + \eta^{(+/-)}_{m,m}$. With the initial condition $c_{0,m} = \delta_{m,J}$, at the first level we have

$$\begin{aligned} c_{1,J+1} &= \frac{J+2\nu}{J+\nu}\left(\frac{\Delta+J}{4} + \frac{\mathbf{a}+\mathbf{b}}{2} + \frac{\mathbf{ab}}{\Delta+J}\right) \\ c_{1,J-1} &= \frac{J}{J+\nu}\left(\frac{\Delta-J-2\nu}{4} + \frac{\mathbf{a}+\mathbf{b}}{2} + \frac{\mathbf{ab}}{\Delta-J-2\nu}\right) \end{aligned} \tag{B.0.14}$$

Higher levels can then be found recursively. We note that the only non-zero coefficients at the second level are $c_{2,J}, c_{2,J+2}$ and $c_{2,J-2}$.

Bibliography

[1] Matthijs Hogervorst and Balt C. van Rees. 'Crossing Symmetry in Alpha Space'. In: *Journal of High Energy Physics* 2017.11 (2017), p. 193. https://doi.org/10.1007/JHEP11(2017)193 doi:10.1007/JHEP11(2017)193.

[2] V. P. Yurov and A. B. Zamolodchikov. 'Truncated Conformal Space Approach to Scaling Lee-Yang Model'. In: *Int. J. Mod. Phys.* A5 (1990), pp. 3221–3246. doi:10.1142/S0217751X9000218X.

[3] Daniel Rutter and Balt C. van Rees. 'Counterterms in Truncated Conformal Perturbation Theory'. In: (2018). arXiv:1803.05798 [hep-th].

[4] S Ferrara, A.F Grillo and R Gatto. 'Tensor Representations of Conformal Algebra and Conformally Covariant Operator Product Expansion'. In: *Annals of Physics* 76.1 (1973), pp. 161 –188. http://www.sciencedirect.com/science/article/pii/0003491673904466 doi:https://doi.org/10.1016/0003-4916(73)90446-6.

[5] A. M. Polyakov. 'Nonhamiltonian Approach to Conformal Quantum Field Theory'. In: *Zh. Eksp. Teor. Fiz.* 66 (1974). [Sov. Phys. JETP39,9(1974)], pp. 23–42.

[6] S. Ferrara, A.F. Grillo, G. Parisi and R. Gatto. 'Covariant Expansion of the Conformal Four-Point Function'. In: *Nuclear Physics B* 49 (1972), pp. 77 –98.

http://www.sciencedirect.com/science/article/pii/0550321372905871
doi:https://doi.org/10.1016/0550-3213(72)90587-1.

[7] A.A. Belavin, A.M. Polyakov and A.B. Zamolodchikov. 'Infinite Conformal Symmetry in Two-Dimensional Quantum Field Theory'. In: *Nuclear Physics B* 241.2 (1984), pp. 333 –380.
http://www.sciencedirect.com/science/article/pii/055032138490052X
doi:https://doi.org/10.1016/0550-3213(84)90052-X.

[8] J. Cardy. *Scaling and Renormalization in Statistical Physics*. Cambridge University Press, May 1996.

[9] Riccardo Rattazzi, Vyacheslav S. Rychkov, Erik Tonni and Alessandro Vichi. 'Bounding Scalar Operator Dimensions in 4D CFT'. In: *JHEP* 12 (2008), p. 031.
doi:10.1088/1126-6708/2008/12/031.
arXiv:0807.0004 [hep-th].

[10] Sheer El-Showk, Miguel F. Paulos, David Poland, Slava Rychkov, David Simmons-Duffin and Alessandro Vichi. 'Solving the 3D Ising Model with the Conformal Bootstrap'. In: *Phys. Rev. D* 86 (2 2012), p. 025022.
https://link.aps.org/doi/10.1103/PhysRevD.86.025022
doi:10.1103/PhysRevD.86.025022.

[11] David Poland, David Simmons-Duffin and Alessandro Vichi. 'Carving Out the Space of 4D CFTs'. In: *JHEP* 05 (2012), p. 110.
doi:10.1007/JHEP05(2012)110.
arXiv:1109.5176 [hep-th].

[12] Zohar Komargodski and Alexander Zhiboedov. 'Convexity and Liberation at Large Spin'. In: *JHEP* 11 (2013), p. 140.
doi:10.1007/JHEP11(2013)140.
arXiv:1212.4103 [hep-th].

[13] Luis F. Alday. 'Large Spin Perturbation Theory for Conformal Field Theories'. In: *Phys. Rev. Lett.* 119.11 (2017), p. 111601. doi:10.1103/PhysRevLett.119.111601. arXiv:1611.01500 [hep-th].

[14] V. K. Dobrev, G. Mack, V. B. Petkova, S. G. Petrova and I. T. Todorov. 'Harmonic Analysis on the n-Dimensional Lorentz Group and its Application to Conformal Quantum Field Theory'. In: *Lect. Notes Phys.* 63 (1977), pp. 1–280. doi:10.1007/BFb0009678.

[15] Denis Karateev, Petr Kravchuk and David Simmons-Duffin. 'Harmonic Analysis and Mean Field Theory'. In: (2018). arXiv:1809.05111 [hep-th].

[16] Simon Caron-Huot. 'Analyticity in Spin in Conformal Theories'. In: *Journal of High Energy Physics* 2017.9 (2017), p. 78. https://doi.org/10.1007/JHEP09(2017)078 doi:10.1007/JHEP09(2017)078.

[17] David Simmons-Duffin. 'The Conformal Bootstrap'. In: *Proceedings, Theoretical Advanced Study Institute in Elementary Particle Physics: New Frontiers in Fields and Strings (TASI 2015): Boulder, CO, USA, June 1-26, 2015*. 2017, pp. 1–74. doi:10.1142/9789813149441_0001. arXiv:1602.07982 [hep-th].

[18] Slava Rychkov. *EPFL Lectures on Conformal Field Theory in D>= 3 Dimensions*. SpringerBriefs in Physics. 2016. doi:10.1007/978-3-319-43626-5. arXiv:1601.05000 [hep-th].

[19] Juan Maldacena. 'The Large-N Limit of Superconformal Field Theories and Supergravity'. In: *International Journal of Theoretical Physics* 38.4 (1999),

pp. 1113–1133.
https://doi.org/10.1023/A:1026654312961
doi:10.1023/A:1026654312961.

[20] S.S. Gubser, I.R. Klebanov and A.M. Polyakov. 'Gauge Theory Correlators from Non-Critical String Theory'. In: *Physics Letters B* 428.1 (1998), pp. 105 –114.
http://www.sciencedirect.com/science/article/pii/S0370269398003773
doi:https://doi.org/10.1016/S0370-2693(98)00377-3.

[21] Edward Witten. 'Anti-de Sitter Space and Holography'. In: *Adv. Theor. Math. Phys.* 2 (1998), pp. 253–291.
doi:10.4310/ATMP.1998.v2.n2.a2.
arXiv:hep-th/9802150 [hep-th].

[22] Eric D'Hoker and Daniel Z. Freedman. 'Supersymmetric Gauge Theories and the AdS/CFT Correspondence'. In: *Strings, Branes and Extra Dimensions: TASI 2001: Proceedings*. 2002, pp. 3–158.
arXiv:hep-th/0201253 [hep-th].

[23] Kenneth G. Wilson. 'The Renormalization Group: Critical Phenomena and the Kondo Problem'. In: *Rev. Mod. Phys.* 47 (4 1975), pp. 773–840.
https://link.aps.org/doi/10.1103/RevModPhys.47.773
doi:10.1103/RevModPhys.47.773.

[24] A. B. Zomolodchikov. 'Irreversibility of the Flux of the Renormalization Group in a 2D Field Theory'. In: *Soviet Journal of Experimental and Theoretical Physics Letters* 43 (June 1986), p. 730.

[25] H. Osborn. 'Derivation of a Four Dimensional c-Theorem for Renormaliseable Quantum Field Theories'. In: *Physics Letters B* 222.1 (1989), pp. 97 –102.
http://www.sciencedirect.com/science/article/pii/0370269389907296
doi:https://doi.org/10.1016/0370-2693(89)90729-6.

[26] Zohar Komargodski and Adam Schwimmer. 'On Renormalization Group Flows in Four Dimensions'. In: *Journal of High Energy Physics* 2011.12 (2011), p. 99.
https://doi.org/10.1007/JHEP12(2011)099
doi:10.1007/JHEP12(2011)099.

[27] Silviu S. Pufu. 'The F-Theorem and F-Maximization'. In: *J. Phys.* A50.44 (2017), p. 443008.
doi:10.1088/1751-8121/aa6765.
arXiv:1608.02960 [hep-th].

[28] P. A. M. Dirac. 'Wave Equations in Conformal Space'. In: *Annals of Mathematics* 37.2 (1936), pp. 429–442.
http://www.jstor.org/stable/1968455.

[29] P. Francesco, P. Mathieu and D. Senechal. *Conformal Field Theory*. Island Press, 1996.
https://books.google.co.uk/books?id=mcMbswEACAAJ.

[30] Miguel S. Costa, Joao Penedones, David Poland and Slava Rychkov. 'Spinning Conformal Blocks'. In: *JHEP* 11 (2011), p. 154.
doi:10.1007/JHEP11(2011)154.
arXiv:1109.6321 [hep-th].

[31] F. A. Dolan and H. Osborn. 'Conformal Partial Waves and the Operator Product Expansion'. In: *Nucl. Phys.* B678 (2004), pp. 491–507.
doi:10.1016/j.nuclphysb.2003.11.016.
arXiv:hep-th/0309180 [hep-th].

[32] Joao Penedones, Emilio Trevisani and Masahito Yamazaki. 'Recursion Relations for Conformal Blocks'. In: *JHEP* 09 (2016), p. 070.
doi:10.1007/JHEP09(2016)070.
arXiv:1509.00428 [hep-th].

[33] Matthijs Hogervorst, Hugh Osborn and Slava Rychkov. 'Diagonal Limit for Conformal Blocks in d Dimensions'. In: *Journal of High Energy Physics* 2013.8 (2013), p. 14.
https://doi.org/10.1007/JHEP08(2013)014
doi:10.1007/JHEP08(2013)014.

[34] M. Billo, M. Caselle, D. Gaiotto, F. Gliozzi, M. Meineri and R. Pellegrini. 'Line Defects in the 3d Ising Model'. In: *JHEP* 07 (2013), p. 055.
doi:10.1007/JHEP07(2013)055.
arXiv:1304.4110 [hep-th].

[35] Ferdinando Gliozzi, Pedro Liendo, Marco Meineri and Antonio Rago. 'Boundary and Interface CFTs from the Conformal Bootstrap'. In: *JHEP* 05 (2015), p. 036.
doi:10.1007/JHEP05(2015)036.
arXiv:1502.07217 [hep-th].

[36] Tom H Koornwinder and Gilbert G Walter. 'The Finite Continuous Jacobi Transform and its Inverse'. In: *Journal of Approximation Theory* 60.1 (1990), pp. 83 –100.
http://www.sciencedirect.com/science/article/pii/0021904590900752
doi:https://doi.org/10.1016/0021-9045(90)90075-2.

[37] David Simmons-Duffin. 'The Lightcone Bootstrap and the Spectrum of the 3d Ising CFT'. In: *Journal of High Energy Physics* 2017.3 (2017), p. 86.
https://doi.org/10.1007/JHEP03(2017)086
doi:10.1007/JHEP03(2017)086.

[38] A. Liam Fitzpatrick, Jared Kaplan, Joao Penedones, Suvrat Raju and Balt C. van Rees. 'A Natural Language for AdS/CFT Correlators'. In: *JHEP* 11 (2011), p. 095.
doi:10.1007/JHEP11(2011)095.
arXiv:1107.1499 [hep-th].

[39] Joao Penedones. 'Writing CFT Correlation Functions as AdS Scattering Amplitudes'. In: *JHEP* 03 (2011), p. 025.
doi:10.1007/JHEP03(2011)025.
arXiv:1011.1485 [hep-th].

[40] Vasco Goncalves, Joao Penedones and Emilio Trevisani. 'Factorization of Mellin Amplitudes'. In: *JHEP* 10 (2015), p. 040.
doi:10.1007/JHEP10(2015)040.
arXiv:1410.4185 [hep-th].

[41] Luis F. Alday and Simon Caron-Huot. 'Gravitational S-matrix from CFT Dispersion Relations'. In: *Journal of High Energy Physics* 2018.12 (2018), p. 17.
https://doi.org/10.1007/JHEP12(2018)017
doi:10.1007/JHEP12(2018)017.

[42] Luis F. Alday, Agnese Bissi and Tomasz Lukowski. 'Large Spin Systematics in CFT'. In: *JHEP* 11 (2015), p. 101.
doi:10.1007/JHEP11(2015)101.
arXiv:1502.07707 [hep-th].

[43] Wolter Groenevelt. 'The Wilson Function Transform'. In: *arXiv Mathematics e-prints*, math/0306424 (2003).
arXiv:math/0306424.

[44] Luis F. Alday, Agnese Bissi and Tomasz Lukowski. 'Large Spin Systematics in CFT'. In: *Journal of High Energy Physics* 2015.11 (2015), p. 101.
https://doi.org/10.1007/JHEP11(2015)101
doi:10.1007/JHEP11(2015)101.

[45] Idse Heemskerk, Joao Penedones, Joseph Polchinski and James Sully. 'Holography from Conformal Field Theory'. In: *JHEP* 10 (2009), p. 079.
doi:10.1088/1126-6708/2009/10/079.
arXiv:0907.0151 [hep-th].

[46] David Simmons-Duffin, Douglas Stanford and Edward Witten. 'A Spacetime Derivation of the Lorentzian OPE Inversion Formula'. In: *Journal of High Energy Physics* 2018.7 (2018), p. 85.
https://doi.org/10.1007/JHEP07(2018)085
doi:10.1007/JHEP07(2018)085.

[47] Matthijs Hogervorst. 'Dimensional Reduction for Conformal Blocks'. In: *Journal of High Energy Physics* 2016.9 (2016), p. 17.
https://doi.org/10.1007/JHEP09(2016)017
doi:10.1007/JHEP09(2016)017.

[48] Matthijs Hogervorst. 'Crossing Kernels for Boundary and Crosscap CFTs'. In: (2017).
arXiv:1703.08159 [hep-th].

[49] Miguel S. Costa, Vasco Goncalves and Joao Penedones. 'Conformal Regge Theory'. In: *JHEP* 12 (2012), p. 091.
doi:10.1007/JHEP12(2012)091.
arXiv:1209.4355 [hep-th].

[50] Simon Caron-Huot. 'Analytical Approaches'. Simons Collaboration Bootstrap Meeting - Azores. 2018.

[51] Petr Kravchuk and David Simmons-Duffin. 'Light-Ray Operators in Conformal Field Theory'. In: *Journal of High Energy Physics* 2018.11 (2018), p. 102.
https://doi.org/10.1007/JHEP11(2018)102
doi:10.1007/JHEP11(2018)102.

[52] Junyu Liu, Eric Perlmutter, Vladimir Rosenhaus and David Simmons-Duffin. 'd-Dimensional SYK, AdS Loops, and $6j$ Symbols'. In: *JHEP* 03 (2019), p. 052.
doi:10.1007/JHEP03(2019)052.
arXiv:1808.00612 [hep-th].

[53] Wolter Groenevelt. 'Wilson Function Transforms Related to Racah Coefficients'. In: *Acta Applicandae Mathematica* 91.2 (2006), pp. 133–191. https://doi.org/10.1007/s10440-006-9024-7 doi:10.1007/s10440-006-9024-7.

[54] Giovanni Feverati, Kevin Graham, Paul A. Pearce, Gabor Zs. Toth and Gerard Watts. 'A Renormalisation Group for the Truncated Conformal Sspace Approach'. In: *J. Stat. Mech.* 0803 (2008), P03011. doi:10.1088/1742-5468/2008/03/P03011. arXiv:hep-th/0612203 [hep-th].

[55] Gerard M. T. Watts. 'On the Renormalisation Group for the Boundary Truncated Conformal Space Approach'. In: *Nucl. Phys.* B859 (2012), pp. 177–206. doi:10.1016/j.nuclphysb.2012.01.012. arXiv:1104.0225 [hep-th].

[56] M. Lencses and G. Takacs. 'Excited State TBA and Renormalized TCSA in the Scaling Potts model'. In: *JHEP* 09 (2014), p. 052. doi:10.1007/JHEP09(2014)052. arXiv:1405.3157 [hep-th].

[57] Philip Giokas and Gerard Watts. 'The Renormalisation Group for the Truncated Conformal Space Approach on the Cylinder'. In: (2011). arXiv:1106.2448 [hep-th].

[58] M. Beria, G.P. Brandino, L. Lepori, R.M. Konik and G. Sierra. 'Truncated Conformal Space Approach for Perturbed Wess-Zumino-Witten SU(2)k Models'. In: *Nuclear Physics B* 877.2 (2013), pp. 457 –483. http://www.sciencedirect.com/science/article/pii/S055032131300518X doi:https://doi.org/10.1016/j.nuclphysb.2013.10.005.

[59] Gabor Zsolt Toth. 'A Study of Truncation Effects in Boundary Flows of the Ising Model on the Strip'. In: *J. Stat. Mech.* 0704 (2007), P04005.

doi:10.1088/1742-5468/2007/04/P04005.

arXiv:hep-th/0612256 [hep-th].

[60] Matthijs Hogervorst, Slava Rychkov and Balt C. van Rees. 'Truncated Conformal Space Approach in d Dimensions: A Cheap Alternative to Lattice Field Theory?' In: *Phys. Rev. D* 91 (2 2015), p. 025005.

http://link.aps.org/doi/10.1103/PhysRevD.91.025005

doi:10.1103/PhysRevD.91.025005.

[61] Slava Rychkov and Lorenzo G. Vitale. 'Hamiltonian Truncation Study of the ϕ^4 Theory in Two Dimensions'. In: *Phys. Rev.* D91 (2015), p. 085011.

doi:10.1103/PhysRevD.91.085011.

arXiv:1412.3460 [hep-th].

[62] Slava Rychkov and Lorenzo G. Vitale. 'Hamiltonian Truncation Study of the ϕ^4 Theory in Two Dimensions. II. The $\mathbb{Z}_2$ -Broken Phase and the Chang Duality'. In: *Phys. Rev.* D93.6 (2016), p. 065014.

doi:10.1103/PhysRevD.93.065014.

arXiv:1512.00493 [hep-th].

[63] J. Elias-Miro, M. Montull and M. Riembau. 'The Renormalized Hamiltonian Truncation Method in the Large E_T Expansion'. In: *JHEP* 04 (2016), p. 144.

doi:10.1007/JHEP04(2016)144.

arXiv:1512.05746 [hep-th].

[64] Joan Elias-Miro, Slava Rychkov and Lorenzo G. Vitale. 'NLO Renormalization in the Hamiltonian Truncation'. In: *Phys. Rev.* D96.6 (2017), p. 065024.

doi:10.1103/PhysRevD.96.065024.

arXiv:1706.09929 [hep-th].

[65] Joan Elias-Miro, Slava Rychkov and Lorenzo G. Vitale. 'High-Precision Calculations in Strongly Coupled Quantum Field Theory with Next-to-Leading-Order Renormalized Hamiltonian Truncation'. In: *JHEP* 10

(2017), p. 213.
doi:10.1007/JHEP10(2017)213.
arXiv:1706.06121 [hep-th].

[66] Andrew J. A. James, Robert M. Konik, Philippe Lecheminant, Neil J. Robinson and Alexei M. Tsvelik. 'Non-Perturbative Methodologies for Low-Dimensional Strongly-Correlated Systems: From Non-Abelian Bosonization to Truncated Spectrum Methods'. In: *Rept. Prog. Phys.* 81.4 (2018), p. 046002.
doi:10.1088/1361-6633/aa91ea.
arXiv:1703.08421 [cond-mat.str-el].

[67] Matthijs Hogervorst, Slava Rychkov and Balt C. van Rees. 'Unitarity Violation at the Wilson-Fisher Fixed Point in $4-\epsilon$ Dimensions'. In: *Phys. Rev. D* 93 (12 2016), p. 125025.
http://link.aps.org/doi/10.1103/PhysRevD.93.125025
doi:10.1103/PhysRevD.93.125025.

[68] Duccio Pappadopulo, Slava Rychkov, Johnny Espin and Riccardo Rattazzi. 'OPE Convergence in Conformal Field Theory'. In: *Phys. Rev.* D86 (2012), p. 105043.
doi:10.1103/PhysRevD.86.105043.
arXiv:1208.6449 [hep-th].

[69] W. Feller. *An Introduction to Probability Theory and its Applications*. Wiley Series in Probability and Mathematical Statistics: Probability and Mathematical Statistics. Wiley, 1971.

[70] Matthijs Hogervorst and Slava Rychkov. 'Radial Coordinates for Conformal Blocks'. In: *Phys. Rev. D* 87 (10 2013), p. 106004.
doi:10.1103/PhysRevD.87.106004.

[71] R. C. Brower, G. T. Fleming and H. Neuberger. 'Lattice Radial Quantization: 3D Ising'. In: *Phys. Lett.* B721 (2013), pp. 299–305.

doi:10.1016/j.physletb.2013.03.009.

arXiv:1212.6190 [hep-lat].

[72] Baur Mukhametzhanov and Alexander Zhiboedov. 'Analytic Euclidean Bootstrap'. In: (2018).

arXiv:1808.03212 [hep-th].

[73] F. A. Dolan and H. Osborn. 'Conformal Partial Waves: Further Mathematical Results'. In: *ArXiv* (2011).

arXiv:1108.6194 [hep-th].